REACTOR CORE MATERIALS

UNIVERSITY OF MICHIGAN
JUL 9 1961
PHOENIX LIBRARY

A Quarterly Technical Progress Review

Prepared for U. S. ATOMIC ENERGY COMMISSION by BATTELLE MEMORIAL INSTITUTE

May 1961

VOLUME 4

NUMBER 2

TECHNICAL PROGRESS REVIEWS

To meet the needs of industry for concise summaries of current atomic developments, the Atomic Energy Commission is publishing this series, Technical Progress Reviews. Issued quarterly, each of the reviews digests and evaluates the latest findings in a specific area of nuclear technology and science.

The four journals published in this series are:

Nuclear Safety, W. B. Cottrell, editor, R. A. Charpie, advisory editor, and associates, Oak Ridge National Laboratory

Power Reactor Technology, Walter H. Zinn and associates, General Nuclear Engineering Corporation

Reactor Core Materials (covering solid material developments), R. W. Dayton, E. M. Simons, and associates, Battelle Memorial Institute

Reactor Fuel Processing, Stephen Lawroski and associates, Chemical Engineering Division, Argonne National Laboratory

Each journal may be purchased ($2.00 per year for subscription and individual issues $0.55) from the Superintendent of Documents, U. S. Government Printing Office, Washington 25, D. C. See back cover for remittance instructions and foreign postage requirements.

The views expressed in this publication do not necessarily represent those of the United States Atomic Energy Commission, its divisions or offices, or of any Commission advisory committee or contractor.

Availability of Reports Cited in This Review

Unclassified AEC reports are available for inspection at AEC depository libraries and are sold by the Office of Technical Services, Department of Commerce, Washington 25, D. C. Some of the reports cited are not available owing to their preliminary nature; however, the information contained in them will eventually be made available in formal progress or topical reports.

Unclassified reports issued by other Government agencies or private organizations should be requested from the originator.

Unclassified British and Canadian reports may be inspected at AEC depository libraries. British reports are sold by the British Information Service, 45 Rockefeller Plaza, New York, N. Y.; Canadian reports (AECL series) are sold by the Scientific Document Distribution Office, Atomic Energy of Canada, Ltd., Chalk River, Ontario, Canada.

Classified U. S. and foreign reports identified in this journal as Classified may be purchased by properly cleared Access Permit Holders from the Office of Technical Information Extension, U. S. Atomic Energy Commission, P. O. Box 1001, Oak Ridge, Tenn. Such reports may be inspected at classified AEC depository libraries.

REACTOR CORE MATERIALS

A REVIEW OF RECENT DEVELOPMENTS

Prepared for U. S. ATOMIC ENERGY COMMISSION
by BATTELLE MEMORIAL INSTITUTE

● MAY 1961

● VOLUME 4

● NUMBER 2

foreword

Reactor Core Materials, one of a series of four quarterly reviews broadly covering the field of nuclear science and technology, is prepared by Battelle personnel from worldwide literature and covers materials and fabrication processes applicable to a nuclear reactor core. The coverage of this subject, however, is limited to materials that are solid at reactor operating temperatures. Pure chemistry, physics, core instrumentation, fuel processing, and source materials are not covered by this Review.

The authors and editors of *Reactor Core Materials* attempt to incorporate new developments and significant findings. This Review can serve as a useful summary of current research for both management and the technical specialist. For the latter group of readers, it is intended that the extensive referencing will aid in locating sources of more detailed information.

R. W. DAYTON
E. M. SIMONS
R. W. ENDEBROCK
Battelle Memorial Institute

contents

Foreword

1 I FUEL AND FERTILE MATERIALS

1 Unalloyed Uranium
1 Alpha-Phase Uranium Alloys
2 Epsilon-Phase Uranium Alloys
2 Gamma-Phase Uranium Alloys
4 Plutonium and Its Alloys
5 Thorium
6 Refractory Fuel and Fertile Materials
9 Dispersion Fuels
11 Mechanism of Corrosion of Fuel Alloys
12 Basic Studies of Irradiation Effects in Fuel Materials
14 References

17 II MODERATOR MATERIALS

17 Graphite
18 Beryllium Metal and Alloys
24 Beryllium Compounds
24 Solid Hydrides
25 References

28 III NUCLEAR POISONS

28 Metallic Poison Materials
30 Dispersion Absorber Materials
31 References

32 IV CLADDING AND STRUCTURAL MATERIALS

32 Corrosion
35 Radiation Effects in Nonfuel Materials
41 Selected Metallurgical Aspects of Cladding and Structural Materials
46 Selected Mechanical Properties of Cladding and Structural Materials
48 References

51 V SPECIAL FABRICATION TECHNIQUES

51 Melting and Casting
52 Cladding
60 Welding and Brazing
61 Nondestructive Testing
62 References

Issued quarterly by the U. S. Atomic Energy Commission. Use of funds for printing this publication approved by the Director of the Bureau of the Budget on November 1, 1960.

Section I

FUEL AND FERTILE MATERIALS

Unalloyed Uranium

An investigation of the adiabatic elastic moduli of single-crystal alpha uranium has been completed by Argonne.[1] The nine single-crystal elastic moduli pertaining to principal crystallographic axes of alpha uranium at 25°C were determined from measurements of high-frequency wave velocities for 21 modes in seven single-crystal specimens. A special orienting and lapping technique was used for preparing the specimens from small single crystals. The probable errors in each measurement, computed from estimated uncertainties, agree well with the internal consistency of the data. The stiffness moduli, in units of 10^{12} dynes/cm^2, are as follows: $C_{11} = 2.147 \pm 0.14\%$, $C_{12} = 0.465 \pm 0.6\%$, $C_{13} = 0.218 \pm 1.5\%$, $C_{22} = 1.986 \pm 0.14\%$, $C_{23} = 1.076 \pm 0.34\%$, $C_{33} = 2.671 \pm 0.14\%$, $C_{44} = 1.2444 \pm 0.10\%$, $C_{55} = 0.7342 \pm 0.10\%$, $C_{66} = 0.7433 \pm 0.10\%$. From these results the elastic compliances, compressibilities, and Poisson's ratios have been computed for the principal axes, and the variations with crystal direction of the stiffness moduli, Young's moduli, and rigidity moduli have been plotted. The nature of the anisotropy for the different moduli indicates that the nearest neighbor interatomic bonds are considerably stiffer than the next nearest bonds, which are, however, only slightly larger in atomic distance.

The heat capacity of uranium metal containing less than 0.01 per cent impurities was measured[2] from 5 to 350°K. From these data the entropy, enthalpy, and free-energy function were calculated. The values of C_p, S^0, $(H^0 - H_0^0)$ and $(F^0 - H_0^0)/T$ at 298.15°K are 6.612 ± 0.013 cal/(deg)(mole), 12.00 ± 0.02 cal/(deg)(mole), 1521 ± 3 cal/mole and −6.893 ± 0.014 cal/(deg)(mole), respectively.

Experiments on the alpha-beta cycling of the core of a bar of uranium while the rims remain in the alpha phase show that dimensional distortions of the bar occur when more than about 10 per cent of the bar diameter is transformed to beta.[3] The extent of the damage depends on the fraction of the bar diameter transformed (e.g., +0.5 diameter strain with 30 per cent transformed). Damage is not observed to increase with increasing numbers of cycles between 13 and 100. Tubular specimens suffer more severe damage than solid bars when compared on a basis of the percentage of outside diameter transformed. The striking feature of these results is the large increase in internal diameter. The distortions are dependent on the direction of movement of the interface between the phases, and the detailed results are consistent with a general model of phase-change cycling. Metallographic examination after cycling shows that recrystallization took place in all metal heated to above 560 ± 10°C. No porosity which can be attributed to cycling was detected. (M. S. Farkas)

Alpha-Phase Uranium Alloys

Fuel pins of type 304 stainless-steel-clad uranium−2 wt.% zirconium and uranium−3 to 7.5 wt.% fissium were irradiated by Argonne[4] to burnups varying from 0.4 to 1.56 per cent, while maximum centerline temperatures of 700 to 1200°F were maintained. Typical operating conditions include a pin-surface heat flux of 300,000 Btu/(hr)(sq ft) and a 60°F centerline-to-surface temperature drop. During the irradiation, 200 to 300 thermal cycles occurred from operating temperature to reactor ambient temperature.

No significant fuel-element warpage was noted. The entire surface of each fuel pin was pimpled in appearance, which in general was more pronounced in the high-temperature areas. The 7.5 wt.% fissium alloys showed less tendency toward surface coarsening than the low-fissium alloys and the zirconium alloys. All the fuel alloys were embrittled to the extent that it was very difficult to handle the specimens remotely without breakage. The density of all fuel specimens decreased upon irradiation. However, despite the importance of fuel burnup, the dominant factor controlling volume expansion of the fuel was the operating temperature. In all the irradiated samples, the largest volume expansion also occurred in the radial direction. The 5 wt.% fissium alloy showed less tendency toward diametral expansion than the 2 wt.% zirconium alloy at a given burnup and temperature. With respect to stability, the 7.5 wt.% fissium alloy appeared to be slightly better than the 5 wt.% alloy. An overall evaluation of the data accumulated leads to the postulation that the 5 wt.% fissium alloy will perform well up to 2 wt.% burnup with a central metal temperature of approximately 1200°F. The major changes in the fuel will be a decrease in density and a considerable roughening of the fuel surface. Fission-gas release is not expected to be troublesome. Accordingly, the 5 wt.% cast fissium alloy was selected for the first core loading of the Experimental Breeder Reactor No. 2 (EBR-II). (M. S. Farkas)

Epsilon-Phase Uranium Alloys

A German report[5] summarizes the properties and behavior of uranium-silicon alloys and compounds, with emphasis on the U_3Si compound. It is concluded that U_3Si cannot be considered for use as a fuel at elevated temperatures.

Gamma-Phase Uranium Alloys

Uranium-Molybdenum

A report issued by Atomic Power Development Associates (APDA)[6] presents the results obtained on three prototype fuel pins for the Enrico Fermi reactor. The pins are zirconium clad and contain uranium–10 wt.% molybdenum alloy fuel. Irradiation data and test results are summarized in Figs. I-1 to I-3. The severe swelling noted for the CP-5-1 pin in the range of 800 to 1050°F is believed to be associated with transformation to the thermally stable alpha-plus-delta phases. Transformation of gamma was observed in the CP-5-2 pin, but transformation was not accompanied by swelling. Irradiation behavior at temperatures above 1100°F is summarized in Fig. I-4 and compared with previous data obtained on specimens irradiated in the Materials Testing Reactor (MTR). A strong temperature and burnup dependence is indicated.

The results of thermal cycling transformed uranium–10 wt.% molybdenum specimens for 504 cycles between room temperature and 525°C are reported by Detroit Edison.[7] Only slight dimensional changes and no metallographic changes in structure were observed after cycling.

A companion report[8] presents the results of thermal cycling gamma-stabilized specimens between 675 and 475°C for 70 cycles, holding the specimens at these temperatures for 2 and 46 hr, respectively. Slight increases in diameter and decreases in length were noted. The 2-hr treatment at 675°C was sufficient to produce gamma in the specimens, whereas the 46-hr treatment at 475°C produced partial transformation. The degree of transformation varied, probably as a result of homogenization of the alloy, from about 90 per cent at the start of the test to 25 per cent at the end of the test.

A study of the thermal-cycling behavior of the uranium–10 wt.% molybdenum alloy both in the stable gamma region and in the metastable gamma region is also reported.[9] No distortion or growth of either retained or partially transformed gamma structures as a result of 1000 thermal cycles was noted.

The results of a study[10] of oxidation rates in air of the uranium–10 wt.% molybdenum alloy indicate no difference in the behavior of either as-cast or gamma-heat-treated material. At 600°F, weight-change data exhibit a parabolic relation with exposure time. In the first ½ hr the maximum weight gain is 0.125 mg/(cm^2)(hr), whereas at 24 hr the weight gain levels off at 0.015 mg/(cm^2)(hr). Only a slight amount of spalling was noted after 24 hr. At 900°F, however, the oxide apparently is not protective, and a linear weight gain of 1.8 mg/(cm^2)(hr) was observed over the greater portion of the 24-hr test period.

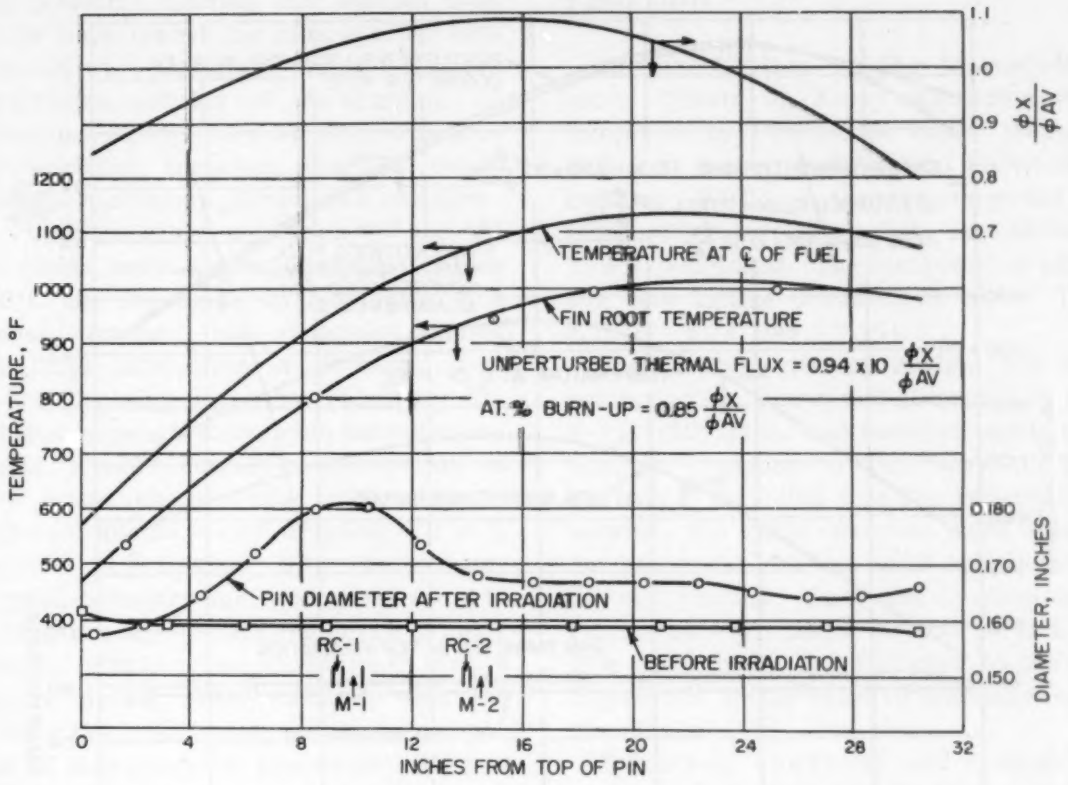

Fig. I-1 Irradiation results of CP-5-1 test.[6] M, specimens taken for metallographic examination. RC, specimens taken for radiochemical burnup analysis.

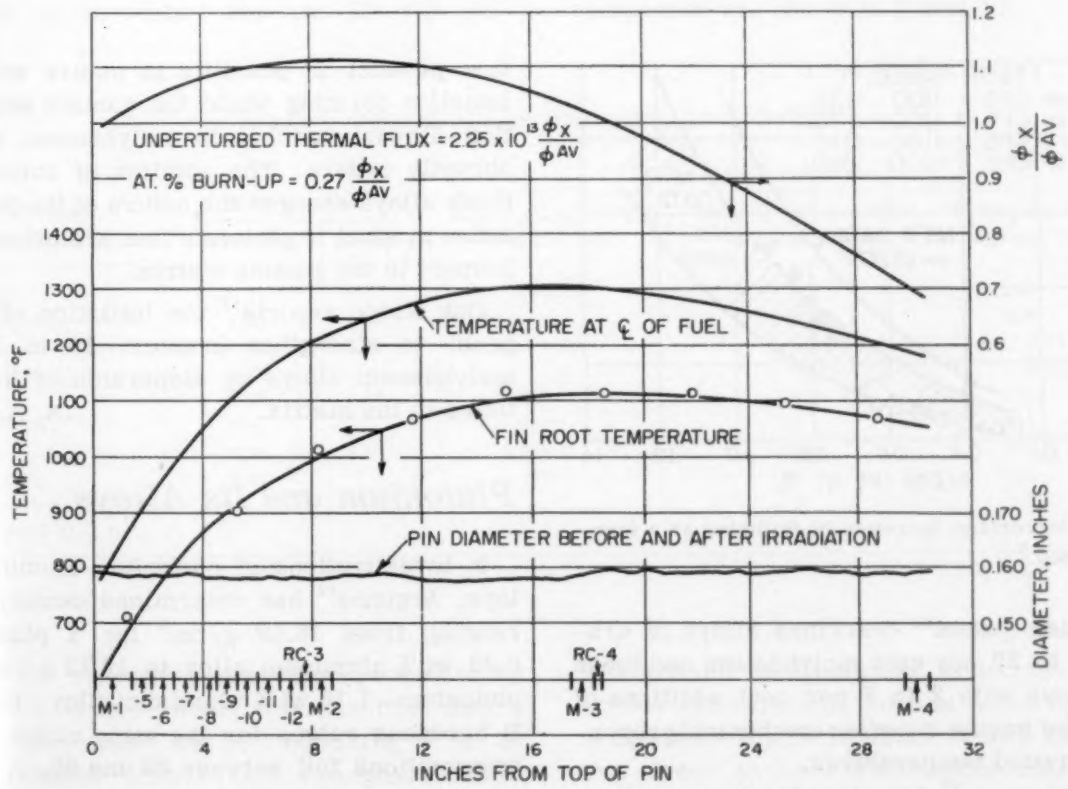

Fig. I-2 Irradiation results of CP-5-2 test.[6] M, specimens taken for metallographic examination. RC, specimens taken for radiochemical burnup analysis.

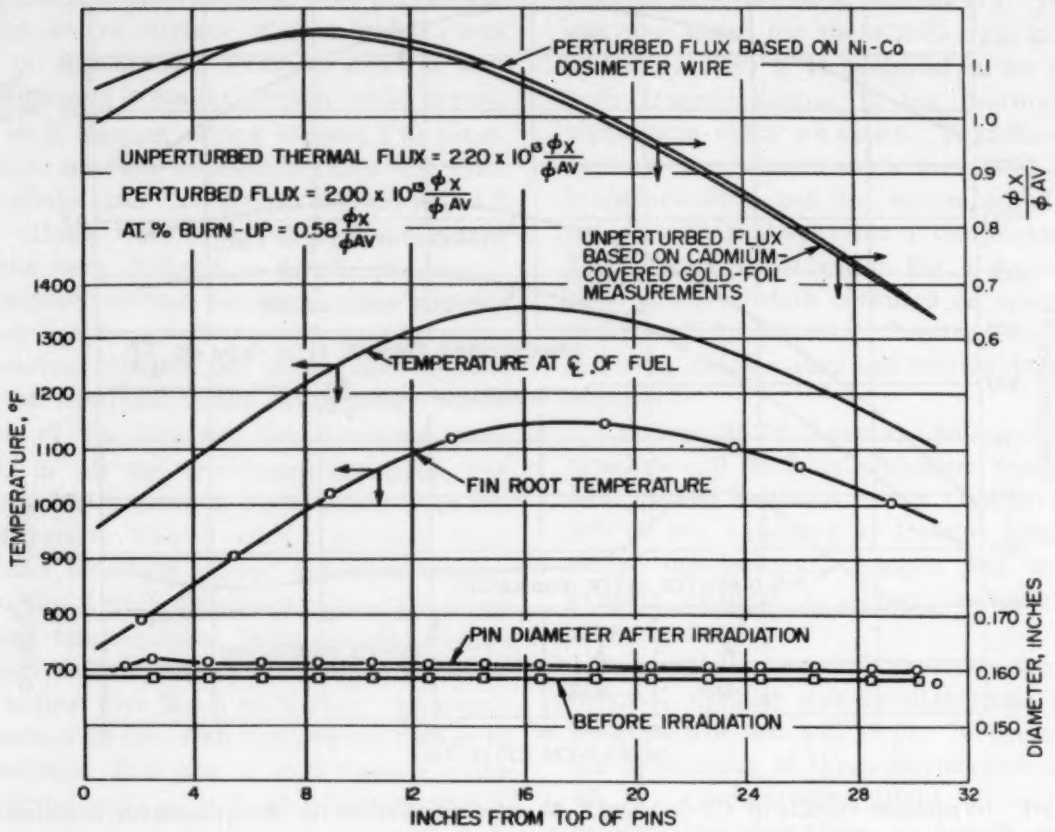
PERTURBED FLUX BASED ON Ni-Co DOSIMETER WIRE
UNPERTURBED THERMAL FLUX = 2.20 x 10^13 φx/φAV
PERTURBED FLUX = 2.00 x 10^13 φx/φAV
AT % BURN-UP = 0.58 φx/φAV
UNPERTURBED FLUX BASED ON CADMIUM-COVERED GOLD-FOIL MEASUREMENTS
TEMPERATURE AT ℄ OF FUEL
FIN ROOT TEMPERATURE
PIN DIAMETER AFTER IRRADIATION
BEFORE IRRADIATION
TEMPERATURE, °F
DIAMETER, INCHES
φx/φAV
INCHES FROM TOP OF PINS

Fig. I-3 Irradiation results of CP-5-3 test.[6]

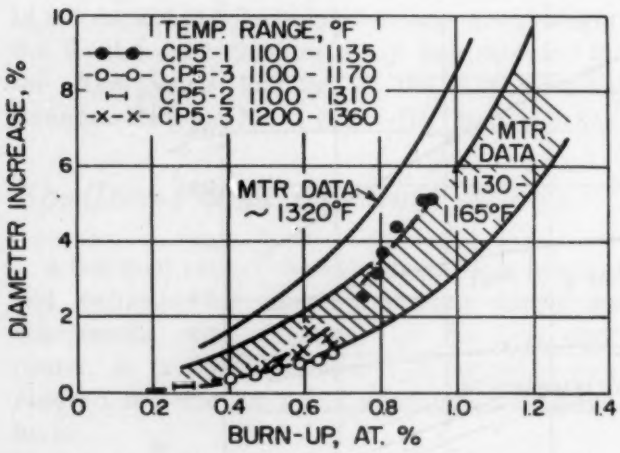

Fig. I-4 Percentage increase in diameter as a function of burnup.[6]

A British patent[11] describes alloys of uranium–10 to 27 per cent molybdenum and these same alloys with 2 to 6 per cent additions of tantalum as having superior mechanical properties at elevated temperatures.

A French paper[12] describes the decomposition of the gamma phase in alloys of 8 to 20 at.% molybdenum. In binary alloys the decomposition product is pearlitic in nature with alpha lamellae forming while the gamma solid solution slowly enriches in molybdenum and then abruptly orders. The addition of ruthenium to these alloys changes the nature of the decomposition product to platelets that are oriented with respect to the gamma matrix.

Oak Ridge reports[13] the initiation of a program to strengthen uranium–10 to 15 wt.% molybdenum alloys by dispersion of fine particles in the matrix. (A. A. Bauer)

Plutonium and Its Alloys

In investigations of plutonium-aluminum alloys, Argonne[14] has determined density values ranging from 16.09 g/cm^3 for a plutonium–0.23 wt.% aluminum alloy to 15.13 g/cm^3 for a plutonium–1.16 wt.% aluminum alloy. Rockwell B hardness values for the same range of alloy compositions fell between 88 and 96. A linear-expansion coefficient for a plutonium–0.68 wt.% aluminum alloy was tentatively determined to be 10.5 μin./(in.)(°C) between 100 and 350°C.

Several potential canning and barrier materials have been tested for compatibility with a uranium–20 wt.% plutonium–10 wt.% fissium alloy.[15] Diffusion couples of the uranium–20 wt.% plutonium–10 wt.% fissium alloy with molybdenum, niobium, tantalum, titanium, vanadium, yttrium, zirconium, Zircaloy-2, niobium–5.3 wt.% vanadium alloy, and types 347 and 430 stainless steels were studied at temperatures up to 800°C and for times up to 60 days. The molybdenum, titanium, and vanadium couples exhibited little interdiffusion. Niobium, zirconium, and Zircaloy-2 showed relatively extensive diffusion penetration, whereas the stainless steels showed extensive penetration at 500°C, a liquid phase being present above 600°C. Cored, injection-cast uranium–20 wt.% plutonium–10 wt.% fissium alloy exhibits extensive grain-boundary melting when heated to 800°C. This cored, cast alloy appears to react with niobium, tantalum, and vanadium to form a liquid phase which, under vacuum, wets and travels along the jacket-material surface.

Studies of thorium-base plutonium alloys at Battelle[16] have shown that a 10 wt.% ternary addition of zirconium to a thorium–10 wt.% plutonium alloy has a greater strengthening effect than does increasing the plutonium content up to 30 wt.%. A cast thorium–10 wt.% plutonium–10 wt.% zirconium alloy proved to be essentially single phase, whereas cast binary thorium-plutonium alloys containing 5 to 30 wt.% plutonium exhibited two phases. The amount of second phase in the binary alloys increased with plutonium content. (V. W. Storhok)

Thorium

An investigation of the thorium-tungsten-boron system by X-ray diffraction has been completed by Pitman and Das.[17] Samples subjected to X-ray identification techniques were fired at 1800°C. A ternary compound having a composition corresponding approximately to $ThWB_4$ was found. The compound is monoclinic and has lattice parameters of $a = 12.25$, $b = 3.75$, $c = 6.14$, and $\beta = 104.1°$.

The thorium-yttrium system has been investigated by Evans and Raynor[18] by means of X-ray diffraction and metallographic examination. In contrast to the work of Eash and Carlson,[19] they find that the two-phase region between the cubic thorium solid solution and the hexagonal yttrium solid extends from 49 to 69 at.% yttrium. Eash and Carlson found this region between about 39 and 53 at.% yttrium. The discrepancy is attributed to the effect of impurities on the relative stabilities of the two structures.

Refractory thorium and thorium-uranium compounds having low thermal-neutron cross sections and high metal densities are being studied at Battelle.[16,20,21] Preliminary density and corrosion data obtained on some of these compounds are shown in Table I-1.

Table I-1 PROPERTIES OF THORIUM COMPOUNDS[16,20,21]

Nominal composition	Density, g/cm³		Weight-gain data		
	Measured	X-ray	In dry air at 1200°F, mg/(cm²)(hr)	In Santowax at 350°C, mg/(cm²)(day)	In CO_2 at 1200°F, mg/(cm²)(hr)
Th_2Al	9.59	9.67	144		200
$(Th_9U)_2Al$	9.89			0.04	125
$ThBe_{13}$	4.10	4.10	0.02	0.3	1.35
$(Th_9U)Be_{13}$	4.28		1.0	0.07	0.048
Th_3Si_2	9.65	9.81	597	9	512
$(Th_9U)_3Si_2$	9.87		202	15	117
ThSi	8.95	8.99	268	54	480
$(Th_9U)Si$	9.05		339	39	690
ThC–10 at.% UC				2	
ThC_2–10 at.% UC_2				0.3	

Argonne[22] is attempting to improve the corrosion resistance of thorium metal by alloying. A thorium–1 wt.% titanium–1 wt.% carbon alloy was found to have a corrosion rate of 4 mg/(cm²)(day) in the course of a 12-day test in water at 260°C. (W. Chubb)

Refractory Fuel and Fertile Materials

Properties and Behavior of Uranium Oxide Fuels

Several recent reports deal with the thermal conductivity of UO_2. Chalk River[23] has performed thermal-conductivity measurements at 60°C on polycrystalline UO_2 specimens having densities varying from 8.5 to 10.7 g/cm^3 and on uranium oxides in the UO_2-U_3O_8 region. Data are also reported for postirradiation measurements made at 60°C on unannealed and annealed UO_2 specimens which had been irradiated below 500°C to various exposures up to 6.8×10^{19} nvt. Measurements at higher temperatures on both unirradiated and irradiated UO_2 were made by Battelle.[24–26] Bettis[27] has completed a series of in-pile measurements of the effective thermal conductivity of UO_2 as a function of the diametral clearance between fuel and cladding, the gas in the gap, and the central temperature of the fuel.

An extensive bibliography of unclassified references on irradiation testing of UO_2 has been prepared by Bost.[28] The effects of excess oxygen on the behavior of UO_2 during irradiation has been discussed by Robertson.[29]

Fission-fragment-damage studies are in progress at Bettis.[30] A series of UO_2 samples, which included some that had been heated in vacuum to 1800°F for 30 hr, have been examined with an X-ray double-crystal spectrometer. In general, only a barely significant change from 5.469 to 5.475 A in the unit cell size has been noted for exposures up to 10^{17} fissions/cm^3, and little change has been noted for exposures from 10^{17} to 20×10^{20} fissions/cm^3. Specimens of UO_2 which accumulated exposures ranging from 23×10^{20} to 30×10^{20} fissions/cm^3 showed a progressive disappearance of the cubic pattern. High-temperature microscopic examinations of UO_2 specimens irradiated to burnups of 40, 125, 440, and 1500 Mwd/ton have been completed at Hanford.[31] The melting points of these materials were 2830, 2890, 2920, and 3040°C, respectively, whereas the melting point observed for unirradiated UO_2 was 2790°C.

Experiments have been conducted[32] to determine the stability of UO_2 in contact with water vapor under irradiation at 80°C and at pressures below 1 atm. The data indicate that oxidation is caused mainly by oxygen produced by radiolytic decomposition of the water vapor.

The compatibility of tungsten, rhenium, tantalum, molybdenum, and niobium with UO_2 was tested at temperatures up to 2660°C at Chalk River.[33] None of the metals showed any evidence of reaction; however, there was a slight adherence of the UO_2 to molybdenum, tantalum, and niobium.

The investigation of the stabilizing effects of oxide additions to UO_2 was continued at Battelle.[34] Previous work indicated that solid solutions of UO_2 containing trivalent oxides such as La_2O_3 or Y_2O_3 are stable at temperatures to at least 1750°C. Recent results show that CaO may be partially substituted for La_2O_3 and Y_2O_3. Hanford[35] has observed that, at 2700°C, crystal growth in UO_2 containing 0.4 wt.% Nb_2O_7 and 0.7 wt.% TiO_2 was three times slower than in pure UO_2. The presence of 22 wt.% Y_2O_3 in UO_2 forms a stable compound corresponding to the formula $Y_6U_3O_7$ which is not affected by exposure to hydrogen or oxygen[36] at 525°C.

Studies dealing with the use of ZrO_2-UO_2 in a compartmented-plate configuration for PWR core 2 are in progress.[30,37] Lattice-parameter measurements made on ZrO_2-UO_2 platelets that were sintered for 65 hr at 1750°C, annealed at 1740°C for 620 hr, and quenched are presented in Table I-2. Metallographic studies on ZrO_2-UO_2 sintered at 1740 to 1750°C for 640 hr, annealed for 66 hr at 1875°C, and cooled rapidly indicate the existence of a two-phase region between 35.4 and 53.5 wt.% UO_2. Coefficients of thermal expansion from room temperature to 1100°C for dense UO_2, 25 wt.% UO_2–ZrO_2, and 34 wt.% UO_2–ZrO_2 were determined to be 10.1, 10.9, and 10.9×10^{-6} in./(in.)(°C), respectively. Platelets of 25 wt.% UO_2–ZrO_2 and 34 wt.% UO_2–ZrO_2 which were exposed to 650°F

Table I-2 LATTICE PARAMETERS FOR VARIOUS ZrO_2-UO_2 COMPOSITIONS[30]

UO_2, mole %	Lattice parameter, A		Structure	Theoretical density, g/cm^3
	a_0	c_0		
100	5.470		Cubic	10.97
90.3	5.438		Cubic	10.57
80.4	5.403		Cubic	10.18
70.1	5.378		Cubic	9.66
60.4	5.350		Cubic	9.21
50.2	5.315	5.344	Tetragonal	8.67

water and 750°F steam for three days showed negligible weight change. The results of 24-day exposures are given in Table I-3. The diffusion of Xe^{133} in high-density platelets of

Table I-3 WEIGHT GAIN BY UO_2-ZrO_2 EXPOSED TO 650°F WATER AND 750°F STEAM FOR 24 DAYS[30]

Composition	Weight gain, mg/cm²	
	650°F water	750°F steam
25 wt.% UO_2-ZrO_2	0.12	0.30
34 wt.% UO_2-ZrO_2	0.18	0.45

slightly irradiated 25 wt.% UO_2-ZrO_2 has been measured at 800, 900, and 1000°C during post-irradiation heating. Tentative diffusion coefficients are given in Table I-4, along with values for UO_2, which are about two orders of magnitude smaller.

Table I-4 DIFFUSION COEFFICIENTS FOR Xe^{133} IN ZrO_2–25 WT.% UO_2

Temp., °C	Diffusion coefficient, cm²/sec	
	ZrO_2–25 wt.% UO_2	UO_2
800	1.4×10^{-17}	4.0×10^{-20}
900	3.5×10^{-17}	2.2×10^{-19}
1000	8.9×10^{-16}	2.0×10^{-18}

The stable single-phase face-centered cubic region of the ZrO_2-rich portion of the UO_2-ZrO_2-CaO system has been investigated by Combustion Engineering.[38] Irradiation studies in a hot-water loop are reported for ZrO_2–13 wt.% CaO–17 wt.% UO_2 and ThO_2–14 wt.% UO_2 fuel materials.[39] The two-phase ZrO_2–13 wt.% CaO–17 wt.% UO_2 was only slightly affected by irradiations of 11.8×10^{20} fissions/cm³. This same fuel, however, showed dimensional instability when exposed to corrosion and an irradiation of 9.9×10^{20} fissions/cm³, simultaneously. Irradiation of the solid-solution ThO_2–14 wt.% UO_2 to an exposure of 12.5×10^{20} fissions/cm³ resulted in no significant dimensional changes.

Dispersion type metal-oxide bodies consisting of an Al_2O_3 matrix containing 20 vol.% UO_2 are being developed[40] for use as fuel in the Maritime Gas-Cooled Reactor (MGCR). There is some evidence that migration of the fuel occurs during sintering. This might be associated with the concentration of impurities such as sodium or potassium in the Al_2O_3. Tests show that Na_2O concentrations of 1 wt.% cause severe UO_2 migration. At concentrations of less than 0.1 wt.%, no migration was noticed in pellets sintered in hydrogen for 2 hr at 1700°F. Investigation of the UO_2-Al_2O_3 system has confirmed that the pseudobinary UO_2-Al_2O_3 is a simple eutectic system.

The liquidus curve for the PuO_2-UO_2 system in both helium and hydrogen has been determined at Knolls.[41] The curve is presented in Fig. I-5. The melting point of pure PuO_2 in helium was found to be 2295 ± 30°C.

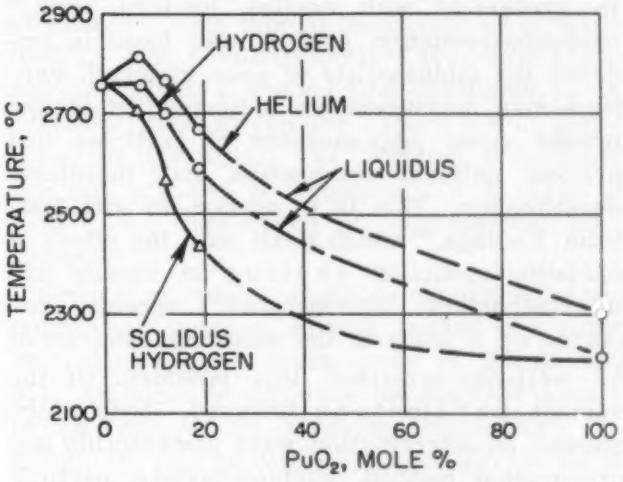

Fig. I-5 The system UO_2-PuO_2.[41]

Argonne[42] has irradiated ThO_2-UO_2 specimens containing molybdenum or niobium fibers. These specimens, which contained 10, 30, or 50 wt.% UO_2, were bare or in Zircaloy-2 jackets with lead or helium bonding. Postirradiation examination of the specimens has shown that the metal fibers effectively increase thermal conductivity, permitting greater heat fluxes.

Uranium silicate glasses are under investigation. Glasses containing up to 45 wt.% UO_2 with at least 40 wt.% SiO_2 in the presence of additives such as Na_2O, CaO, Al_2O_3, and TiO_2 exhibit reasonable devitrification resistance.[43] At Argonne,[15] fueled glasses involving the Na_2O-K_2O-UO_2-SiO_2 and PbO-UO_2-SiO_2 systems are under consideration. (R. H. Barnes)

Fabrication of UO_2-Containing Ceramics

An investigation to determine how the conditions under which ammonium diuranate is prepared influence the sinterability of UO_2 powders made by pyrolysis of the diuranate is

in progress at Nuclear Materials and Equipment Corporation (NUMEC).* The work, which complements earlier research at Chalk River,† reemphasizes the need for careful control of powder-preparation processes if a reproducible, sinterable powder is to be obtained.

Considerable differences in powder characteristics and sinterability in commercial UO_2 powders have been found by NUMEC. This is in agreement with results obtained by Olin Mathieson Chemical Corporation[44] and others. Olin Mathieson reports about as great a variance from lot to lot of UO_2 powder from a given source as for lots from different sources. In agreement with earlier Hanford work,[45] oxidation-reduction cycling was found to improve the sinterability of poor material. Particle-size measurements indicated that cycling breaks down agglomerates of particles that prevent uniform compaction and, therefore, densification. This is in agreement with Battelle findings,[46] which dealt with the effect of oxidation-reduction cycling on density and microstructure. Westinghouse[39] recently reported on a study of the sintering behavior of 35 well-characterized UO_2 powders. Of the various parameters involved, those which showed an interrelation were sinterability and preparation method, surface texture, particle size and shape, and agglomerate size and shape.

The development of a method of forming flat UO_2 plates has been reported by Gladding, McBean & Company.[47] The method consists of passing UO_2 powder, mixed with appropriate binders, through a set of rolls to form plates which then are dried and fired in a conventional manner. The process reportedly can be used to produce high-density plates (95 per cent of theoretical) with good dimensional uniformity.

Hanford[48] has remotely fabricated a UO_2-containing fuel element, a technique that appears promising for recycling fuel. Electrodeposited UO_2 was vibrationally compacted into a $\frac{5}{8}$-in.-diameter Zircaloy tube. The technique for electrodepositing UO_2 was described previously.[49]

(H. D. Sheets)

Properties of Refractory Fuels Other Than Uranium Oxides

Properties of oxides and carbides of plutonium are being investigated at Hanford.[48,50,51] The oxygen-to-plutonium ratio of PuO_2 after heating at 1500°C in wet or dry hydrogen or in helium is reduced to as low as 1.8 but appears to be affected by prior calcining treatment. X-ray-diffraction studies reveal that the reduction of PuO_2 pellets, in the above atmospheres, is largely at the surface. X-ray studies of PuO_2-ZrO_2 specimens after reactions at 1400°C revealed only the face-centered cubic solid-solution phase up to 62 wt.% ZrO_2. At higher ZrO_2 contents the cubic phase was not completely stabilized, and the monoclinic modification of ZrO_2 was observed in the diffraction patterns. PuO_2-ThO_2 bodies are being studied at Battelle. Weight losses and solid-state reactions were studied on bodies sintered at 1180°C. Hanford[51] observed complete vaporization of PuO_2 when heated with carbon in vacuum at 2000°C. Studies on the vaporization of PuC indicate that the above PuO_2 + carbon specimens reacted to form PuC, which decomposes and vaporizes at temperatures above 1750°C. Hanford[51] and Argonne[14] are evaluating PuC-UC solid-solution type fuels. UC appears to stabilize PuC to higher temperature. A transformation in PuC specimens containing 45 to 50 at.% carbon was revealed[14,15] by metallographic examination after quenching from 700°C. Argonne[15] reported the thermal-expansion coefficient for PuC to be 10×10^{-6}/°C. The transformed product, which can be obtained by working, has a slightly higher thermal-expansion coefficient at 700°C.

A review[52] of the Battelle Developments in UC fuels summarizes the studies of cladding materials for UC, self-diffusion behavior, and results of irradiation experiments on UC. Two ternary aluminum-uranium-carbon compounds are reported to exist by Cirilli and Brisi.[53] Neutron-pulse heating of natural and 8 per cent enriched UC fuel rods in the Kinetic Experiment on Water Boilers (KEWB) reactor was investigated by Atomics International.[54] A uniform temperature change was observed throughout the specimen containing natural uranium, whereas the change of surface temperature in the enriched sample

* Nuclear Materials and Equipment Corporation, 1960. (Unpublished)

† L. C. Watson, Production of Uranium Dioxide for Ceramic Fuels, in Fuel Elements Conference, Paris, November 18–23, 1957, USAEC Report TID-7546(Bk. 2), pp. 384–401, March 1958.

was approximately twice that of the center temperature. The high-temperature cubic modification of UC_2 was confirmed by Bredig.[55]

Investigations of properties of uranium monosulfide at Argonne[56] include heat of dissociation (121 kcal/mole), melting point (2735°K), resistivity (100×10^{-6} ohm-cm), and lattice parameter (5.4903 A). The vapor species were determined to be mainly uranium and sulfur atoms.

Thermal-expansion coefficients for U_2Si_3 and UN are given[57] as 16×10^{-6}/°C and 8×10^{-6}/°C, respectively.

Thermoelectric materials containing fissile materials, such as the compounds of uranium-sulfur, uranium-selenium, and uranium-tellurium, are reported[58] to be of primary interest. Preliminary reactor-arrangement studies are proposed. Russian workers[59] are evaluating the electron and ion emission of ThC as a function of temperature. (D. A. Vaughan)

Fabrication of Ceramic Fuels Other Than Uranium Oxides

The fabrication of uranium carbide fuels and of mixed fuels containing uranium carbide continues to be of interest at many laboratories. An investigation at Olin Mathieson,[44] on alternate methods of preparing the carbide powder to achieve greater purity and density in the finished product, has revealed that the reaction of UH_3 with propane gave higher purity than the reaction with methane. Attempts to obtain high density in sintered carbide bodies resulted in further evidence that an excess of uranium over the stoichiometric amount promotes densification. Contrary to some previous indications, nitrogen in the atmosphere was not beneficial in the absence of free uranium. The results of an extensive study of the preparation and fabrication of uranium carbide by several alternative methods at Battelle[52] were summarized in a recent report. The following carbide preparations are included: reaction of the metal with methane and propane, reaction of the oxide and carbon, and reaction of the metal and carbon. In addition, the fabrication of bodies by cold pressing and sintering and by hydrostatic and conventional hot pressing is covered.

Mixed fuels of plutonium and uranium carbide are under study at Argonne.[14,15,22] Attempts to prepare PuC from PuO_2 and carbon have resulted in poor stoichiometry; the effect of varying the proportions of the reactants is being studied.[14]

In studies[60] of uranium sulfide, the type of atmosphere selected during sintering was shown to affect densification. Sintering in argon gave greater density than sintering in vacuum. Preparation and fabrication of uranium sulfide, selenide, and telluride as potential thermoelectric nuclear fuels are being studied at Westinghouse.[58] These compounds are being prepared by reacting mixtures of the elements in an evacuated quartz tube at temperatures of about 1000°C. The resulting powders are cold pressed and are given a second heat-treatment in an evacuated tube to remove excess sulfur, selenium, or tellurium. The purified compounds are hot pressed at temperatures of 1150 to 1300°C for fabrication of experimental elements.

Several alternative methods for preparing and fabricating uranium nitride bodies are being studied at Battelle (references 16, 20, 21, and 61). Attempts to increase the sintered density by an increase in sintering temperature resulted in loss of nitrogen at temperatures of 2000 to 2100°C. Isostatic hot pressing using steel capsules gave densities of 87 to 91 per cent of the theoretical density. The use of molybdenum or Armco iron capsules to allow higher temperatures during isostatic hot pressing is under study. Preliminary experiments in melting and casting under a nitrogen atmosphere indicate that it is necessary to heat the uranium nitride uniformly and to hold it at or near the melting temperature for a long enough time to achieve equilibrium with the nitrogen atmosphere.

Thorium sulfide was found to sinter readily to yield strong, fine-grained bodies having densities of about 98 per cent of the theoretical density when sintered in a vacuum[22] at 2000 to 2400°C. (M. J. Snyder)

Dispersion Fuels

The construction of a low-power research reactor is under consideration by Junta de Energía Nuclear (JEN)[62] in Spain. A plate type fuel element with 20 g of U^{235} per plate will be

incorporated as 20 per cent enriched uranium in the form of U_3O_8. Aluminum or aluminum-base alloy will be used as cladding and matrix material. Also, the possibility of fabrication of single plates with varying amounts of U^{235} will be considered. The plates are similar to those used in the American Argonaut reactors, except for the fact that the fuel plates are completely clad.

Depleted-uranium-bearing Fiberglas has been consolidated[63] into compacts by either hot pressing or cold pressing followed by hot pressing. Densities attained by these methods averaged 99 per cent of the theoretical density. Fabrication techniques have not been successful to date for producing dummy fuel plates to specifications from the uranium-bearing Fiberglas. This may be due to the high glass content of this material (i.e., 54.3 vol.%) as compared to a 40 vol.% glass in the Fiberglas drawn from uranium-free glass.

The fiber orientation has little effect on the tensile properties of fabricated material. The as-hot-pressed, Fiberglas-reinforced aluminum has an average tensile strength of 18,450 psi in the temperature range from 250 to 800°F. The tensile strength of the fabricated material decreases at elevated temperatures, but it is far superior to 1100 aluminum (the matrix metal in the composites). The Fiberglas-reinforced aluminum has tensile strengths up to 20, 700, 14,600, and 11,850 psi at temperatures of 72, 400, and 600°F, respectively. At the same temperatures, cold-worked 1100 aluminum has tensile strengths of 18,000, 9500, and 2500 psi, respectively.

Since yttrium and uranium are completely immiscible in both the solid and liquid states, a series of dispersions of the two metals was prepared[64] by powder-metallurgy techniques. Powder mixtures containing up to 85 wt.% uranium in yttrium were pressed at 50 tsi and sintered at 1100°C in vacuum to 100 per cent density. The dispersions showed no dimensional changes after 50 hr at 1000°C and no reaction with sodium after 300 hr at 650°C. Hot-hardness and tensile tests proved the dispersions to have reasonable mechanical strength up to 600°C. A series of dispersions has been prepared for irradiation testing.

Scheinhartz[65] has reported investigations of the use of uranium carbide and uranium sulfide as dispersants in matrices of molybdenum, niobium, niobium-titanium alloy, vanadium, zirconium, and aluminum for matrix type fuel elements. At the fabrication temperature of 1200°C, uranium carbide reacted with all the matrix materials under investigation, whereas uranium sulfide appeared to be a promising dispersant material. Zircaloy-2 prepared by powder metallurgy was compared with conventionally prepared Zircaloy-2, but due to improper equipment the tests did not produce any positive conclusions.

Highly enriched UO_2–stainless steel cermet is planned for the first loading of Pathfinder,[66] and a detailed study of available data on its irradiation stability is being made. This information will be used to establish the design parameters for the high-enrichment fuel elements.

Instrumented fuel plates of the blocked-channel design incorporating SM-1 reactor fuel plates have been fabricated at Battelle.[16,20,61] The plates contain a Zircaloy filler, clad with niobium to prevent reaction with the stainless steel during the bonding treatment.

Six capsules containing SM-2 reactor reference and alternate fuel specimens are being irradiated in the Engineering Test Reactor (ETR). It is planned to irradiate the specimens to a burnup of 70 per cent of the contained U^{235}. Work has been concluded on the material-development and the fuel-element thermodynamics studies.

Also at Battelle,[21] cermet fuels consisting of 80 vol.% UO_2 combined with 20 vol.% chromium, molybdenum, and niobium have been selected for irradiation testing. The conditions of testing will be designed for obtaining a central-core temperature approximately 0.7 of the melting temperature of the matrix metals. Irradiations in the ETR are planned and are expected to begin in late spring. Hastelloy X and type 430 stainless steel are being investigated as cladding materials. Gas-pressure bonding is being used as the fabrication technique for producing and cladding cermets for irradiation.

Sintering and gas-pressure-bonding techniques are being investigated as methods of producing UN cermets containing a minimum fuel loading of 60 vol.% UN. Compatibility tests of UN with iron, molybdenum, tantalum, titanium, tungsten, and zirconium are reported. The UN

appears to be more refractory than UO_2 or UC, and consequently it is more difficult to densify.
(D. L. Keller)

Mechanism of Corrosion of Fuel Alloys

Uranium Fuel Elements

The mechanism of corrosion of zirconium-clad uranium fuel elements in high-temperature water has been described in a paper from Hanford, which was presented at the 1960 AEC Corrosion Symposium in Boston.[67] It was found that large areas of exposed uranium oxidized uniformly at a constant rate of 2 mils/min at 300°C and at a rate of 0.1 mil/min at 200°C. However, at the lower temperature the uranium was hydrided from hydrogen released during corrosion. The uranium hydride, in turn, was oxidized to UO_2 with more hydrogen being released. The hydride reaction occurred along carbide stringers in the uranium. This caused severe distortion, which increased the exposed area and accelerated the corrosion attack. The accelerating effect of the hydride penetration was believed to be responsible for the frequent anomaly where more total corrosion occurred at 200°C than at 300°C.

Attack at small (intentional) defects through the cladding resulted in blister formation that was attributed to hydride penetration into the core-cladding bond. Blisters beneath a thin zirconium cladding ruptured readily and thus prevented extensive hydride penetration into the bond. Blisters associated with thick cladding did not rupture as soon because of their increased mechanical strength. However, total corrosion was greater with thick cladding because of extensive hydriding at the core-cladding bond.

The hydriding mechanism proposed for the corrosion of zirconium-clad uranium fuel elements in high-temperature water is somewhat similar to that generally accepted for the corrosion of aluminum-clad uranium elements in boiling water. In the latter, uranium hydride blisters frequently form at some distance from the defect in the cladding. These blisters may rupture, and the hydride is then oxidized. Apparently the hydrogen, produced during corrosion at the defect, diffuses through voids or rolling seams in the uranium. Hydriding occurs at an area of bare uranium which is free of oxide film.

Uranium

The various mechanisms proposed for the aqueous corrosion of uranium are critically reviewed in a paper presented[68] at the AEC-Euratom Conference on Aqueous Corrosion of Reactor Materials held in Brussels, Belgium, in October 1959. Particular attention is given to the role of hydrogen and to lattice mismatch between the oxide film and the underlying uranium metal surface.

Recent work at Argonne has shown that an aggregate or array of pieces of uranium ignites at a considerably lower oxygen temperature than an individual piece.[15] This phenomenon apparently is the result of self-heating and is attributed to the condition of decreased heat loss from an interior piece which is completely surrounded by other pieces which also are generating heat.

Uranium Oxide

The kinetics and mechanism of oxidation of UO_2 sintered pellets containing from 0 to 5 wt.% fission-product oxides (fissia) have been studied at Atomics International.[69] Experiments were conducted at oxygen pressures ranging from 3 to 800 mm Hg and temperatures ranging from 0 to 450°C.

The proposed steps, in the mechanism for the oxidation of UO_2 to U_3O_8, are as follows:

1. Oxygen is chemisorbed on the UO_2 surface, followed by adsorption of oxygen on the chemisorbed layer.
2. Simultaneously with the above step, oxygen diffuses into the UO_2 lattice until a sufficient amount is present to form a thin layer of U_3O_7 or U_4O_9. The oxidation is controlled by oxygen diffusion through this thin layer.
3. Later, sufficient oxygen is absorbed at grain boundaries to result in the formation of U_3O_8 in these areas. This causes the surface layer to spall.
4. New surfaces are exposed, and eventually the UO_2 pellet is pulverized by this process.
5. The entire powder is then converted to U_3O_8 by oxidation.

Activation energies and diffusion coefficients were determined for the various steps involved. The effect of fissia in the UO_2 was to lower the

activation energy of the diffusion and adsorption processes. (W. E. Berry)

Basic Studies of Irradiation Effects in Fuel Materials

Metallic Fuels

The research that is reviewed here is concerned with mechanisms of irradiation-induced swelling in uranium and uranium alloys and of irradiation-induced anisotropic growth in uranium.

At Harwell[70] a study has been made of phenomena thought to contribute to swelling in alpha uranium irradiated up to about 0.5 at.% burnup at 450 to 650°C. An array of small bubbles has been observed in all specimens. These bubbles, 0.1 μ in diameter and spaced about 1 μ apart, presumably contain most of the fission gas. In about one in three of the specimens, grain-boundary cracks contribute about 1 per cent of the volume increase and are probably due to a combination of irradiation embrittlement and internal stressing caused by thermal cycling. In specimens irradiated at 450 to 500°C, ragged holes at the grain boundaries are thought to be partly due to irradiation growth. In only three specimens, holes up to 2 mm in diameter were formed, accompanied by distortion of the specimen and large local volume increases. This may have been due to severe overheating caused by film boiling in sodium. Acceleration of swelling leading to breakaway due to joinup of the small gas bubbles is not expected below 1.5 per cent burnup in alpha uranium, provided that the gas bubbles are always on the fine scale observed so far, but breakaway swelling at 0.5 per cent burnup could be caused by internal cracks collecting sufficient fission-product gas to blow up into round bubbles.

The mechanism of nucleation and growth of fission-gas bubbles in alpha uranium and the role of surface tension in controlling bubble size are discussed at length.[70] The arguments for the following are presented: homogeneous nucleation on dislocation lines, heterogeneous nucleation, growth of fission-product gas bubbles by vacancy diffusion, and growth by plastic deformation of the matrix. The possible effects of bombarding bubble nuclei and bubbles by fission fragments are also discussed.

The results reviewed[70] cover (1) irradiation of uranium from room temperature to 350°C and subsequent heating at 500 to 650°C and (2) investigations of gas diffusion and precipitation.

Dimensional and density changes and optical and electron microscope observations are reported from Harwell[71] on irradiated cubic uranium alloys that are not subjected to severe internal stresses of the type occurring in alpha uranium on thermal cycling or irradiation growth.

These cubic materials showed little change of shape on irradiation even up to volume changes of 100 per cent. No irradiation-induced cracks were found. Swelling was due to bubbles which were nearly spherical, except when they were large enough to link together. Average bubble sizes ranged from small fractions of a micron in specimens with small volume increases up to a few hundred microns in specimens with 100 per cent volume increase, but generally adequate vacancies were supplied for bubbles to grow at such a rate that surface tension was the major restraining force.

For a given burnup and irradiation temperature, volume increases were largely determined by bubble spacing, indicating the importance of the scale of bubble nucleation. Nucleation was not closely related to microstructural features, but some nonuniform bubble distributions were apparently related to heterogeneity of composition in some alloys.

The behavior of helium injected by alpha-particle irradiation and of krypton injected by glow discharge into various uranium alloys has been studied at Nuclear Metals.[72] Helium-gas bubbles were observed in the cyclotron-irradiated samples following various heat-treatments between 475 and 1075°C. The majority of the bubbles in any sample, regardless of heat-treatment, were between 0.05 and 2 μ in diameter (10^{10} to 10^{14}/cm^3) and accounted for up to 10 per cent porosity. Postirradiation heat-treatments above 900°C gave rise to the formation of about 10^5 bubbles/cm^3 between 10 and 150 μ in diameter, accounting for porosities up to several hundred per cent.

The effects of recrystallization and of phase transformation on the behavior of the helium bubbles were observed. Also, the nucleation and growth characteristics of small and large bubbles are discussed.

Uranium-base metallic reactor fuels show good resistance to swelling if the gas-bubble

concentration remains as high as $10^{13}/cm^3$. Working on the hypothesis that the particles of a second precipitate can act as bubble-nucleation sites, finely dispersed phases have been produced in uranium-molybdenum alloys with ternary additions of tin and silicon by suitable heat-treating. Particles as small as 0.2 μ, having densities as high as $10^{13}/cm^3$ and showing good thermal stability at 670°C, have been produced in certain alloys at Atomics International.[73] These alloys have not yet been irradiated.

The number of lattice defects formed in uranium by neutron irradiation have been studied in France.[74] A rapid saturation of defects can be demonstrated by electrical-conductivity measurements. Separation of the production and diminution effects associated with fission spikes causing these electrical changes resulted in an estimated fission-spike volume of 2.10×10^{-16} $cm^3 \pm 0.20 \times 10^{-16}$ cm^3.

An X-ray method of predicting the stability of natural uranium at low burnup has been sought at Savannah River,[75] and a generalized growth index based on X-ray-diffraction data has been formulated which eliminates effects due to asymmetry in the set of planes used. This effect is referred to as "formalistic" to distinguish it from other deleterious effects such as those which result from the use of too few diffraction planes or poor experimental measurements.

Another formalistic effect results from the normalization of growth index in which the planes used for the calculation of $\Sigma TC_{hkl} \cos^2 B_{hkl}$ were not all the same as those used to calculate $\Sigma TC_{hkl} \cos^2 \alpha_{hkl}$. This normalization was used to obtain a growth index of zero for random orientation and to obtain equal numbers of diffraction planes for evaluating the calculation of these quantities. (F. A. Rough)

Fundamental Studies of Irradiation Effects in UO_2

In studies[76] on thin films of UO_2, observations of fission-fragment tracks by electron microscopy can be made with 100 per cent efficiency if the films are less than 100 A thick. Only when the fragment kinetic energy is dissipated at greater than 1000 ev/A does the track become visible. Tracks of length less than 1 μ occur more frequently than expected, but tracks of length greater than 1 μ occur less frequently than expected from geometric considerations. The upper limit on track length is about 4 μ. Occasional forked tracks, suggesting direct fragment-lattice atom collision, are reported. Another beginning effort[48] is aimed at detecting fission-fragment tracks in aluminum foils.

A change in the fracture mode of sintered UO_2 from transgranular to intergranular has not been definitely explained but might be associated with formation of grain-boundary microporosity or cumulative fission-spike stresses.[77] Free surfaces suffer from microdistortion, but there is no major microstructural change. Increasing irradiation results in progressive lowering of the UO_2 melting point from 2790°C ± 15°C in unirradiated UO_2 to 2760°C ± 20°C after 8.4 at.% burnup and 2660°C ± 20°C after 11.25 at.% burnup.[48]

Several programs of study of fission-gas release from UO_2 under in-pile and postirradiation conditions are in progress. Gas-release rates have been determined[16,20] for sintered and for fused single crystalline UO_2. In the temperature range 1205 to 1400°C, xenon postirradiation diffusion coefficients in single-crystal UO_2 were 6.15×10^{-18} cm^2/sec to 2.14×10^{-17} cm^2/sec. In-pile gas release from similar material was not diffusion controlled in the temperature range 260 to 816°C. During postirradiation heating of sintered UO_2 (79 to 97 per cent theoretical density), xenon was released with diffusion constants $D' = D/a^2$ of between 10^{-15}/sec and 10^{-18}/sec for the temperature range 1200 to 1550°C, where a is the radius of a sphere having the surface-to-volume ratio of the sintered specimen. Similar experiments at another laboratory* resulted in values of D' of 1.72×10^{-11}/sec to 3.59×10^{-11}/sec at 1400°C for UO_2 of 90 to 93 per cent theoretical density. Data obtained between 1000 and 1500°C for single-crystal UO_2 (powdered fused material) reveal a sharp increase in activation energy for xenon diffusion at 1300°C. However, after a preirradiation hydrogen anneal at 1650°C, the D versus $1/T$ relation was linear between 1000 and 1500°C, with a single-valued activation energy of 123 kcal/mole.

Enhanced gas release rates at the early stages of postirradiation heating are considered to result from a high oxygen-to-uranium ratio

*W. H. Stevens, Atomic Energy of Canada, Ltd., 1960. (Unpublished)

at the surface. This effect is reduced by pre-irradiation annealing at 1500°C in hydrogen, but diffusion of oxygen into the UO_2 during the hydrogen heat-treatment results in generally higher xenon diffusion rates than were observed in UO_2 that was free of excess oxygen. Experiments at Oak Ridge[76] reveal a dependence of gas release rates on density, stoichiometry, and temperature in the temperature range 1700 to 3150°F. Nonstoichiometric UO_2 (oxygen-to-uranium ratio >2.1) released from 25 to 40 per cent of fission gases above 2800°F. Stoichiometric UO_2 (oxygen-to-uranium ratio <2.1) released up to 25 per cent of fission gases at 3100°F.

(F. A. Rough and J. B. Melehan)

References

1. E. S. Fisher, The Adiabatic Elastic Moduli of Single-Crystal Alpha Uranium at 25°C, USAEC Report ANL-6096, Argonne National Laboratory, June 1960.
2. H. E. Flotow and H. R. Lohr, The Heat Capacity and Thermodynamic Functions of Uranium from 5 to 350°K, *J. Phys. Chem.*, 64: 904–906(July 1960).
3. J. J. Stoto, Alpha-Beta Cycling of Uranium, *J. Nuclear Materials*, 2: 97–109(June 1960).
4. J. H. Monaweck and E. S. Sowa, Summary Report on Irradiation of Prototype EBR-II Fuel Elements, USAEC Report ANL-6010, September 1960.
5. H. Steinkopff and F. Thümmler, Uranium-Silicon Alloys and Compounds, German Report ZFK-WF-1, September 1959.
6. M. S. Silliman et al., Irradiation Testing of Enrico Fermi Prototype Fuel Pins in the CP-5, USAEC Report APDA-130, Atomic Power Development Associates, April 1960.
7. J. J. Bodzin, Thermal Cycling Experiments on Blanket Elements and Fuel Pins To Determine the Effect of Cycling in the Alpha-Plus-Epsilon Phase on Physical Size and Microstructure, Report NP-9131, Detroit Edison Co., Mar. 21, 1960.
8. J. J. Bodzin, Thermal Cycling Experiments on Fuel and Blanket Elements To Determine the Effect of Phase Transformation on Physical Size and Microstructure, Report NP-9130, Detroit Edison Co., Mar. 14, 1960.
9. B. Minushkin, Thermal Cycling Tests on U–10 Wt.% Mo for the ORNL Fast Burst Reactor, USAEC Report NDA-Memo-2136-2, Nuclear Development Corp. of America, July 30, 1960.
10. J. Gioseffi, Oxidation Rates of U–10 Wt.% Mo in Air, USAEC Report NAA-SR-Memo-4845, Atomics International, Jan. 6, 1960.
11. P. C. L. Pfeil, Improvements in or Relating to Alloys of Uranium, British Patent 836,692, June 9, 1960.
12. G. Donze and G. Cabane, Mechanism of Gamma-Phase Decomposition in Uranium-Molybdenum and Uranium-Molybdenum-Ruthenium Alloys, *Mém. sci. rev. mét.*, 57: 450–458 (June 1960).
13. Oak Ridge National Laboratory, Metallurgy Division Annual Progress Report for Period Ending July 1, 1960, USAEC Report ORNL-2988, Sept. 30, 1960.
14. Argonne National Laboratory, Reactor Development Program Progress Report, October 1960, USAEC Report ANL-6253, Nov. 15, 1960.
15. Argonne National Laboratory, Reactor Development Program Progress Report, August 1960, USAEC Report ANL-6215, Sept. 16, 1960.
16. R. W. Dayton and C. R. Tipton, Jr., Progress Relating to Civilian Applications During November 1960, USAEC Report BMI-1480, Battelle Memorial Institute, Dec. 1, 1960.
17. D. T. Pitman and D. K. Das, A Study of the Thorium-Tungsten-Boron System, *J. Electrochem. Soc.*, 107: 763–766 (September 1960).
18. D. S. Evans and G. V. Raynor, Lattice Spacings in Thorium-Yttrium Alloys, *J. Nuclear Materials*, 2(3): 209–215 (September 1960).
19. D. T. Eash and O. N. Carlson, Investigation of the Thorium-Yttrium System, *Trans. Am. Soc. Metals*, 52: 1097–1114 (1960).
20. R. W. Dayton and C. R. Tipton, Jr., Progress Relating to Civilian Applications During October 1960, USAEC Report BMI-1473, Battelle Memorial Institute, Nov. 1, 1960.
21. R. W. Dayton and C. R. Tipton, Jr., Progress Relating to Civilian Applications During December 1960, USAEC Report BMI-1489(Rev.), Battelle Memorial Institute, Jan. 1, 1961.
22. Argonne National Laboratory, Reactor Development Program Progress Report, September 1960, USAEC Report ANL-6234, Oct. 14, 1960.
23. A. M. Ross, The Dependence of the Thermal Conductivity of Uranium Dioxide on Density, Microstructure, Stoichiometry, and Thermal Neutron Irradiation, Canadian Report CRFD-817(AECL-1096), September 1960.
24. R. W. Dayton and C. R. Tipton, Jr., Progress Relating to Civilian Applications During June 1960, USAEC Report BMI-1448(Rev.), Battelle Memorial Institute, July 1, 1960.
25. R. W. Dayton and C. R. Tipton, Jr., Progress Relating to Civilian Applications During July 1960, USAEC Report BMI-1455, Battelle Memorial Institute, Aug. 1, 1960.
26. R. W. Dayton and C. R. Tipton, Jr., Progress Relating to Civilian Applications During August 1960, USAEC Report BMI-1464, Battelle Memorial Institute, Sept. 1, 1960.
27. I. Cohen et al., Measurement of the Thermal Conductivity of Metal-Clad Uranium Oxide Rods During Irradiation, USAEC Report WAPD-228,

Westinghouse Electric Corp., Bettis Atomic Power Laboratory, August 1960.

28. W. E. Bost, Irradiation Testing of UO_2: A Literature Search, USAEC Report TID-3559, November 1960.
29. J. A. L. Robertson, Concerning the Effects of Excess Oxygen in UO_2, Canadian Report CRFD-973(AECL-1123), October 1960.
30. Westinghouse Electric Corp., Bettis Atomic Power Laboratory, Technical Progress Report, Pressurized Water Reactor (PWR) Project for the Period June 24, 1960, to August 23, 1960, USAEC Report WAPD-MRP-87.
31. F. W. Albaugh, Reactor and Fuels Research and Development Operation Monthly Report for August 1960, USAEC Report HW-66644-A, Hanford Atomic Products Operation, Sept. 15, 1960. (Classified)
32. B. R. Harder and R. G. Sowden, The Oxidation of Uranium Dioxide by Water Vapour Under Reactor Irradiation, British Report AERE-M-725, August 1960.
33. J. J. Byerley, The Compatibility of UO_2 with the Refractory Metals and Refractory Metal Thermocouples at Temperatures Above 1750°C, Canadian Report CRFD-971(AECL-1126), October 1960.
34. W. B. Wilson and A. F. Gerds, Stabilizing Effects of Oxide Additions to Uranium Dioxide, USAEC Report BMI-1467, Battelle Memorial Institute, Sept. 13, 1960.
35. L. H. McEwen, comp., Unclassified Research and Development Programs Executed for the Division of Reactor Development and the Division of Research, October 1959, USAEC Report HW-62759, Nov. 10, 1959.
36. N. C. Orrick and K. E. Rapp, Compound Formation Between Uranium and Yttrium Oxides, USAEC Report TID-6571, Oak Ridge Gaseous Diffusion Plant, Apr. 1, 1959.
37. Westinghouse Electric Corp., Bettis Atomic Power Laboratory, Technical Progress Report, Pressurized Water Reactor (PWR) Project for the Period August 24, 1960, to October 23, 1960, USAEC Report WAPD-MRP-88.
38. Combustion Engineering, Inc., The Development and Testing of Homogeneous Ceramic Fuels, USAEC Report NYO-2992(CEND-98), September 1960.
39. Westinghouse Electric Corp., Bettis Atomic Power Laboratory, Bettis Technical Review, Reactor Technology, USAEC Report WAPD-BT-20, September 1960.
40. General Atomic Div., General Dynamics Corp., Maritime Gas-Cooled Reactor Program, Quarterly Progress Report for the Period Ending December 31, 1959, USAEC Report GA-1195.
41. S. W. Pijanowski and L. S. DeLuca, Melting Points in the System PuO_2-UO_2, USAEC Report KAPL-1957, Knolls Atomic Power Laboratory, Apr. 15, 1960.
42. Argonne National Laboratory, Metallurgy Division Annual Report for 1959, USAEC Report ANL-6099.
43. C. D. Wirkus and D. R. Wilder, Uranium Glasses: II. Uranium Silicate Glasses, USAEC Report IS-158, Ames Laboratory, Sept. 16, 1960.
44. Olin Mathieson Chemical Corp., Nuclear Fuel Research Fuel Cycle Development Program, Quarterly Progress Report, July 1 to September 30, 1960, USAEC Report NYO-2690, Nov. 11, 1960.
45. D. R. Stenquist and R. J. Anicetti, Fabrication Behavior of Some Uranium Dioxide Powders, USAEC Report HW-51748, Hanford Atomic Products Operation, Dec. 1, 1957.
46. R. W. Dayton and C. R. Tipton, Jr., Progress Relating to Civilian Applications During December 1959, USAEC Report BMI-1403, Battelle Memorial Institute, Jan. 1, 1960.
47. Gladding, McBean & Co., Development of Flat Plate Ceramic Fuel Elements, USAEC Report TID-6569, Mar. 23, 1960.
48. F. W. Albaugh, Reactor and Fuels Research and Development Operation Monthly Report for October 1960, USAEC Report 67254-A, Hanford Atomic Products Operation, Nov. 15, 1960. (Classified)
49. W. L. Lyon and E. E. Voiland, The Preparation of Uranium Dioxide from a Molten Salt Solution of Uranyl Chloride, USAEC Report HW-62431, Hanford Atomic Products Operation, Oct. 20, 1959.
50. F. W. Albaugh, Reactor and Fuels Research and Development Operation Monthly Report for September 1960, USAEC Report HW-66960-A, Hanford Atomic Products Operation, Oct. 15, 1960. (Classified)
51. Hanford Atomic Products Operation, Reactor and Fuels Research and Development Operation Monthly Report for November 1960, USAEC Report HW-67532-A, Dec. 15, 1960. (Classified)
52. F. A. Rough and W. Chubb, eds., Progress on the Development of Uranium Carbide Type Fuels, USAEC Report BMI-1488, Battelle Memorial Institute, Dec. 27, 1960.
53. V. Cirilli and C. Brisi, Solid State Equilibrium in the Uranium-Aluminum-Carbon System, *Atti accad. sci. Torino, Classe sci. fis. mat. e nat.*, 94: 424–431 (1959–1960).
54. E. L. Gardner and S. G. Barnes, Transient Heating of UC Fuel Elements in the KEWB Facility, USAEC Report NAA-SR-Memo-4333, Atomics International, Sept. 1, 1960.
55. M. A. Bredig, The High-Temperature Cubic Phases of Uranium and Lanthanum Dicarbide, *J. Am. Ceram. Soc.*, 43: 498 (September 1960).
56. E. D. Cater, The Vaporization, Thermodynamics, and Phase Behavior of Uranium Monosulfide, USAEC Report ANL-6140, Argonne National Laboratory, March 1960.

57. K. M. Taylor, Synthesis and Fabrication of Refractory Uranium Compounds, USAEC Report ORO-331, Carborundum Co., Oct. 13, 1960.
58. W. P. Blankenship et al., Thermoelectric Nuclear Fuel Element, Quarterly Progress Report for January–March 1960, USAEC Report WCAP-1545, Westinghouse Electric Corp., Atomic Power Dept., Apr. 10, 1960.
59. N. D. Morgulio and Y. P. Korchevoi, Thermionic Conversion of Heat Energy into Electrical Energy Using Thorium Carbide, *At. Energ.*, 9: 49–51 (1960).
60. Argonne National Laboratory, Reactor Development Program Progress Report, November 1960, USAEC Report ANL-6269, Dec. 15, 1960.
61. R. W. Dayton and C. R. Tipton, Jr., Progress Relating to Civilian Applications During September 1960, USAEC Report BMI-1469, Battelle Memorial Institute, Oct. 1, 1960.
62. J. Redondo et al., A Dispersion Type Fuel Element for Low Power Research Reactors, Spanish Report NP-9353, October 1959.
63. R. H. Baskey, Fuel-Bearing Fiberglas in Aluminum Base Fuel Elements, USAEC Report ORO-300, Clevite Corp., June 2, 1960.
64. I. Sheinhartz and J. L. Zambrow, Yttrium-Uranium Alloys for High Temperature Fuel Elements, *Trans. Am. Nuclear Soc.*, Session 22, Paper 3, p.444 (Dec. 12–15, 1960).
65. I. Scheinhartz, Dispersion Type Materials for Fuel Elements. Part II. Uranium Carbide and Uranium Sulfide Dispersion Materials, USAEC Report SCNC-273, Sylvania-Corning Nuclear Corp., March 1959.
66. Allis-Chalmers Mfg. Co., Pathfinder Atomic Power Plant Technical Progress Report for January 1960–March 1960, USAEC Report ACNP-6006, June 15, 1960.
67. J. P. Pemsler, Proceedings of the Ninth Annual AEC Corrosion Symposium, May 10–12, 1960, USAEC Report NMI-1220, Nuclear Metals, Inc., July 18, 1960.
68. J. T. Waber, Aqueous Corrosion of Uranium and Its Alloys, in AEC-Euratom Conference on Aqueous Corrosion of Reactor Materials, USAEC Report TID-7587, p.307, July 1960.
69. T. Smith, Kinetics and Mechanism of the Oxidation of Uranium Dioxide and Uranium Dioxide Plus Fissia Sintered Pellets, USAEC Report NAA-SR-4677, Atomics International, Nov. 1, 1960.
70. S. F. Pugh, Swelling in Alpha Uranium Due to Irradiation, British Report AERE-R-3458, August 1960. (To be published in *J. Nuclear Materials.*)
71. G. W. Greenwood, The Effects of Neutron Irradiation of Gamma Uranium and Some Fissile Alloys of Cubic Crystal Structure, British Report AERE-R-3468, September 1960. (To be published in *J. Nuclear Materials.*)
72. A. Boltax et al., A Metallographic Study of the Swelling of Uranium and Uranium Alloys, USAEC Report NMI-1239, Nuclear Metals, Inc., 1960.
73. D. Kramer, Finely Dispersed Phases in Uranium-Molybdenum Ternary Alloys, USAEC Report NAA-SR-5507, Atomics International, Nov. 1, 1960.
74. Y. Quere and F. Nakache, Evaluation du Volume d'Une Pointe de Fission dans l'Uranium (in French), *J. Nuclear Materials*, 2: 203–209(1960); also, Estimation of the Volume of a Fission Spike in Uranium, French Report CEA-1304, 1959.
75. E. F. Sturcken, A Generalized Growth Index Formalism, in USAEC Report NLCO-804, p.9, National Lead Co. of Ohio, July 15, 1960.
76. F. Ward, ed., Solid State Division Annual Progress Report for Period Ending Aug. 31, 1960, USAEC Report ORNL-3017, Oak Ridge National Laboratory, Dec. 6, 1960.
77. H. W. Newkirk et al., Electron Microscope Studies of Damage in Irradiated Uranium Dioxide, *J. Nuclear Materials*, 2(3): 269–293 (September 1960).

Section II

MODERATOR MATERIALS

Graphite

Hawker Siddeley Nuclear Power Company, Ltd. (Great Britain), has produced impermeable graphite by furfural alcohol impregnation.[1] The graphite is impregnated under pressure and then heated to 1000°C to polymerize and carbonize the trapped furfural alcohol. The impregnated bodies are graphitized at temperatures up to 3000°C in a nitrogen atmosphere to prevent impurity pickup. In fine-grained graphite, gas permeabilities as low as 10^{-6} cm^3/sec under a pressure differential of 1 atm were obtained. A vacuum of less than 10 μ could be held by graphite tubes for several hours at 1800°C in a nitrogen atmosphere. Properties of treated and untreated graphites are compared in Table II-1.

Table II-1 PROPERTIES OF GRAPHITE PROCESSED BY HAWKER SIDDELEY[1]

	Untreated	HSNP treated
Flexural strength, psi	3600	5700
Elastic modulus, 10^6 psi	1.8	3.0
Electrical resistivity, milliohm-cm	1.9	1.5
Thermal expansion, 10^{-6}/°C:		
At 300°C	2.0	2.1
At 600°C	2.2	2.7
At 900°C	2.6	3.0
Ultimate tensile strength, psi	3200	5900

In a study to develop improved graphite bodies, workers at Armour Research found that furfural alcohol has several advantages over pitch for use as a binder.[2] These include:

1. Only about half as much furfural alcohol is required as pitch for the same green density. Since less binder is required, the weight loss in carbonization is reduced and a higher carbonized density results.

2. Since the binder is thermosetting, there should be no distortion due to plastic flow during carbonization.

3. Although thermosetting binders are usually difficult to graphitize, this is not the case for furfural alcohol.

4. Shrinkage during graphitization is sufficient to compensate for the loss of volatiles on carbonizing, resulting in a graphitized density about as high as that of a green body.

5. Since the binder is a synthetic, it can be closely reproduced with a high degree of purity.

6. Since furfural alcohol is a liquid at room temperature, the batch can be mixed cold in a variety of mixing equipment.

The British have studied the reaction of graphite with oxygen.[3] The depth of oxidation, L, is given theoretically by $L = (Z/k_v)^{0.5}$, where Z is the effective diffusion coefficient of oxygen through the gas in the pores of the graphite and k_v is the rate constant expressed in terms of the volume consumed. If L is much smaller than the thickness of a graphite block, the rate of oxidation at a distance x from the surface is proportional to exp $(-x/L)$. Similar results apply approximately to the reaction of CO_2 with graphite.

The rate of reaction between UO_2 and graphite is being investigated as a function of temperature, UO_2 particle size, and CO pressure at Oak Ridge.[4] Data obtained for the reaction between −60 +80-mesh (250 to 175 μ) UO_2 and graphite at CO pressures of 10^{-3} and 10^{-4} mm Hg were fitted to the equation $X = kt^{0.5}$, where X is the fraction of UO_2 converted to carbide, k is the temperature-dependent rate constant, and t is the time, in hours, at temperature. The values of k obtained were 0.18, 0.33, and 0.44 at 1275, 1325, and 1375°C, respectively. These results, when compared with results[5] for −325-mesh

(<44 μ) UO_2, indicate that the reaction rate is sensitive to particle size below 1325°C and relatively insensitive above this temperature.

An evaluation of candidate graphites for the New Production Reactor (NPR) was completed.[6] The aim of this program was to find the graphite which was most resistant to radiation-induced dimensional changes above an exposure temperature of 500°C. Some of the findings are listed below:

1. Graphites made from needle cokes contract less than does graphite from any other type of coke.
2. Graphites fabricated from coke ground to what the industry terms a "50 flour" particle size (45 to 55 wt.% passes through a 200-mesh screen) contract less than those fabricated using a coarser coke particle size.
3. Graphites that have not been pitch impregnated contract less than those which have been impregnated.
4. Graphites that have been graphitized at 3000°C or above contract less than those graphitized at lower temperatures.

On the basis of this work, the best graphite moderator for high-temperature applications would be fabricated from a fine-grained needle coke that is graphitized at 3000°C or above without a pitch impregnation. (J. Koretzky)

Beryllium Metal and Alloys

Nuclear Metals was awarded a major contract[7] on beryllium research for the Air Force. Twelve projects were set up in three major categories: purification, joining, and flow and fracture. The objectives are to increase the usability of beryllium by improved processing and understanding of the technology and by improvement of the metal by various means. About 60 per cent of the effort has been subcontracted to seven firms.

Beryllium Casting and Alloy Development

The most promising alloys encountered to date in an Armour study[8,9] of the liquid-phase sintering approach to produce ductile beryllium alloys are found in the beryllium-aluminum-silver-germanium system. These alloys are very tough and can withstand considerable amounts of cold deformation.

Alloying additions of lanthanum were reported[10] to give increasing columnar grain refinement to the structure of cast beryllium with increasing alloy additions. Zirconium as an alloying grain refiner has an optimum concentration of 0.40 to 0.60 wt.% for maximum columnar grain refinement. In studies of cold reduction of the cast structure, a trend has been observed for an optimum percentage cold reduction for a given heat-treatment for maximum grain refinement.

At the conclusion of a two-year effort[11] under joint AEC and Air Force sponsorship to develop wrought beryllium alloys of improved properties, it was reported that no metallic alloying addition to beryllium was found that resulted in improved properties for elevated-temperature applications. New data were reported on the strength properties of beryllium with higher than normal BeO content in the hot-extruded and hot-extruded, cross-rolled forms over an extended temperature range.

Fabrication of Beryllium

The growing importance of beryllium fabrication is accented by the announcement[12] of Brush Beryllium that they will build a $3,000,000 plant in Cleveland to expand by 50 per cent their capacity to finish, fabricate, and machine beryllium. This importance was further emphasized by the announcement of a $300,000 research and development contract from the Air Force to the Beryllium Corporation to study the development needed for the roll forming of channels, angles, zees, tees, rounds, and squares. Subcontractors are Allegheny Ludlum, The Budd Company, and Nuclear Metals. Final objective of the program is the production of a quantity of these shapes at least 60 in. long. The Beryllium Corporation recently completed a joint program with Wyman-Gordon on the development of closed-die forging techniques in cooperation with the Massachusetts Institute of Technology. Small parts successfully forged from their unclad beryllium planks showed greatly improved properties.

A current article[13] gives data for machining, forming, and joining beryllium and for inspection techniques. Extremely high-tolerance parts that would be impossible to machine from titanium or aluminum can be machined from beryllium. Precision tolerances include: wall thicknesses of 4 mils, drilled holes 2 mils deep and

30 in. deep (with $^3/_{16}$-in. diameters), and spheres with sphericity tolerances of up to 2 millionths of an inch with complex internal geometries.

On the Air Force forging program, it was reported that beryllium forged at 1375°F had a tensile strength of 81,700 psi, a yield strength of 50,500 psi, and an elongation of 9.7 per cent at room temperature. This forged material showed a basal-plane alignment in planes parallel to the forging face of six to eight times that of random orientation.[14]

Aeronca's monthly report on the development of beryllium honeycomb[15] notes that mechanical polishing of the edges of beryllium tensile specimens increased the apparent tensile strength about 20,000 psi over that of specimens with machined edges. Application of silver-braze alloys decreased the strength of the beryllium.

Beryllium Tubing. Arrangements have been announced for developing methods of fabricating finned beryllium tubing as follows:

1. The Brush Beryllium Company for warm extrusion and drawing.
2. Nuclear Metals for hot extrusion, including filled billet and ribbed die techniques.
3. Sylcor for isostatic pressing and Dynapack forming.

The Beryllium Corporation is expected to submit a proposal for the direct extrusion of tubing from cast billet.[16]

For the testing and evaluation of the smooth-wall tubing purchased from Tube Investments, Ltd., for the Heavy-Water Power-Reactor Program, negotiations are in progress with Aero Projects, Inc., for development of ultrasonic welding for joining end caps to finned tubes; with Oak Ridge for nondestructively testing tubing; with Combustion Engineering Laboratories for destructive (mechanical and corrosion) testing; and with General Electric Testing Reactor (GETR) for in-pile corrosion testing.[16]

It was reported[17,18] that the lowest degree of preferred orientation is found in tubes extruded by the filled billet method from hot-compacted cores contained within a thick-walled can. Tubes that were extruded from hot-compacted cores by extrusion with a mandrel had a high degree of preferred orientation but also had the highest room-temperature burst strengths. Tubing 0.750 in. in outside diameter by 0.030 in. in wall thickness was produced by extrusion of hot-compacted billets over a mandrel. Extrusion ratios were limited by the equipment available. Tubes that were extruded at lower reduction ratios cracked more severely than those extruded at higher ones.

Beryllium Rolling. Commercial production processes for beryllium and the fabrication and properties of beryllium sheet are discussed in a recent report of the Materials Advisory Board.[19]

Work at the Beryllium Corporation on a Lockheed subcontract[20] has resulted in the production of reasonably fine-grained rolled beryllium strip from cast ingots. Although the properties obtained up to now are inferior to those obtained by powder-metallurgical means, this work represents a significant step toward the utilization of cast beryllium. On another Lockheed subcontract,[21] the feasibility of making beryllium strip by the direct rolling of beryllium powder was demonstrated. The green strip was sufficiently strong to handle through a sintering furnace where it was sintered either in argon or in a vacuum. The finished sheet was only 8 mils thick, which was the minimum the available equipment could produce. The thin strip could be wrapped cold around a pencil without cracking; however, on a tensile test it showed an ultimate tensile strength of 45,000 psi and only 0.2 per cent elongation. The sheet had a random crystallographic structure.

Beryllium Joining. From Oak Ridge it was reported[17] that crack-free joints were obtained on end-sealed closures by inert-arc fusion welding. The crack-free joints were made by utilizing press-fitted end caps of high-purity material. Crack-free joints were made on Brush Beryllium hot-pressed, hot-extruded, and warm-extruded material, on Pechiney hot-extruded tube, and Chesterfield hot-extruded tubing. Only the Brush hot-pressed tubing consistently contained no porosity in the weld. Joint efficiencies were highest in the closures made on Chesterfield tubes, presumably because the plugs fitted more tightly in these tubes. In a British paper[22] on fuel-element end-cap designs, the weld, preheat, and subsequent cooling rates were found to be critical factors in eliminating cracking when using flowing argon as an inert-gas shield. Welding in a static pure-argon atmosphere was found to require less critical control of these factors. The report describes apparatus for experimental tungsten arc–inert gas, autogenous fusion welding of beryllium. Satisfactory welding conditions were obtained for a variety of weld designs of beryllium fab-

ricated from ingot and sintered powder materials. Beryllium oxide in quantities up to 2 per cent is not harmful in beryllium fusion welds, so long as it is contained generally in the grain boundaries. Postheat-treatment of beryllium welds is beneficial; temperatures up to 825°C may be used. A much slower welding speed must be used for both manual and automatic welding of beryllium than is used for other materials.

Production of Beryllium Foil. The Russians described[23] the production of beryllium foil by vacuum deposition of beryllium vapor on a polished molybdenum sheet. Beryllium 99.88 per cent pure was heated in a BeO crucible up to 1300 to 1350°C. The molybdenum sheet was preheated to between 50 and 300°C before vapor deposition. The 20- to 300-μ-thick foil obtained was then vacuum heat-treated at 700 to 900°C for 15 hr. Plasticity of the foil was a function of deposition rate, the temperature of the molybdenum sheet, the heat-treatment, and the cooling rate.

Physical Metallurgy of Beryllium

Phase Diagrams. Bedford[24] determined a new tentative phase diagram for the zirconium-beryllium system. The four compounds are $ZrBe_{13}$, Zr_2Be_{17}, $ZrBe_5$, and $ZrBe_2$. The Russian diagram published in the February 1961 issue of *Reactor Core Materials*, Vol. 4, No. 1, showed $ZrBe_6$ instead of $ZrBe_5$ and $ZrBe_9$ instead of Zr_2Be_{17}. Bedford also determined the tentative diagram for the hafnium-beryllium system and identified the following compounds: $HfBe_{13}$, βHf_2Be_{17}, αHf_2Be_{17}, $HfBe_5$, and $HfBe_2$. The relative stability of the two forms of Hf_2Be_{17} appeared to depend on the composition of the system rather than the temperature. βHf_2Be_{17} is found in equilibrium with $HfBe_{13}$, and αHf_2Be_{17} is found in equilibrium with $HfBe_5$. The most refractory compound in the system, Hf_2Be_{17}, melts at 1860 ± 60°C. In the titanium-beryllium system, the phases identified were $TiBe_{12}$, βTi_2Be_{17}, αTi_2Be_{17}, $TiBe_3$, and $TiBe_2$. The alpha and beta modifications of $TiBe_{17}$ occurred in the same way as the Hf_2Be_{17} phases. The titanium beryllides are less refractory than the zirconium or hafnium compounds.

In work sponsored by the U. S. Atomic Energy Commission[25–28] on an attempt to preserve beryllium's high-temperature body-centered cubic beta phase at lower temperatures, nickel proved to be the most effective alloying addition found to date. Alloys examined include beryllium with cerium, chromium, copper, iron, lanthanum, nickel, niobium, palladium, platinum, silicon, silver, vanadium, zirconium, and the ternary beryllium-nickel-palladium. The addition of 8 at.% nickel lowers the transformation temperature of beta to alpha approximately 200°C. Cobalt has an effect similar to that of nickel in that it raises the melting point and lowers the temperature of the beta-to-alpha transformation. A eutectoid exists at a temperature of approximately 1120°C and a cobalt content of approximately 4.5 at.%. Manganese appears to have little solubility in beryllium and causes little or no stabilization of the beta phase.

The solidus lines for iron, cobalt, and nickel in beryllium have been determined from zero concentration to the eutectoid compositions. The solidus line for copper has been partially determined. The maximum beta stabilization that can be achieved appears to increase with increasing atomic number of the solute. Tentative design of a complex alloy was described in which the beta phase will be stabilized to much lower temperatures than any yet obtained. To date, however, it has not been possible to achieve this result. A proposed beryllium-rich portion of the beryllium-cobalt phase diagram was shown. On another AEC project[29] a preliminary investigation of a large number of binary systems with beryllium was carried out. These included zinc, germanium, manganese, chromium, yttrium, lithium, and cadmium binary systems. Lattice-parameter measurements were made on alloys with up to 2 per cent copper made by powder-metallurgy techniques. It was indicated that the amount of copper in solid solution increased with the copper content after a solution heat-treatment at 1000°C for 2 hr, followed by a water quench. The copper in solid solution increased the yield strength and ultimate tensile strength but had little effect on the ductility.

Structure of Beryllium. The effects of reduction ratio and annealing heat-treatment on the structure and orientation of cold-worked beryllium sheet were studied to determine the relative importance of variables in the rolling process. Fused and ground beryllium oxide in varied amounts was added to beryllium powder and hot extruded. The randomness of orientation was increased by the hard particles, but the embrittling effect associated with the BeO addi-

tions was greater than any ductility increase that might have been realized by the decrease in crystallographic anisotropy.[30,31]

It was determined that $(10\bar{1}2)$ type twinning appears to be one of the most predominant modes of deformation at temperatures as high as 1066°C. The prior texture of beryllium appears to affect the development of preferred orientation, especially at low reduction ratios. To date, the most randomly oriented wrought beryllium produced exhibits a ductility of approximately 1 per cent.[32]

Beryllium undergoes large amounts of accommodation kinking on the $\{11\bar{2}0\}$ planes without cracking. Evidence is presented that beryllium may twin on planes other than $\{10\bar{1}2\}$. A stereographic projection of the angular relations between crystallographic planes was presented by Burke[33a] in a standard orientation.

Work at the Atomic Weapons Research Establishment at Aldermaston, England, indicates the possibility of alloying to improve the ductility of beryllium at temperatures between 500 and 600°C, the temperature range where beryllium is to be used in nuclear reactors of the AGR type. At temperatures above 400°C, intergranular failure becomes the dominant fracture mode in extruded beryllium rods.[34]

Heating extruded beryllium ingot of the QMV type to 780°C for 120 hr, followed by slowly cooling to room temperature over another 120 hr, improved the ductility as shown in Fig. II-1. This was accompanied by some loss of strength (Fig. II-2). The improvement in ductility is ascribed to precipitation of a solid phase(s) which artificially strengthens the grain boundaries. Similar effects were not obtained with pure electrolytic type material.[34]

Extrusion reduction determines which of two main types of texture is developed in tubes. In low-reduction (≤6 : 1) textures, the basal planes tend to concentrate parallel to the surface of the tube; in high-reduction (≥12 : 1) textures, the basal planes still lie parallel to the extrusion direction but tend to concentrate at angles ranging from 50° to 90° to the surface. A prism-plane fibered texture is present in all tubes.[35]

The bend ductility of wrought beryllium sheet was correlated with the preferred orientation and strip width. Narrow strips joined at their edges with a ductile brazing material exhibit improved bend ductility, with retention of strength and stiffness in the longitudinal direction. The maximum effect was obtained by cladding slotted beryllium sheet with titanium, taking care to keep the narrow slots free of brazing material. For narrow samples, bend ductility was highest with a highly preferred basal-plane texture. For wide samples, bend ductility was highest with a semirandom basal-plane texture.

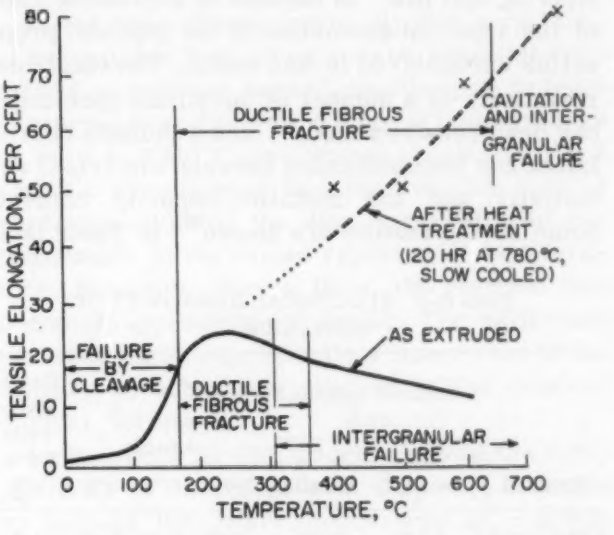

Fig. II-1 Ductility of vacuum-cast pebble beryllium extruded at 1050°C, 44 : 1 reduction.[34]

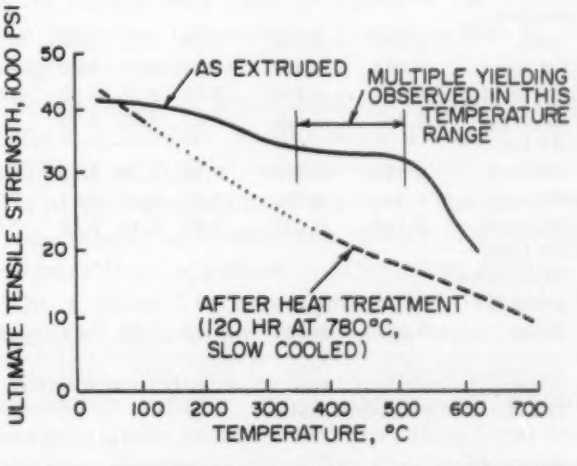
ULTIMATE TENSILE STRENGTH, 1000 PSI
TEMPERATURE, °C
AS EXTRUDED
MULTIPLE YIELDING OBSERVED IN THIS TEMPERATURE RANGE
AFTER HEAT TREATMENT (120 HR AT 780°C, SLOW COOLED)

Fig. II-2 Strength of thermally reduced beryllium, vacuum cast and extruded at 1050°C, 44 : 1 reduction.[34]

In composites formed by cladding, the presence of a cladding did not institute unusual changes in the ductility of the composite; however, the cladding appeared to be significant as a fail-safe and surface-protection medium and is possibly significant for its surface-oxidation protection.[36]

Physical and Mechanical Properties of Beryllium

Physical Properties. An attempt was made[33b] to correlate the structure-insensitive physical properties of beryllium on the basis of the theory of solids. The author concluded that the theoretical model of beryllium proposed by Herring and Hill[37] is capable of explaining most of the apparent anomalies of the physical properties encountered in this metal. The electrical resistivity of a number of beryllium specimens has been redetermined,[33c] and a definite correlation has been indicated between electrical resistivity and the metallic-impurity content. Some of the results are shown[33c] in Table II-2.

Table II-2 ELECTRICAL RESISTIVITY OF BERYLLIUM[33c]

Material	Impurity content,* wt.%		Resistivity, ohm-cm			Resistivity ratio, 300°K/4°K
	Non-metallic	Metallic	300°K	77°K	4°K	
EBM† ingot	0.125	0.794	9.60	5.44	5.40	1.8
Arc melt	0.133	0.727	8.90			
EBM ingot	0.189	0.721	9.73	4.89	4.86	2.0
EBM ingot	0.189	0.721	10.12	5.58	5.53	1.8
EBM ingot	0.189	0.721	9.38	5.15	5.07	1.8
Induction melt	0.090	0.635	7.64	3.23	3.20	2.4
EBM ingot	0.260	0.493	6.52	2.71	2.63	2.5
EBM ingot	0.185	0.376	6.91	3.33	3.33	2.1
EBM ingot	0.185	0.376	6.60	3.32	2.72	2.4
QMV hot pressed	0.886	0.276	5.63	0.79	0.68	8.3
EBM ingot	0.144	0.222	6.03	2.43	2.42	2.5
EBM ingot	0.144	0.222	6.80	2.49	2.40	2.8
EBM ingot (from hot-pressed flake)	0.087	0.094	4.03	0.54	0.54	7.5

*Based on analysis of ingot; not directly from specimen.
†EBM = electron-beam melted.

The surface tension of 99.98 per cent pure beryllium at 1500°C was found experimentally in a vacuum of 5×10^{-5} mm Hg to be 1100 ± 35 ergs/cm^2. This calculation was based on a density of 1.42 ± 0.04 g/cm^3, which was determined simultaneously under the same conditions. The value for surface tension in the literature was 1620 ergs/cm^2 at the melting point, which was calculated by semiempirical relations. After all possible corrections are made, the discrepancy between this and the newly calculated value is greater than 10 per cent.[38]

A redetermination of the lattice parameters of beryllium[39] gave the following values:

$$a = 2.2866 \pm 0.0006 \text{ A}$$

$$c = 3.5833 \pm 0.009 \text{ A}$$

$$\frac{c}{a} = 1.5671$$

The method used gives results of considerable accuracy without the necessity for extremely refined experimental conditions.

Mechanical Properties of Beryllium. Complications can arise in the selection of the classical criteria for yield and fracture strength of beryllium from directionalities that are the result of preferred orientation of the grain lattice structure. Crawford[40] discussed these considerations and introduced modified criteria for yield and fracture to account for preferred orientation.

At the conclusion of the year's study of crack propagation and the effects of surface condition on the mechanical properties of beryllium, it was concluded that surface defects and irregularities which might have had little effect in more ductile materials exerted a pronounced influence on beryllium products. These defects can be removed most effectively by an etching treatment after all other processing is completed. Ductility of beryllium sheet, always low, is limited by the presence of notches and preferred orientation. Ductility can be increased[41] by heating the sheet to between 400 and 600°F.

The mechanical properties of beryllium which are important in gyro applications are discussed in a significant report[42] on dimensional stability of the metal. The results of measurements of precision elastic limit and dimensional stability on six modified forms of beryllium are given. It is shown that fine grain size and high BeO content favor high precision elastic limit and good dimensional stability. It is also shown that the addition of 1 per cent iron as an alloying element improves the precision mechanical properties of beryllium without significantly altering the diamagnetic character. Prestraining likewise improves these properties. Variability of the precision elastic limit is rather large from sample to sample.

Beryllium from the Bureau of Mines plant at Boulder City was zone refined by Franklin Institute workers[43] to produce a single crystal with the basal plane oriented at an angle of 20°

to the long axis of the bar. This was formed into a tensile bar with a 0.140-in.-gauge section diameter. When pulled to fracture, the minimum elliptical gauge section measured 0.140 by 0.113 in., which represents a 20 per cent reduction in cross-sectional area. The elongation was not measured, but the specimen showed a 20 per cent over-all extension and a calculated 25 per cent elongation based on the reduction of area. The final fracture was on the $(11\bar{2}0)$ plane closest to 90° from the tension axis. It is believed that this single crystal has exhibited greater ductility associated with basal slip than any other beryllium crystals reported in the literature. Although proof was lacking, it seemed most probable that the increased ductility was associated with the removal of solid-solution elements.

A very good review[44] of past effort on making beryllium ductile appeared in a recent literature survey. Contrary to indications from the Franklin Institute single-crystal work, this review concludes that the removal of impurities will not lead to extensive ductility. Neither has any marked improvement in ductility been achieved by deoxidation, solid-solution alloying, or grain refinement through alloying. Optimum orientation for maximum ductility is one in which a $[10\bar{1}0]$ direction is parallel to the stress axis. Ductility reaches a maximum at two different temperatures, 400 and 800°C. Two brittle-ductile transition temperature ranges exist, one between 0 and 200°C and the other between −50 and −200°C. Fracture occurs on the (0001) basal, $\{11\bar{2}0\}$ planes, and the twin matrix interface. Fracture is initiated by cracks formed by kinks and $\{11\bar{2}0\}$ bend planes. Beryllium sheet with a ductility of 30 to 40 per cent in all directions in the plane of the sheet has been produced by cross rolling of extrusions. The ductility in the third direction was zero. Under proper conditions thermal treatment improves the ductility of beryllium.

Corrosion and Irradiation Behavior of Beryllium

Trillat and coworkers[45] reported a study of the oxidation of thin films of beryllium under very low pressures by electron-diffraction means. The conditions under which the oxide, BeO, appeared during heating in a vacuum or during ionic bombardment are defined. Carburization is studied also.

The corrosion of beryllium in air[33d] follows a linear rate and is temperature dependent with an activation energy of 1.1×10^5 cal/mole in the range 930 to 1065°C and 1.06×10^4 cal/mole in the range 1065 to 1295°C. An induction period was observed in all experiments on the corrosion of beryllium in air. This period could be considerably lengthened by an oxidizing pretreatment.

It had been shown previously that beryllium, in comparison with other metals, possesses excellent resistance toward oxidation up to temperatures near 1000°C. A study at temperatures of 1110 to 1210°C and oxygen pressures of 0.1 and 0.2 atm showed that the reaction rate is parabolic and that the data agree with an extrapolation of the values reported in the literature. However, after a time, the reaction rate becomes approximately linear. The shift from parabolic to an approximately linear rate is attributed to a buckling process at the oxidized surface.[46]

In the work at Oak Ridge, tests on the compatibility of beryllium with CO_2 were extended to include the effect of pressure on reaction rate. Tests were run at 720, 650, and 600°C in atmospheric and low-pressure CO_2. In all cases the corrosion rates at pressures of 1×10^{-3} mm Hg decreased with time, and only at 720°C were they lower at the reduced pressure than at atmospheric pressure.[17]

Seven types of fabricated beryllium exposed to flowing sodium at 900°F for 47 hr, followed by 520 hr at 1100°F, were covered with a nitride film at the completion of the test. The film was hard, black, and adherent. Below the surface the beryllium appeared unaffected by sodium.[47]

On a second high-temperature beryllium swelling experiment, specimens were held at 500, 600, and 700°C and irradiated during a one-month reactor cycle. Incomplete density measurements indicate that less than 1 per cent swelling occurred. This is considerably less than that observed after the first irradiation experiment.[48] Over 90 per cent (by volume) of the gases formed during irradiation are helium. Below about 600°C no changes in microstructure were noted. Irradiation caused an increase in hardness from about 200 DPH to over 400. Heating at temperatures between 450 and 1100°C decreased this hardness.

Beryllium irradiated with more than 10^{21} fast neutrons while in the temperature range of 280 to 480°C showed no measurable increase in

volume until heated for 1 hr at above 800°C. Tensile specimens of the irradiated beryllium pulled at room temperature to 600°C showed that the strength had more than doubled, whereas the elongation was reduced to practically zero. Some recovery was achieved by annealing[49] at above 800°C.

Miscellaneous Beryllium Studies

Detailed directions for the metallographic polishing techniques used at Tube Investment Research Laboratories including etchants are given in a paper by Meredith.[50]

Hood design, enclosure technique, air flows, and other ideas for solving ventilation problems in all shops handling beryllium or its compounds are described by Breslin and Harris.[51]

Lockheed issued two literature surveys; one[52] contained 228 references to general literature concerning beryllium metal, its alloys, and its compounds. The other[53] contained 141 references to crack propagation in beryllium and related studies.

Another bibliography[54] contains a list of Army, Navy, Air Force, AEC, and other research reports and translated and untranslated literature on beryllium. It covers forging, magnetic properties, metallographic preparation, and corrosion control. (W. Hodge)

Beryllium Compounds

BeO-UO_2 ceramics were irradiated at Bettis and Battelle.[55,56] The compositions, irradiation conditions, and dimensional changes are summarized in Table II-3.

Table II-3 IRRADIATION OF BeO-UO_2 CERAMICS[55,56]

Composition	Fuel particle size, μ	Density, % of theoretical	Average surface temp., °F	Average burnup, fissions/ $cm^3 \times 10^{20}$	Increase in dimensions, %
BeO–25.3 wt.% UO_2*	0–50	96	530	11.1	27.3
BeO–28.7 wt.% UO_2*	150	90	535	12.1	5.8
BeO–56 wt.% UO_2†	0–40	98	1700	1.1	Not significant

*Irradiated at Bettis.
†Irradiated at Battelle.

The difference in expansion of the BeO–25.3 wt.% UO_2 and BeO–28.7 wt.% UO_2 bodies may be due to the difference in fuel particle size. The volume fraction of the BeO matrix damaged by fission fragments decreases with increasing fuel particle size. Approximate calculations indicate that 44 per cent of the BeO is damaged in the fine dispersion, whereas only 5 per cent of the BeO is damaged in the coarse dispersion. The lodging of fission fragments in the matrix destroys the BeO crystal structure. This loss of crystallinity may account for the observed expansions. A large expansion is to be expected in the fine dispersion since a greater portion of the BeO is damaged.

The lack of dimensional changes in the Battelle ceramics may be due to annealing at the high (1700°F) irradiation temperature and to the relatively low burnup. (J. Koretzky)

Solid Hydrides

Zirconium Hydride

Investigation of the structure of zirconium hydride by X-ray diffraction has continued at Denver Research Institute.[57,58] Their results show that the delta-epsilon transformation at room temperature occurs at a composition of 62.5 at.% hydrogen by a diffusionless (martensitic) process. The long-sought gamma phase is concluded to be a decomposition product of the delta phase, occurring at a composition near the end of the eutectoid reaction (56.5 at.% hydrogen), and appears to be the stoichiometric compound, ZrH. High-temperature X-ray studies verified these data on the gamma phase, which disappeared rapidly when the temperature was raised beyond the solubility limit for hydrogen in the delta phase.

The effect of oxygen on the solubility of hydrogen in zirconium has been studied at the University of Alberta.* The equilibrium pressure of hydrogen over the ternary solid solution of zirconium-oxygen-hydrogen was measured as a function of temperature and composition. It was

*K. P. Singh and J. Gordon Parr, Atomic Energy of Canada, Ltd., 1960. (Unpublished)

found that the volume of hydrogen absorbed at the saturation point in the metal was decreased by a volume equal to that of the oxygen present in the zirconium-oxygen solid solution. The solubility of hydrogen in the zirconium-oxygen was a maximum between 400 and 500°C.

Electrical-resistivity measurements made at Atomics International[59] on face-centered cubic $ZrH_{1.54}$ and face-centered tetragonal $ZrH_{1.96}$ between 1.2 and 400°K revealed a sizable optical mode scattering contribution. For compositions approaching ZrH_2, the hydride is a better electrical conductor than pure zirconium. The room-temperature Hall coefficient is 35 to 40×10^{-5} cm^3/coulomb for the face-centered cubic and -20 to -68×10^{-5} cm^3/coulomb for the face-centered tetragonal material. Other studies at Atomics International[60] revealed a large internal friction peak in $ZrH_{1.92}$, which suggests that it is associated with a stress-induced twin interface motion. Stress relaxation appears to be controlled by the diffusion of hydrogen, with an activation energy of about 20 kcal/mole.

Lithium Hydride

A literature survey of the unclassified publications on lithium hydride has been made at Tufts University.[61] In it are discussed the preparation, the physical and thermodynamic properties, the reactivity, and the thermal stability of lithium hydride. Practical considerations such as handling, toxicity, fabrication methods, and analysis are included. Critical comparisons of conflicting data are made where it is appropriate, and extrapolated values of some high-temperature properties are given. Lithium deuteride and LiH vapor are discussed also. The review covers 230 references.

Niobium Hydride

Niobium-hydrogen equilibria have been studied at Armour.[62] The system was examined in the temperature range 300 to 1500°C, between 0 and 760 mm Hg equilibrium hydrogen pressure, by the Sievert's technique. Continuous solid solution formed in this range, which exhibits a body-centered cubic structure, with lattice parameter increasing with hydrogen content. The solubility of hydrogen in niobium was found to be higher than that measured by previous investigators, and this result is attributed to higher purity of the niobium used.

Alloy Hydrides

Data on the SNAP-2 reactor have been published by Atomics International.[63] The fueled-moderator concept is used, with uranium metal dispersed in a zirconium hydride matrix. The composition of the material is 1.71 wt.% hydrogen, 6.88 wt.% uranium, and 91.41 wt.% zirconium, which results in an N_H of 6. Accelerated burnup tests showed no swelling or damage of any sort. The properties of the SNAP-2 fuel are given in Table II-4. (H. H. Krause)

Table II-4 PROPERTIES OF SNAP-2 FUEL (Zr–6.88 WT.% U–1.71 WT.% H)[63]

	Value	Temp. range, °F
Thermal conductivity, Btu/(hr)(ft)(°F)	13 ± 1	200–1200
Compressive strength, psi	90,000	RT
Ultimate tensile strength, psi	25,000	RT–1300
Dynamic elastic modulus, 10^6 psi	9 ± 1	RT
Coefficient of expansion, 10^{-6}/°F	6.56	RT–1300
Density, g/cm^3	5.94	RT

References

1. J. M. Conway-Jones, The New Impermeable Graphite, *Brit. Power Eng.*, 1: 64–66 (June 1960).
2. C. W. Boquist and S. W. Bradstreet, Modified Graphite Technology, Quarterly Report No. 2, USAEC Report ARF-6038-11(LAR-47), Armour Research Foundation, Illinois Institute of Technology, Apr. 18, 1960. (Classified)
3. M. H. Dodson, The Depth of Oxidation of Graphite: A Theoretical Approach, British Report DEGR-148(CA), Sept. 16, 1958.
4. Oak Ridge National Laboratory, Gas-Cooled Reactor Project Quarterly Progress Report for Period Ending Sept. 30, 1960, USAEC Report ORNL-3015, pp.75–76, Nov. 11, 1960.
5. Oak Ridge National Laboratory, Gas-Cooled Reactor Project Quarterly Progress Report for Period Ending June 30, 1960, USAEC Report ORNL-2964, July 11, 1960.
6. R. W. Benoliel, Technical Basis for NPR Core Graphite Specification, USAEC Report HW-65300, Hanford Atomic Products Operation, May 5, 1960. (Classified)
7. S. H. Gelles, Beryllium Research and Development Program, Quarterly Progress Report for the Period April 1, 1960, to June 30, 1960, Report NMI-9502, Nuclear Metals, Inc., July 26, 1960.
8. F. A. Crossley and R. J. Van Thyne, Ductile

Beryllium Alloys, Bimonthly Report No. 3, Report ARF-2187-3, Armour Research Foundation, Illinois Institute of Technology, Mar. 15, 1960.

9. F. A. Crossley et al., Ductile Beryllium Alloys, Bimonthly Report No. 5, Report ARF-2187-5(AD-240614), Armour Research Foundation, Illinois Institute of Technology, July 20, 1960.
10. K. C. Taber and R. C. Harris, Beryllium Casting, Eighth Interim Technical Report on Phase II, Report NP-9477, The Beryllium Corp., 1960.
11. J. G. Klein et al., Development of Wrought Beryllium Alloys of Improved Properties, USAEC Report WADC-TR-58-478(Pt.II), Brush Beryllium Co., Sept. 1, 1959.
12. Beryllium-Rolling Extruding Program Expanded, *Light Metal Age*, 18: 18 (October 1960).
13. G. A. Toczko and Ken Breeze, The Production Man's Guide to Working Beryllium, *Am. Machinist*, 104: 115–126 (Oct. 17, 1960).
14. A. F. Hayes, Beryllium Forging Program, Phase II, Interim Engineering Report No. 3, Report AD-235279, Ladish Co., 1960.
15. J. N. Krusos, Development of Beryllium Composite Structures, Aeronca Monthly Progress Report No. 7, Report ER-344, August 1960.
16. Savannah River Operations Office, Monthly Progress Report on Heavy Water Power Reactor Program, USAEC Report SRO-38, October 1960.
17. Oak Ridge National Laboratory, Gas-Cooled Reactor Project Quarterly Progress Report for Period Ending September 30, 1960, USAEC Report ORNL-3015, Nov. 11, 1960.
18. R. N. Randall and F. M. Yans, Nuclear Metals, Inc., June 30, 1960. (Unpublished)
19. National Research Council, Materials Advisory Board, Development of Manufacturing Processes for Aircraft Materials, Report MAB-165-M, May 31, 1960.
20. B. H. Hessler, Primary Mechanical Working of Beryllium and Beryllium Alloys, Report LMSD-763239, Lockheed Aircraft Corp., June 22, 1960.
21. K. H. Moyer and I. Scheinhartz, Sylvania-Corning Nuclear Corp., January 1960. (Unpublished)
22. T. J. McDonald et al., Fusion Welding of Beryllium, *Brit. Welding J.*, 7: 441–450 (July 1960).
23. V. M. Amonenko et al., Manufacture of Beryllium Foil (in Russian), *Zavodskya Lab.*, 26: 625–626 (May 1960).
24. R. G. Bedford, Phase Diagrams of Zirconium-Beryllium and Related Systems, USAEC Report UCRL-5991-T, University of California Lawrence Radiation Laboratory, July 22, 1960.
25. S. H. Gelles et al., Some Recent Advances in Beryllium Metallurgy, paper presented at AIME Southwest Metals and Minerals Conference, Los Angeles, Calif., Apr. 22, 1960.
26. Nuclear Metals, Inc., Fundamental and Applied Research and Development in Metallurgy, Progress Report for July 1960, USAEC Report NMI-2087, Aug. 31, 1960.
27. Nuclear Metals, Inc., Fundamental and Applied Research and Development in Metallurgy, Progress Report for August 1960, USAEC Report NMI-2088, Sept. 30, 1960.
28. Nuclear Metals, Inc., Fundamental and Applied Research and Development in Metallurgy, Progress Report for September 1960, USAEC Report NMI-2089, Oct. 21, 1960.
29. F. M. Yans, Preliminary Survey of Mechanical Properties and Phase Relationships in Several Binary Beryllium Alloys, USAEC Report NMI-1240, Nuclear Metals, Inc., Sept. 8, 1960.
30. F. M. Yans et al., Development of Randomly Oriented Wrought Beryllium Sheet, Second Quarterly Report to Wright Air Development Division, Report NMI-9605, May 16, 1960.
31. F. M. Yans et al., Development of Randomly Oriented Wrought Beryllium Sheet, Third Quarterly Report to Wright Air Development Division, Report NMI-9608, Nuclear Metals, Inc., May 17, 1960.
32. F. M. Yans and P. Pointu, Preliminary Attempts to Produce Randomly Oriented Wrought Beryllium and Their Relation to Texture Development, USAEC Report NMI-1225, Nuclear Metals, Inc., July 6, 1960.
33. Lockheed Aircraft Corp., General Research in Materials and Propulsion, January 1959 to January 1960: Vol. I, Propulsion Chemistry and Propulsion Physics, Report LMSD-288140(Vol. I).
    - 33*a*. E. C. Burke, Plastic Deformation in Beryllium, in Report LMSD-288140(Vol.II), Paper No. 3.
    - 33*b*. G. C. Kuczynski, Electronic Structure of Beryllium, in Report LMSD-288140(Vol.II), Paper No. 1.
    - 33*c*. J. Ho and E. S. Wright, Electrical Resistivity of Beryllium, in Report LMSD-288140(Vol.II), Paper No. 2.
    - 33*d*. W. Bradshaw and E. S. Wright, High-Temperature Corrosion of Beryllium in Air, in Report LMSD-288140(Vol.II), Paper No. 5.
34. A. Brown et al., An Improvement in the Ductility of Beryllium at High Temperatures, *Nature*, 187: 494–496 (Aug. 6, 1960).
35. N. A. Hill and J. Williams, Textures in Beryllium Rods and Tubes Extruded from Consolidated Powders, *Powder Met.*, 5: 116–129 (1960).
36. J. Greenspan et al., Beryllium Research and Development in the Area of Composite Materials, Report WADD-TR-60-32, Nuclear Metals, Inc., July 1960.
37. C. Herring and A. G. Hill, Theoretical Constitution of Metallic Beryllium, *Phys. Rev.*, 58: 132 (1940).
38. V. N. Eremenko et al., Surface Tension of Liquid Beryllium, *Russ. Met. and Fuels*, No. 3 (May–June 1960).
39. D. R. Schwarzenberger, Accurate Determination of the Lattice Parameters of Beryllium, Report

NP-9203, Tube Investments Research Laboratories, Feb. 11, 1959.

40. R. F. Crawford, On Determining Biaxial-Stress Yield and Fracture Criteria for Hot-Pressed Beryllium at Room and Elevated Temperatures, in Mechanics of Deformable Bodies, Report LMSD-288139(Vol. II), Paper No. 6, January 1959 to January 1960, Lockheed Aircraft Corp.
41. C. O. Matthews et al., Beryllium Crack Propagation and Effects of Surface Condition, Report WADD-TR-60-116, Lockheed Aircraft Corp., July 1960.
42. T. J. Hughel, An Investigation of the Precision Mechanical Properties of Several Types of Beryllium, Report NP-9662, General Motors Corp., Research Staff, Apr. 4, 1960.
43. E. Hein et al., Develop High-Purity Beryllium and Determine the Mechanical Properties of Material Produced, Report NP-9242, Franklin Institute Laboratories, June 30, 1960.
44. Ductile Beryllium (A Literature Survey), Report AD-245149, Dec. 31, 1960.
45. Jean-Jacques Trillat et al., The Oxidation and Carburization of Thin Layers of Beryllium (in French), *Compt. rend.*, 251: 10–13 (July 4, 1960).
46. M. M. Nakata, A Thermogravimetric Balance for the Investigation of High-Temperature Reaction Kinetics and the Results of a Beryllium Oxidation Study, USAEC Report NAA-SR-4737, Atomics International, Nov. 1, 1960.
47. W. W. Kendall, Corrosion of Beryllium in Flowing Sodium, USAEC Report GEAP-3333, General Electric Co., Atomic Power Equipment Dept., Jan. 15, 1960.
48. Oak Ridge National Laboratory, Nov. 4, 1960. (Unpublished)
49. J. B. Rich et al., The Mechanical Properties of Some Highly Irradiated Beryllium, British Report AERE-R-3449, September 1960. (To be published in *J. Nuclear Materials.*)
50. J. E. Meredith, Metallographic Polishing Techniques for Beryllium, Report NP-8990, Tube Investments Research Laboratories, Jan. 20, 1960.
51. A. J. Breslin and W. B. Harris, Practical Ways To Collect Beryllium Dust: I, *Air Eng.*, 2(7): 34 ff (July 1960).
52. K. D. Carroll, comp., Beryllium—A Survey of the Literature, Report LMSD-288190(Suppl.2), Lockheed Aircraft Corp., August 1960.
53. K. D. Carroll, Beryllium Crack Propagation and Related Studies, Report NP-9274, Lockheed Aircraft Corp., Aug. 24, 1960.
54. Beryllium (1945–1960), OTS Selective Bibliography, Report SB-413, Office of Technical Services, June 1960.
55. Westinghouse Electric Corp., Bettis Atomic Power Laboratory, Bettis Technical Review, Reactor Technology, USAEC Report WAPD-BT-20, September 1960.
56. D. G. Freas et al., A Study of Radiation Stability of UO_2 Dispersion in BeO, USAEC Report BMI-1484, Battelle Memorial Institute, Dec. 9, 1960.
57. R. L. Beck, Reactor Materials Study, USAEC Report LAR-8, Denver Research Institute, April 1960. (Classified)
58. R. L. Beck, Reactor Materials Study, USAEC Report LAR-9, Denver Research Institute, July 1960. (Classified)
59. P. W. Bickel and T. G. Berlincourt, Optical Mode Scattering Contribution to Electrical Resistivity in Zirconium Hydride, *Phys. Rev.*, 119: 1603–1604 (September 1960).
60. R. Chang, Phase Transformation, Twinning, an Anelastic Phenomenon Associated with Zirconium Hydride, USAEC Report NAA-SR-5537, Atomics International, Sept. 15, 1960.
61. C. E. Messer, A Survey Report on Lithium Hydride, USAEC Report NYO-9470, Tufts University, Oct. 27, 1960.
62. S. Komjathy, Columbium-Hydrogen System, USAEC Report ARF-2120-5, Armour Research Foundation, Illinois Institute of Technology, May 1960.
63. J. B. Vetrano, A Uranium Dispersion, Zirconium Hydride Matrix Fuel for Compact Space Power Systems, *Trans. Am. Nuclear Soc.*, Session 22, Paper 4 (December 1960).

Section III

NUCLEAR POISONS

Metallic Poison Materials

The Bureau of Mines[1] has been investigating the iron-gadolinium, nickel-gadolinium, and titanium-iridium alloy systems. A tentative iron-gadolinium equilibrium diagram is shown in Fig. III-1. Three eutectic points were found in the nickel-gadolinium system at about 10 to 15, 70 to 75, and 90 to 95 wt.% gadolinium. Three secondary phases, Ni_9Gd, Ni_5Gd, and Ni_2Gd, have been identified, and two other secondary phases have been observed but not identified. The Ni_9Gd phases decompose incongruently in a peritectic type isotherm. The Ni_5Gd phase melts congruently. Approximately 15 at.% iridium was found to dissolve in titanium at 1400°C. Thermal analysis of alloys containing 25, 30, and 35 wt.% iridium showed evidence of an iso-

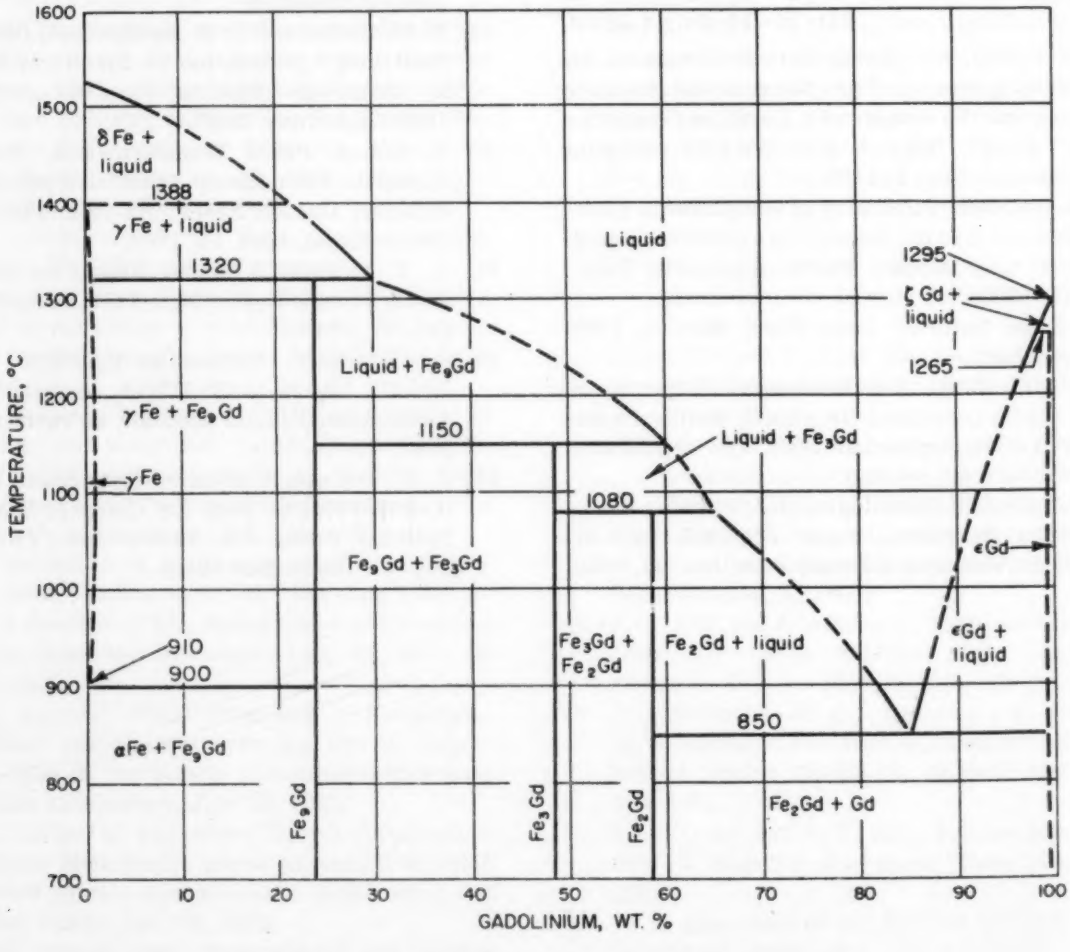

Fig. III-1 Tentative iron-gadolinium phase diagram.[1]

Table III-1 RESULTS OF CORROSION TESTS* OF VARIOUS CONTROL-ROD MATERIALS[2]

Material, wt.%	100-hr exposure		900-hr exposure		2000-hr exposure	
	Weight change, mg	Corrosion rate, mg/(cm²)(yr)	Weight change, mg	Corrosion rate, mg/(cm²)(yr)	Weight change, mg	Corrosion rate, mg/(cm²)(yr)
80 Ag–15 In–5 Cd	0.0	0.0	−2.3	−0.9	−1.8	−0.3
	−0.1	+0.3	−1.8	−0.7	−1.5	−0.3
	0.0	0.0	−1.3	−0.5	−1.9	−0.3
	−0.1	+0.3	−0.7	−0.3	−1.8	−0.3
80 Ag–15 In–4.5 Cd–0.5 Sn	0.0	0.0	−1.6	−0.6	−1.4	−0.2
	+0.1	+0.3	−0.3	−0.1	−1.2	−0.2
	+0.1	+0.3	−0.4	−0.2	−0.4	−0.1
	+0.1	+0.3	−1.1	−0.4	−0.3	−0.1
Boronated stainless steel (1.0 boron)	−0.2	+0.7	+0.5	+0.2	0.0	0.0
	−0.1	+0.3	+0.3	+0.1	0.0	0.0
			+0.2	+0.1	−0.2	−0.03
	−0.1	+0.3	+0.3	+0.1	+0.1	+0.02
Boronated stainless steel (1.5 boron)	+0.1	+0.3	+0.6	+0.2	+0.4	+0.1
	0.0	0.0	+0.7	+0.3	+0.1	+0.02
	+0.1	+0.3	+0.7	+0.3	+0.1	+0.02
	0.0	0.0	+0.6	+0.3	+0.2	+0.04
Boronated stainless steel (2.0 boron)	0.0	0.0	+0.3	+0.1	−0.1	−0.02
	0.0	0.0	+0.5	+0.2	−0.3	−0.1
	0.0	0.0	+0.4	+0.2	0.0	0.0
	−0.1	+0.3	+0.9	+0.4	+0.1	+0.02
Boral–35 B_4C in aluminum matrix	+30.2	+62.5	+138.1	+28.6	+143.3	+14.8
	+22.6	+46.7	+73.7	+15.2	+77.5	+8.0
			+108.6	+22.4	+114.8	+11.8

*Test conditions: medium, demineralized water; temperature, 190°F; *p*H, 7.0 ± 0.3; pressure, atmospheric.

Table III-2 SUMMARY OF TENSILE PROPERTIES OF HAFNIUM[3]

Condition	Test		Yield strength (0.2% offset), 1000 psi		Ultimate tensile strength, 1000 psi		Total elongation, %		Reduction of area, %	
	Temp., °C	No. of samples	$\bar{X}$	Range	$\bar{X}$	Range	$\bar{X}$	Range	$\bar{X}$	Range
700°C Vacuum Heat-Treated and Hot Rolled										
Longitudinal	RT	18	30.6(34)*	19.6–40.7	73.8(64)	57.9–87.4	23.7(23)	8.6–30.5	29.1(37)	9.1–36.5
Transverse	RT	20	40.9(37)	24.9–53.7	70.5(60)	55.0–83.8	17.1(26)	5.5–26.0	22.4(38)	6.6–45.0
	260	20	23.6(26)	14.5–31.1	38.1(35)	29.4–44.7	47.2(36)	38–58.0	48.7(44)	38.0–59.0
700°C Vacuum Heat-Treated and Cold Rolled										
Longitudinal	RT	5	56.6(33)	53.6–61.7	79.6(62)	74.0–86.3	19.8(26)	8.0–26.0	32.2(37)	13.0–40.0
Transverse	RT	6	68.5(44)	59.0–79.2	82.9(58)	74.2–93.8	16.3(22)	10.9–19.0	34.7(40)	16.0–43.0
	260	9	44.8(34)	40.0–49.7	52.0(43)	47.6–56.5	28.6(40)	22.0–33.0	55.2(58)	43.0–61.0
850°C Vacuum Heat-Treated										
Hot rolled, transverse	RT	18	39.1(39)	24.3–50.7	69.9(63)	55.2–81.5	24.0(31)	13.3–28.9	32.9(35)	13.7–41.6
Cold rolled, transverse	RT	5	39.4(34)	33.3–48.0	70.6(51)	65.4–76.9	22.4(28)	7.0–30.0	33.0(36)	9.0–66.0

*Values in parentheses are values for crystal-bar plate.

therm at 1480°C. It is believed that the compound Ti_3Ir decomposes peritectically at this temperature.

Westinghouse[2] has corrosion tested silver-indium-cadmium, silver-indium-cadmium-tin, boronated stainless steels, and boral (aluminum with B_4C) for 2000 hr in 190°F demineralized water. Results are listed in Table III-1. Except for the boral, all performed satisfactorily.

A study to compare the properties of sponge hafnium with the properties of crystal-bar hafnium has been conducted at Bettis.[3] Sponge hafnium was found to be similar to crystal-bar hafnium with respect to corrosion resistance and weldability. Density of the sponge material was found to be slightly less than that observed for crystal-bar hafnium, possibly due to internal porosity. Sponge ingots were readily fabricated by hot forging and rolling but were very difficult to cold roll. Table III-2 lists the mechanical properties of the two types of hafnium.

(V. W. Storhok)

Dispersion Absorber Materials

Workers at Argonne[4] are attempting to develop new absorber materials and are placing emphasis on dispersions of 25 and 38 wt.% Dy_2O_3 in X-8001 aluminum alloy and composite plates consisting of an inner core of 20 wt.% gadolinium-samarium-europium oxide mixture plus 10 wt.% Er_2O_3 dispersed in cobalt and an outer core of 30 wt.% Sm_2O_3 dispersed in cobalt.

Muccigrosso et al.[5] have published a detailed report on the production of spherical B_4C particles. Four methods are described: (1) resistance hot-press method, (2) graphite-tube furnace process, (3) mechanical-abrasion process, and (4) plasma-spray process. In the first process, one part of angular particles of B_4C is blended with three parts of graphite powder, held in a hot press 15 min at 2300°C, and cooled in place. The surface tension is sufficient to spheroidize the B_4C. The graphite-tube furnace process was similar. A mixture of B_4C and graphite was heated in the furnace for ½ hr at 2350°C, the temperature was raised to 2450°C for 5 min, and the sample was pushed into the furnace cold zone. The mechanical-abrasion process consists of grinding the particles to a smooth shape in an air mill. The plasma-spray process consists of feeding sintered B_4C rods into a plasma jet, melting to form droplets that quench into spheres as they are carried out of the high-temperature region.

Bettis[6] is evaluating burnable-poison plates containing platelets of B_4C and B_4C plus SiC. Four of the eight samples comprising the burnable-poison plates of one test have been examined after irradiation to a burnup of approximately 60 per cent of the original B^{10} atoms present. The interim examination consisted of visual and dimensional analysis; the results are noted in Table III-3. Although the plates had swelled considerably, no cladding defects were detected. The plates were subsequently returned to the MTR for continued irradiation.

Helium-evolution measurements have been completed on slightly irradiated SiC–50 vol.% B_4C and SiC–30 vol.% B_4C platelets at 700°C (30 hr), 800°C (127 hr), 900°C (60 hr), 1000°C (138 hr), and 1100°C (300 hr). The amount of helium evolved for the same irradiation and annealing conditions is compared with that from

Table III-3 DIMENSIONAL CHANGES ON IRRADIATED B_4C-CONTAINING PLATELETS[6]

Plate	Composition and thickness	Dimensional changes				
		Interim examination 1		Interim examination 2		
		10^{20} captures/cm^3	Δ thickness, in.	B^{10}, %	10^{20} captures/cm^3	Δ thickness, in.
PB 7-8	B_4^DC (0.0952 to 0.0969 in.)	29	0.0021 to 0.0079	60	60	0.0128 to 0.0172
PB 33-34	B_4^NC (0.0663 to 0.0671 in.)	59	0.0022 to 0.0049	60	122	0.015 to 0.020
PB 11-12	B_4^NC–50 vol.% SiC (0.0950 to 0.0958 in.)	31	0.0063 to 0.0107	60	64	0.0153 to 0.0208
91-92	B_4^DC (0.0921 to 0.0928 in.)	29	0.0028 to 0.0057	60	60	0.0128 to 0.0295

pure B_4C in Table III-4. The rate and amount of helium released are greater for B_4C than for SiC-B_4C platelets.

Table III-4 HELIUM EVOLUTION IN B_4C AND B_4C-SiC PLATELETS[6]

Sample	10^{22} B^{10} atoms/cm^3	Annealing conditions		Helium evolved, 10^{-4} cm^3
		Temp., °C	Time, hr	
B_4C	2.18	700	30	141
SiC–50 vol.% B_4C	1.09	700	30	23
SiC–30 vol.% B_4C	0.65	700	30	13
B_4C	2.18	800	62	642
SiC–50 vol.% B_4C	1.09	800	61	41
SiC–30 vol.% B_4C	0.65	800	61	31
B_4C	2.18	900	34	1260
SiC–50 vol.% B_4C	1.09	900	33	48
SiC–30 vol.% B_4C	0.65	900	33	37

The Russian workers Tresvyatskiy et al.[7] have investigated the systems BeO-Sm_2O_3 and BeO-Gd_2O_3. Both systems are simple eutectics, and no new phases were detected. It was concluded that in the range 1300 to 1500°C no solid solutions occur. (G. W. Cunningham)

References

1. Bureau of Mines, Albany Metallurgy Research Center, Quarterly Metallurgical Progress Report No. 8 for the Period July 1 to September 30, 1960, USAEC Report USBM-U-761.
2. Carolinas-Virginia Nuclear Power Associates, Inc., Research and Development Program Quarterly Progress Report for the Period January 1 to March 31, 1960, USAEC Report CVNA-52, May 1960.
3. Westinghouse Electric Corp., Bettis Atomic Power Laboratory, Bettis Technical Review, Reactor Technology, USAEC Report WAPD-BT-20, September 1960.
4. Argonne National Laboratory, Reactor Development Program Progress Report, USAEC Report ANL-6269, November 1960.
5. A. T. Muccigrosso et al., Methods of Forming Spherical Boron Carbide Particles, USAEC Report KAPL-M-ATM-3, Knolls Atomic Power Laboratory, June 1960.
6. Westinghouse Electric Corp., Bettis Atomic Power Laboratory, Technical Progress Report, Pressurized Water Reactor (PWR) Project for the Period August 24 to October 23, 1960, USAEC Report WAPD-MRP-88.
7. S. G. Tresvyatskiy et al., Investigation of the Systems BeO-Sm_2O_3 and BeO-Gd_2O_3, *At. Energ.*, 9(1): 54–55 (January 1960).

Section IV

CLADDING AND STRUCTURAL MATERIALS

Corrosion

Zirconium Corrosion

An undesirable white corrosion product was found on many Pressurized-Water Reactor (PWR) seed 1 type fuel-element clusters following standard corrosion tests employed to establish the integrity of the Zircaloy-2 cladding. The white corrosion product was associated with acid staining resulting from acid drying on the surface prior to rinsing. These results indicated a need for either improving or eliminating the pickling operation. A study at Bettis[1] has indicated that machined surfaces given a surface-cleaning treatment without pickling exhibit satisfactory corrosion behavior. The only appearance of white corrosion products was found in the heat-affected zone of the welds. This attack, however, was found to be substantially reduced by the application of a black corrosion-resistant film prior to welding.

Hydrogen pickup in Zircaloy-2 and related alloys is being studied at Chalk River.* Samples of Zircaloy exposed in the reactor flux picked up about twice as much hydrogen with almost double the oxidation rate as those exposed in the same coolant out of the flux. X-ray-diffraction patterns of stripped corrosion films did not reveal any differences between those formed in flux or out of flux. Spectrographic analyses, however, indicated a higher level of contamination of the in-flux films by iron, chromium, lead, and silicon than was found for out-of-flux films.

Corrosion-produced hydrogen pickup by zirconium-base alloys also is being studied at Hanford,[2] where it was found that, in low-oxygen-content water (0.1 ppm O_2, *p*H 10) at 300°C, Zircaloy-2 picked up about 8 per cent of the hydrogen available from corrosion. With 3- to 4-ppm oxygen present in the water, the pickup was reduced to 1 per cent. Two samples of Zircaloy-4, on the other hand, picked up 11 and 17 per cent, respectively, of the available hydrogen. The somewhat contradictory nature of these results suggests that further study of the effect of water quality on hydrogen pickup is needed.

A fundamental study of the mechanism of corrosion of zirconium alloys in high-temperature steam is being conducted at Nuclear Metals.[3] Emphasis is being placed on (1) thermodynamics of the interaction of gases with zirconium intermetallic compounds, (2) structure and properties of the metal substrate beneath the oxide film on corroding zirconium, and (3) growth of the oxide film. (W. K. Boyd)

Aluminum Corrosion

A series of high-purity aluminum-base alloys containing an iron-to-nickel ratio of 1.5 to 1, but varying total alloy additions, is being tested in 360°C deionized water at Hanford.[2] Alloys down to 0.25 wt.% nickel–0.37 wt.% iron evince good corrosion properties. However, a 0.1 wt.% nickel–0.15 wt.% iron alloy failed in 10 days. In other studies, a 1 wt.% nickel–9 wt.% silicon alloy, similar to that used by the Russians for high-temperature-water service, exhibits a penetration in 360°C deionized water, after 4000 hr, of 6.23 mils, as compared with 5.85 mils for the X-8001 alloy exposed at the same time.

A program to develop corrosion-resistant aluminum-base alloys is being conducted at Nuclear Metals.[4] Experimental materials comprised of mixtures of a matrix of atomized

*W. R. Thomas, Atomic Energy of Canada, Ltd., 1960. (Unpublished)

aluminum powder with dispersed compound phase of iron and/or nickel are being evaluated at 200°C with a 15 to 1 ratio of specimen surface area to water volume. Although it is premature to reach conclusions regarding corrosion behavior of present materials, it is interesting to note that the dispersed-phase materials are less resistant than atomized aluminum.

Studies at Argonne[5,6] are being directed toward improving the mechanical properties of corrosion-resistant aluminum alloys. Ternary alloys containing titanium and iron show promise. An alloy containing 1.5 wt.% titanium plus 0.5 wt.% iron has shown good resistance to distilled water at 360°C. Other data indicated that, for alloys containing say 1 wt.% zirconium, at least .1 wt.% iron is necessary to ensure corrosion resistance after hot and cold rolling. (W. K. Boyd)

Carburization of Stainless Steels

Current gas-cooled-reactor studies at Oak Ridge[7] appear to confirm earlier hypotheses that the variations observed in the extent of carburization of Type 304 stainless steel depend on the CO_2-to-CO ratio. For example, at 982°C with a CO_2-to-CO ratio of 0.07, the final carbon content was 0.49 wt.%, whereas only 0.099 wt.% carbon was detected in samples exposed to gas having a CO_2-to-CO ratio of 0.46. At temperatures below about 775°C, oxidation and carburization are insignificant.

(W. K. Boyd)

Niobium Oxidation

The niobium-oxygen phase diagram has been established by Armour Research Foundation.[8] The three oxides, NbO, NbO_2, and Nb_2O_5, melt congruently at 1945, 1915, and 1495°C (3535, 3480, and 2725°F), respectively. The solid solubility of oxygen in niobium increases from 0.25 wt.% at 500°C to 0.72 wt.% at 1915°C.

The low-temperature oxidation behavior of niobium is improved by halide pretreatments, according to Lockheed.[9] Heating in an HCl-O_2 mixture at 480°C (900°F) reduces the oxidation rate during subsequent air exposures at the same temperature.

Silicide-base coatings for niobium are under development at Thompson Ramo Wooldridge[10] and Fansteel.[11] The Thompson Ramo Wooldridge coating consists of titanium–50 wt.% chromium overlaid with silicon. It is applied by vacuum distillation in two stages and is protective for 15, 5, and 1 hr at 1430, 1480, and 1540°C (2600, 2700, and 2800°F), respectively. Fansteel has applied a molybdenum silicide coating to niobium by depositing a molybdenum-rich layer on the substrate and subsequently converting this to molybdenum disilicide by a vapor-phase reaction. This coating, which is superior to a straight silicide coating on niobium, is protective for 70 hr at 1260°C (2300°F).

Studies at Battelle[12] have indicated that a niobium–20 wt.% uranium alloy may be useful as an intermediate-temperature fuel element. This alloy is resistant to air oxidation to about 300°C (570°F). It also had moderately good corrosion resistance in water and steam at 315 to 400°C (600 to 750°F), corroding about three times faster than Zircaloy-2. (W. D. Klopp)

Tantalum Oxidation

Recent Russian work[13] has shown that cold-worked tantalum oxidizes up to 50 per cent faster than recrystallized tantalum in the temperature range 650 to 900°C. Cold working, however, does not change the oxidation mechanism. Platinum-marker experiments indicated that oxidation proceeds by oxygen diffusion through the Ta_2O_5 scale.

Oak Ridge[14] has determined from single-crystal studies that tantalum oxidizes faster at 500°C on the (1 1 0) and (1 1 1) planes than on the (1 0 0) planes. This is also true for niobium.

(W. D. Klopp)

Molybdenum Coating

A silicide-base coating (W-2) for protecting molybdenum from oxidation is under study by the National Aeronautics and Space Administration (NASA).[15] A 2-mil coating will protect molybdenum in static oxidation for 140 hr at 1150°C (2100°F) and about 20 hr at 1320 to 1540°C (2400 to 2800°F). Above 1430°C (2600°F), the coating contains a liquid phase. Corrugated molybdenum sections coated after assembly with 1 mil of W-2 tended to fail at the spot-welded joints. (W. D. Klopp)

Corrosion of Base-Metal Alloys (Iron, Nickel, Cobalt)

Aqueous Corrosion. Poor corrosion resistance in oxygenated hot water has been a deterrent to use of carbon and low-alloy steels

as cladding materials. Recent tests at Argonne[16] indicated that proper control of oxygenated hot water may result in acceptable corrosion rates. Electrolytic iron specimens were exposed to water at temperatures from 100 to 260°C. The amount of dissolved oxygen was controlled at 45 and 530 ppm. At the higher oxygen concentration, corrosion rates were low at all temperatures. Under these conditions, the corrosion product was an apparently passive film displaying interference colors. At the low oxygen concentration, passivation occurred only at the highest temperature (260°C), and the corrosion rate was correspondingly low. At 200°C and lower, the corrosion product was not protective, and corrosion rates were excessive and increased with decreasing temperature. Carbon steel behaved similarly to the iron under the conditions tested. The test times (not stated in the reference) were apparently short. The Argonne workers concluded that, by maintaining sufficient dissolved oxygen in hot water, corrosion of low-carbon steel can be inhibited. Less oxygen is required for inhibition at higher temperatures.

Gaseous Corrosion. The results of a mechanistic study of the oxidation reaction of binary iron-chromium alloys in water-saturated argon were reported recently by Naval Research Laboratory (NRL) workers.[17] Pertinent oxidation measurements are given in Table IV-1. From these data, NRL concluded that, at 700 and 900°C, parabolic oxidation occurred, and at 1100°C the oxidation was linear. Atmosphere adjustment through decreasing the partial pressure of water vapor, or by adding hydrogen, decreased the oxidation rate. (E. S. Bartlett)

Table IV-1 OXIDATION OF BINARY IRON-CHROMIUM ALLOYS IN H_2O-SATURATED ARGON AT VARIOUS TEMPERATURES[17]

Cr content (balance Fe), wt.%	Temp., °C	Weight gain, mg/dm², after indicated time			
		7 hr	20 hr	30 hr	40 hr
5	1100	30	71	104	131
10	1100	30	79	111	146
15	1100	25	69	107	137
20	1100	3	12	18	23
5	900	14	28	36	44
10	900	16	41	53	62
15	900	17	37	43	53
5	700	4	8	11	13
10	700	5	9	13	14

Corrosion by Liquid Metals

The proceedings of a recent joint NASA-AEC Liquid-Metals Corrosion Meeting have been published.[18] Representatives attended from 18 laboratories engaged in various facets of liquid-metal research, much of which is directed toward nuclear vapor-cycle space power systems. Extensive high-temperature-corrosion and heat-transfer work in progress was described, although only meager results have been obtained to date. As a whole, the materials receiving most attention for containment of sodium, NaK, potassium, rubidium, and lithium at temperatures in the 2000°F range are niobium-zirconium alloys. Candidate containment materials for lower temperature mercury systems include carbon steels which are clad with materials such as 1¼ wt.% chromium–½ wt.% molybdenum steel and Inconel.

Information obtained from studies of the corrosion behavior of molten uranium-bismuth alloys conducted at Brookhaven has been summarized in previous issues of *Reactor Core Materials* (the most recent being Vol. 3, No. 4). This research has demonstrated the importance of magnesium and zirconium additives in forming corrosion-resistant films on exposed surfaces. With these additives present, it has been possible to operate 550°C peak-temperature forced-convection loops, fabricated of various ferritic steels of interest, for several thousand hours without evidence of more than trace corrosion effects.

To explore the influence of nuclear radiation and fission-fragment bombardment in this corrosion situation, Brookhaven conducted a series of in-pile capsule experiments with specimens of laboratory-proven materials exposed to zirconium-magnesium-inhibited uranium-bismuth alloy.[19,20] Irradiation conditions included temperatures up to about 650°C, fluxes in the neighborhood of 10^{13} neutrons/(cm²)(sec), and exposure times up to 90 days. Postirradiation observations indicated that the effectiveness of the film protection created by the magnesium and zirconium additives was appreciably reduced in the irradiation environment. A leading example of behavior is that for 1¼ wt.% chromium–0.5 wt.% molybdenum steel. After over 20,000 hr of service (in a

laboratory loop with a hot-leg temperature of about 550°C), this material did not exhibit hot-zone corrosion; a 60-day capsule exposure of the material at 590°C produced heavy intergranular corrosion. Increasing the zirconium content from 250 to 1000 ppm reduced such attack somewhat, leading to the speculation that a higher zirconium concentration might be beneficial. (J. H. Stang)

Radiation Effects in Nonfuel Materials

Defects: Structure and Properties

Metals. The dynamics of radiation events is being studied by means of machine calculations.[21] The model used represents copper at absolute zero with event energies below 400 ev. Orbits of the displaced atoms are found, as well as the resulting damage configuration. Permanent damage consists of vacancies and interstitials as has previously been assumed. The model consists of "crystals" of either 500 or 1000 atoms in which reasonable interaction forces are used along with classical collision theory. A variety of initial conditions have been investigated. Energy thresholds for interstitial formation were found to be about 25 ev in the ⟨100⟩ directions, 25 to 30 ev in the ⟨110⟩ directions, and 85 ev in the ⟨111⟩ directions. Collision chains in the ⟨100⟩ and ⟨110⟩ directions are prominent at low energies. These chains are found to defocus at high energies. Local heating effects and a process similar to a displacement spike have been observed. Various static configurations of defects have also been studied. For example, the interstitial is found to reside in a position where it shares a lattice site with another atom. Crowdions are not found to be stable, and Frenkel pairs are found to be stable only beyond minimum separations which are very dependent on orientation.

Blewitt et al.[22] investigated the differences between the recovery of neutron damage and electron damage in copper and aluminum at temperatures below 45°K. It was felt that neutron damage which arises from primary displacements where the energy is several orders of magnitude greater than the displacement threshold would result in recovery dependent on the energy of the primary displacement. The change in energy is accomplished by using the U^{235} fission reaction and the $B^{10}(n,\alpha)Li^7$ reaction. The results showed that the U^{235} fission produced about 900 times as many defects as a reactor neutron, whereas the B^{10} fission produced about eight times as many. Isochronal annealing of neutron-irradiated copper showed no peaks below ~40°K. Uranium-235 doped copper and aluminum show exponential saturation of damage, with the same character as the damage produced by fast-neutron irradiation, but there is a strong suppression of the 40°K peak at high damage concentrations. The B^{10} doped copper shows peaks at lower temperatures similar to those produced by electron irradiation. Defect production rates for these experiments were inferred from length-change measurements. The recovery of neutron damage in silver, gold, nickel, palladium, platinum, and aluminum was also studied between 4°K and room temperature. The observed annealing structure was not similar to that produced by electron or deuteron irradiations.

Thompson et al.[22] made room-temperature measurements of the internal friction in copper single crystals during neutron irradiation at frequencies from 10 to 110 Mc, using the pulse-echo method. The pinning of dislocation lines by radiation defects causes a transition from damping-limited dislocation motion to line-tension-limited motion as predicted for this case by Granato and Lucke [*J. Appl. Phys.*, 27: 583, 789 (1956)].

Displacement spikes have been observed in gold films by transmission electron microscopy[23] after irradiation with 4.2×10^{17} fast neutrons/cm^2. This directly supports Brinkman's theory. The gold was in the form of thin vacuum-deposited discrete particles (a discontinuous film). Spikes were observed as small black spots with a mean density of 3×10^{16}/cm^3 (this is in good agreement with the theoretical calculations of 9×10^{16}/cm^3 under these conditions). The average diameter of the displacement spikes was found to be 65 ± 7 A, again in good agreement with the theory.

Goland[24] attempted to transform gray tin into white tin as a result of localized heating produced by thermal spikes generated during irradiation. X-ray diffraction showed no increase in the white tin content after an 87-hr irradiation of 7.2×10^{12} neutrons/(cm^2)(sec) at 0°C. This irradiation should have transformed 16 per cent of the gray tin according to a modest es-

timate of the theory. He suggests the following explanations: (1) the time was too short to produce thermal equilibrium, (2) the temperature of the spikes was too low to produce transformation, or (3) strain fields might have returned the white tin to gray.

The range of relative rates of energy loss for five products of the thermal-neutron-induced U^{235} fission has been measured radiochemically in aluminum and gold.[25] Range-velocity relations were obtained from these measurements. The functional forms of these relations are assumed to hold for fission products of any mass. Observations were interpreted in terms of the average component of the range perpendicular to the original velocity. The value of this component in gold was estimated to be about one-fifth of the total range.

X-ray line broadening due to fast-neutron irradiation (1.4×10^{20} neutrons/cm^2 at 22°C) has been observed by the Canadians in gold and platinum. Strain, as opposed to a decrease in crystalline size, is believed to be the cause of the broadening. A smaller effect was noted in palladium and molybdenum, while the broadening in aluminum was negligible. After exposure to 1.4×10^{20} fast neutrons/cm^2 at 50°C, the following density changes were observed in high-purity materials: copper, -0.009 ± 0.003 per cent; molybdenum, -0.011 ± 0.002 per cent; and tungsten, -0.015 ± 0.004 per cent. Changes for the same exposure were undetectable or insignificant in aluminum, palladium, gold, and zirconium.*

Nenno and Kauffman[26] have also determined the equilibrium vacancy concentration near melting in high-purity aluminum. Their method consisted primarily in combining the bulk and lattice thermal-expansion measurements made simultaneously on the same specimen. This is essentially the same method as that used by Simmons and Balluffi[27] which has been previously reported. The results of the two experiments are in agreement. Nenno reports a fractional vacancy concentration of $1.1 \pm 0.2 \times 10^{-3}$ at melting, with a formation energy per vacancy of 0.64 ± 0.12 ev.

Lattice vacancies have been observed to decrease the elastic modulus of aluminum while using dynamic measurements.[28] Annealing of this decrease shows the same dependence on time and temperature as the annealing of the electrical resistivity due to vacancies.

The increased yield stress in niobium due to neutron irradiation (~10^{20} neutrons/cm^2 at 16°C) has been explained in terms of a vacancy mechanism.[29] A further increase is observed during annealing between 125 and 175°C, forming a yield drop at the start of deformation. The activation energy is 1.30 ± 0.1 ev, and it is concluded that this process is due to vacancy migration, the yield drop being due to the condensation of irradiation-produced vacancies on dislocations.

After neutron irradiation (1×10^{18} nvt), pure iron with a permeability of about 150,000 shows a decrease in permeability (about 20 per cent) and an increase in coercive force.[30] Preliminary annealing experiments indicate this effect is due to the formation of large (of the order of 1000 A) defects during the irradiation as well as the formation of anisotropic defects which interact with the magnetization vector. Future experiments are planned to investigate the relative importance to the magnetic properties of each type of defect.

An effect of total neutron exposure on the annealing kinetics of irradiated molybdenum has been observed[31] by means of X-ray diffraction. Irradiations of 10^{18} and 10^{19} nvt produced a large decrease in lattice parameter when the specimens were annealed between 50 and 200°C. No decrease is observed in this temperature range if the samples were previously irradiated to exposures of 5×10^{19} nvt or greater. This behavior is explained by the formation of interstitial clusters during irradiations. The higher exposures apparently tied up a fundamental defect (interstitial) which was produced during initial stages of the irradiation. This results in a type of damage that is stable and does not anneal out until high temperatures are reached.

Recovery of irradiated iron also has been studied[32] at 175 and 375°C. Recovery at 375°C after a dose of 1.5×10^{20} nvt is characterized by first-order kinetics. The activation energy for this reaction, calculated on the basis of incomplete data, was 0.5 ev (11,400 cal). A possible mechanism is the radiation-induced resolution of Fe_4N or a complex nitride upon annealing. Recovery at an exposure of 4.4×10^{18} nvt at 175°C involves an activation energy of

*G. R. Piercy and R. H. Tuxworth, The Effect of Fast-Neutron Irradiation on the Density, X-ray Lattice Parameter, and Line Breadth of Metals, Canadian Report CRRM-1010, April 1961.

0.3 ev. The reaction order appears to be intermediate, indicating a complex reaction.

Defects in Other Materials. Klick[32] proposes an explanation for the formation of Frenkel defects in alkali halides at low temperatures. Frenkel defects are felt to be the cause of sites that produce coloration at low temperatures. The suggested mechanism is free of some of the objections to previous proposals. Klick proposes that the double ionization of a halide ion, or single ionization of two adjacent halide ions, leads to the formation of an uncharged halogen molecule which occupies two adjacent halide-ion sites. There is a high probability that this molecule will be localized at one of these sites by the jump of a nearby halide ion into the other site. This forms the interstitial-vacancy Frenkel pair.

Fission tracks have been observed[33,34] in UO_2 and in nonfissionable materials.[35] Transmission electron microscopy was used for direct observation of UO_2 films having a thickness of 100 A or less. Thicker films show a decrease in sensitivity. The observed tracks result from redistribution of surface material either in a hill-and-valley configuration[33] or in a group of hills[34,35] whose density increases near the end of the track. The minimum range of energy loss which registers a track is of the order of 1000 ev/A. The low number of observed long (4 to 12 μ) tracks, however, indicates that some unrecognized free-surface effect is contributing to the track register. Forked tracks produced by the interaction of a fission fragment and an oxygen atom have also been observed. Bierlein and Mastel's studies have been done in materials that have received heavier doses of neutron irradiation (up to 4.4×10^{19} nvt), whereas Noggle and Stiegler looked at individual fission tracks. The observed tracks are uniform in cross section (100 to 150 A); thus it is not obvious exactly where the fission event occurred. Also, the direction of the fission fragment cannot be determined. Likewise, the termination of the observed track is not necessarily indicative of the fission fragment's loss of energy, since it might have left the film. At the higher doses the UO_2 aggregated into isolated outgrowths with little material remaining in intimate contact with the substrate. Tracks in ZrO_2 were of similar character to those in UO_2, whereas tracks in platinum showed discrete perforations along the path length which may have resulted from local vaporization that occurred as well as from the observed deformation.

Nondestructive investigations of surface radiation damage in solids has been initiated by Young.[36] The procedure consists in studying the physical adsorption of an inert gas at low temperatures. The materials used initially were α-Al_2O_3 with krypton adsorption. The materials were exposed to neutron irradiation up to 2×10^{18} fast neutrons/cm^2 at 40°C. The shape of the adsorption isotherm and the differential molar entropy of the adsorbed phase have been studied. Young states that, in favorable cases, the defects should be separated into groups depending on their heats of adsorption.

The $\alpha \rightleftharpoons \beta$ inversion of pure SiO_2 cristobalite is markedly displaced to lower temperatures[37] by fast-neutron irradiation (1.3×10^{19} neutrons/cm^2) at 50°C. The lattice parameters increase. Tempering to 500°C does not change the irradiated state, whereas tempering at 1600°C gives a full recovery as well as a restoration of the inversion temperature to its preirradiated value. Addition of TiO_2 produces the same type of increase in lattice parameters and change in inversion temperature. (T. G. Knorr)

Theories of Radiation Effects

The binding energies of threefold complexes have been investigated,[38] treating the electrons as quasi-free and solving the Schrodinger equation by the partial-wave method. The ion core interactions are represented by a Born-Mayer potential. Threefold complexes are found to have binding energies about three times that of a twofold complex. Triangular arrangements and tetrahedral ones with a central atom are both considered; either may represent the more stable form, depending on the details of the potential. Entropy and displacement energy are also discussed briefly.

Calculations using a Morse-potential function in copper show that two vacancies will attract each other if they are less than 7 A apart.[39] At separations greater than 7 A, the vacancies do not interact appreciably. The most stable separation is the nearest-neighbor separation or divacancy configuration. The binding energy for the divacancy was found to be 0.64 ev. This energy corresponds to the recovery process observed in deuteron-irradiated copper at 220°K with an activation energy of 0.69 ev. Divacancies are also found to be active in the mechanism of self-diffusion in copper.

Lattice distortions about point defects in copper have been calculated[40] using the general method of Tewordt. Five hundred atoms are considered in the case of an interstitial, and 50 atoms are used for the vacancy. The elastic solutions that are joined to the displacements of the discrete particles are determined for an anisotropic continuum. The changes in volume of the crystal arising from the interstitial are found to be 0.911, 1.219, and 1.441 atomic volumes, respectively, for the Morse potential, V_M, and the two Born-Mayer potentials, V_1 and V_2, which have been used. The corresponding values for the vacancy are −0.441, −0.378, and −0.321 atomic volume. The relaxation of the lattice is calculated around three configurations of interstitial pairs with axes in the ⟨1 0 0⟩, ⟨1 1 0⟩, and ⟨1 1 1⟩ directions, considering about 100 atoms as movable in each case. The contributions to the binding energies arising from the potential V_1 turn out to be 0.81, 0.18, and −0.26 ev, respectively. This strongly indicates that interstitial pairs can attract one another. The stability of the 10 closed interstitial-vacancy pairs (Frenkel pairs) is examined. All pairs smaller than 1.5 lattice constants in diameter are found to be unstable; the other pairs are stable and give a discrete spectrum of Born-Mayer energies. The results are discussed in connection with recent experiments in the field of radiation damage.

Rossin[41] reported on calculations of neutron damage in iron with various fluxes available at different installations. He used a simple model where the average number of defects produced per neutron is proportional, to the first approximation, to the product of the cross section for elastic scattering by target atoms and the neutron energy.

Simple arguments have been advanced to prove that an arbitrary body filled with a finely distributed random distribution of defects will be homogeneously dilated, regardless of whether the strains are elastic (as shown before) or not.[42] This assumes, of course, that the defects are acting as centers of dilation. In taking measurements on nonuniformly irradiated specimens, caution must be observed, since such damage produces inhomogeneous stresses (macroscopically).

Impurity resistance in metals has been calculated[43] by means of a many-particle formulation. Emphasis was placed on the role of electron-electron interactions. The model assumed was that of a dense Fermi gas of electrons moving in a uniform background of a few positively charged impurities. Expressions result which are of the form of the standard classical transport coefficients. Present restrictions are absolute zero temperature and a simple electron conductivity produced by an external field. However, Langer feels that the methods developed will be useful in extending the calculations beyond these limits.

March and Murray[44] have developed a theory to replace Mott's first-order approximation for dealing with imperfections in metals. This is accomplished by showing that, for a nonspherical potential energy, the work of Green on the quantum-mechanical partition function may be utilized to yield a perturbation theory for the Dirac matrix. (T. G. Knorr)

Surveys on Radiation-Induced Defects

An extensive report on the effects of neutron irradiation on the properties of iron and steel has been prepared by Harries.[45] Not only are the mechanical properties discussed, but also the magnetic properties and annealing of the radiation damage. Mechanisms based on defects are incorporated as explanations for all the property changes.

A short survey of the research effort on the effects of radiation on structural materials has appeared.[46] The properties reported are: electrical, thermal stored energy, elastic, diffraction, diffusion, and mechanical. (T. G. Knorr)

Effects of Radiation on Mechanical Properties

As indicated in Table IV-2, the British[47] found that the increase in transition temperature of steels as a result of fast-neutron exposures to 10^{20} nvt was greater when the irradiation temperature was 130 to 140°C than when it was 50 to 60°C. Since increased temperatures are known to anneal out radiation damage, there appears to be a peak in the irradiation temperature–transition temperature relation. Similar increases were caused by 10 to 20 per cent compressive strain and aging 1 hr at 200°C.

Oak Ridge[22] is studying the effects of annealing on the recovery of properties after irradiation at 1 to 3×10^{19} neutrons/cm^2 in the Oak Ridge Research Reactor (ORR) pool-side facility. After as many as five stages of impact transition-temperature recovery, ASTM A-212

Table IV-2 EFFECT OF NEUTRON IRRADIATION ON THE BEND TRANSITION TEMPERATURE OF TWO STEELS[47]

(Evaluation Was by a Slow-Bend Test Using Standard Izod Specimens of 4⅝-In.-Thick Plate. The Transition Was Determined Visually When Fracture Was 50 Per Cent Fibrous and 50 Per Cent Brittle.)

Irradiation temp., °C	Bend transition temperatures for the indicated conditions, °C		
	Unirradiated	5×10^{19} neutrons/cm^2	1×10^{20} neutrons/cm^2
Low-Alloy Steel: 1.2 Mn, 0.5 Cr, 0.25 Mo, 0.15 C			
50–60	0	+40	+72
130–140	0	+65	+77
Plain Carbon Steel: 0.14 C			
50–60	−75	−45	
130–140	−75	−25	

grade B steel recovered 90 per cent after annealing 1.5 hr at 850°F. A similar steel containing higher manganese (Swedish 21YY) required somewhat lower temperatures and appeared to recover in a less complex manner.

The Russians[48] have studied the effect of irradiation on the mechanical properties of iron, nickel, molybdenum, and some austenitic steels. As indicated in Table IV-3, an irradiation of 1.8×10^{20} fast neutrons/cm^2 at 40 to 70°C increased strength, hardness, and electrical resistivity and decreased ductility. There were no changes in the microstructures of iron, nickel, or molybdenum as a result of the irradiation or postannealing. By analyzing the decrease of hardness of the irradiation specimens with annealing time and temperature, the authors found that the hardening was caused by two types of defects which annealed out with activation energies of 16,500 and 28,700 cal/mole without involving diffusion.

In other Russian work[49] the effect of 0.9 to 3.4×10^{20} thermal neutrons/cm^2 (fast flux one-fourth thermal) at 450 to 650°C was determined on the mechanical properties of three chromium-nickel austenitic, six 17 Cr ferritic, five 13 Cr ferritic-martensitic steels, and commercially pure molybdenum. Control specimens were given similar heat-treatments outside the reactor. Results indicate that hardening in the austenitic steels was caused by precipitation and not by the irradiation. The environment did not significantly affect the properties of the other steels in the stabilized conditions. However, the strength of molybdenum was found to increase and the ductility to decrease. The authors conclude that, because of its high melting point, molybdenum is hardened by irradiation at 450 to 650°C, which is apparently high enough to anneal out radiation-induced defect production in the steels.

The effect of irradiation on the tensile properties of molybdenum has been investigated in British research.[50] Subsize cylindrical tensile specimens were made from arc-cast, wrought,

Table IV-3 ROOM-TEMPERATURE PROPERTIES OF CERTAIN METALS AFTER A NEUTRON IRRADIATION[48] OF 1.8×10^{20} FAST NEUTRONS/CM^2 AT 40 TO 70°C

Material, wt.%	Ultimate tensile strength, kg/mm^2		Elongation, %		Microhardness, kg/mm^2		Electrical resistivity, μohm-cm		Minimum postannealing temp. to remove hardness increase, °C
	Before irradiation	After irradiation	Before irradiation	After irradiation	Before irradiation	After irradiation	Before irradiation	After irradiation	
Metals Annealed 1 Hr at 760°C									
99.84 Fe	39.5	59.5	36.5	15.0	117.0	185.0	15.2	16.4	450
99.97 Ni	43.0	59.0	49.5	26.0	115.0	199.0	7.8	8.2	600
99.9 Mo	69.0		27.0	2.0	215.0	303.0	5.5	7.3	1050
Steels Water Quenched from 1100°C									
0.14 C, 16.0 Cr, 9.5 Ni	62.0	71.0	69.0	47.0	157.0	252.0			650
0.11 C, 16.7 Cr, 9.2 Ni, 0.6 Ti	63.5	75.0	77.0	49.0	150.0	260.0			650
0.09 C, 16.6 Cr, 12.0 Ni	54.5	66.5	65.0	41.0	135.0	235.0			650
0.10 C, 17.2 Cr, 12.4 Ni, 2.1 Mo, 0.5 Ti	60.0	70.5	71.5	43.5	143.0	241.0	77.0	77.6	650
1.12 C, 16.1 Cr, 16.9 Ni	51.5	63.0	58.0	36.0	131.0	232.0	76.9	77.6	600

and recrystallized material with grain diameters ranging from 0.03 to 0.26 mm. The specimens were subjected to 2×10^{19} epithermal neutrons/cm^2 (10 per cent having energies >1 Mev). The results of Fig. IV-1 indicate that the yield

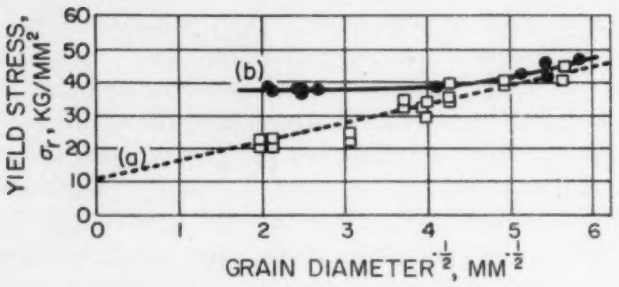

Fig. IV-1 The effect of grain size on the yield stress of molybdenum (*a*) before irradiation and (*b*) after irradiation.[50]

strength is increased, especially for large grain sizes. The mechanism of irradiation embrittlement appears more complex than that analyzable by Petch equations (relating yield strength and grain size) for EN2 steel.[51]

Oak Ridge[22] is conducting tube burst tests on Inconel, Zircaloy-2, type 304 stainless steel, and niobium. Results for types 304 and 304 ELC steel showed that the rupture life decreased by a factor of about 2 at stresses of 2500 and 3500 psi at 1500°F in air for material irradiated to about 10^{19} neutrons(>1 Mev)/cm^2. At 1300°F there was little radiation-induced change in rupture life at 9000 or 1300 psi.

The effect of irradiation on the room-temperature properties of tantalum has been studied at Battelle.[52] Electron-beam refined, cold-rolled, 30-mil tantalum-sheet tensile specimens were irradiated in the MTR to produce conversions of tantalum to tungsten of about 1.5 and 3.0 per cent. Unirradiated tantalum and arc-melted and cold-rolled tantalum–1.5 wt.% tungsten and tantalum–3.0 wt.% tungsten alloys were tested for comparison with the unirradiated material. As indicated in Table IV-4, the tensile and yield strengths increased, and the ductility decreased for the irradiated material. However, the unirradiated tantalum-tungsten alloys had properties similar to those of unirradiated tantalum. The results indicate that irradiation increased the strength of tantalum primarily by defect production, and to a much lesser extent by conversion to tungsten.

The effect of irradiation (about 10^{20} thermal neutrons/cm^2) on two ceramics, B_4C and BN, and on three stainless-steel-clad particulate cermets, BN-Ni, CaB_6-Fe, and Cu-B_4C containing natural boron, has been studied at Oak Ridge.[53] B_4C retained dimensional stability at 1 per cent average B^{10} burnup at temperatures up to 815°F. Property changes and gas evolution were measured in irradiated hot-pressed and powder BN. There was good dimensional stability up to 6 per cent burnup at 1780°F. The BN-Ni and CaB_6-Fe cermets showed damage at burnups of 38 per cent at 345°F. The Cu-B_4C material showed damage above 790°F at 18 per cent burnup. This damage was thought to be caused primarily by thermal cycling.

(B. C. Allen)

Table IV-4 ROOM-TEMPERATURE MECHANICAL PROPERTIES OF UNIRRADIATED AND IRRADIATED TANTALUM AND TANTALUM-TUNGSTEN ALLOYS[52]

Specimen description	Integrated flux, 10^{20} thermal nvt*	Ultimate tensile strength, 1000 psi	Yield strength (0.2% offset), 1000 psi	Elongation in 1 in., %	Hardness (100-g load), KHN
Unirradiated Ta	0	42.0	30.0	40	103
Unirradiated Ta–1.5 wt.% W	0	44.9	31.0	39	151
Unirradiated Ta–3.0 wt.% W	0	52.4	38.5	35	170
Irradiated Ta (analyzing 0.6 to 0.8 wt.% W)	7.8	69.5	65.8	16	274
Irradiated Ta (analyzing 0.8 to 2.2 wt.% W)	15.7	86.3	81.4	7	309

*Fast neutron flux about one-tenth the thermal flux. Irradiation temperature was about 200°F.

Selected Metallurgical Aspects of Cladding and Structural Materials

Zirconium

Transformation studies on zirconium–2.5 wt.% niobium alloys are reported by Chalk River.[54] After being annealed at 650, 700, 800, and 900°C and then quenched, the zirconium–2.5 wt.% niobium alloy shows a structure which indicates that the alloy had been in the alpha-plus-beta region before quenching. For example, after 66 hr at 650°C, followed by air quenching, this alloy exhibits a structure of alpha grains and a constituent identified as transformed beta. These results suggest that the phase diagram by Ivanon et al., which places the maximum solubility of niobium in alpha zirconium at about 1.5 wt.%, is probably correct.

Workers at Case Institute of Technology, who are also examining the transformation characteristics of zirconium-niobium alloys,[55] have presented some interesting observations. The hypermonotectoid alloys are relatively complex and involve at least two, and possibly three, transformation mechanisms. A cellular mode of decomposition has been observed at temperatures both above and below the monotectoid temperatures. Thus this mode of decomposition appears to reflect primarily the tendency of the system to segregate into niobium-rich and niobium-poor regions, as contrasted to a eutectoidal type of decomposition of beta (zirconium rich) simultaneously supersaturated with respect to both alpha and beta (niobium rich). Further evidence for this is provided by the fact that direct precipitation of alpha from beta competes with the cellular reaction at sufficiently low temperatures.

Single-crystal studies of the omega reaction[55] confirm conclusions reached earlier that omega present in quenched zirconium–12 wt.% niobium alloys is supersaturated with niobium. The temperature at which this omega forms on quenching appears to be near 300°C. The quenched omega is a highly imperfect structure and consists of thin platelets parallel to beta (1 1 0) planes. Quenched omega can be interpreted as a highly faulted structure, and preliminary results suggest that the degree of faulting increases with niobium content of the alloy. Changes that occur on aging of quenched omega reflect annealing out of stacking faults and adjustments of composition to the values demanded by metastable equilibrium of omega with beta.

Tempering of martensite in the zirconium–5 wt.% niobium alloy appears to be a relatively simple process involving the precipitation of a niobium-rich beta phase from supersaturated alpha. Substantial hardening accompanies this precipitation.

Zirconium alloys containing additions of copper and molybdenum are under investigation at Oak Ridge,[56] where specimens of zirconium–1 wt.% copper, zirconium–1.6 wt.% copper, zirconium–4 wt.% molybdenum, and zirconium–7.5 wt.% molybdenum were transformed isothermally or by beta quench and reheat aging at 400, 500, 600, and 700°C for times up to 60 min. Hardness data collected show that an age-hardening reaction occurs in all four alloys for both types of transformation at temperatures of 400 and 500°C and that the hardness continually decreases for transformation by both techniques at 600 and 700°C. Metallographic examination has been difficult and of little aid in following the transformation behavior. Transformation studies are being extended to both shorter and longer times at several temperatures intermediate to those already used.

Russian data[57] indicate that the solubility of niobium in zirconium at 750°C is less than 1.4 wt.%. Thermal methods of analysis indicate the solubility of niobium in zirconium at 600°C to be about 5 wt.%, whereas X-ray data indicate that the solubility is less than 0.5 wt.%.

(J. A. DeMastry)

Refractory Metals

Tantalum. The solid-solubility limits of carbon, nitrogen, and oxygen in tantalum are reported by Battelle.[58] For carbon, the solid solubility is 0.07 at.% at 1500°C, decreasing to less than 0.07 at.% at 1000°C. Nitrogen dissolves to the extent of 3.70 at.% at 1500°C, decreasing linearly with temperature to 2.75 at.% at 1000°C and 1.8 at.% at 500°C. The oxygen solubility is reported to be 3.65 at.% at 1500°C, 2.95 at.% at 1000°C, and 2.5 at.% at 500°C. The phase Ta_2C, the low-temperature modification of Ta_2O_5, and the phase Ta_xN of unknown structure based upon the original body-centered cubic tantalum lattice have been identified as the initial precipitates in the respective systems.

Molybdenum. The English[59] have investigated the molybdenum-rhodium system above 1500°C

in the compositional range of 40 to 100 at.% rhodium. They report that the system contains intermediate hexagonal close packed or epsilon phase extending from roughly 45 to 82 at.% rhodium, the freezing point of which rises to a maximum at about 67 at.% rhodium. Rhodium can dissolve about 15 at.% molybdenum at high temperatures. The lattice spacing–composition relations of the epsilon phase are such that both a and c spacings diminish with increasing rhodium content, but the axial ratio c/a passes through a maximum in the region of 75 at.% rhodium.

Fabrication studies of molybdenum made by the University of California[60] have produced the following conclusions:

1. Large-grained molybdenum specimens are more susceptible to brittle fracture at low temperatures than are single crystals. Both transgranular and intergranular cracking occur in polycrystals strained at low temperature.
2. Twin bands form when polycrystalline molybdenum fractures at low temperatures.
3. The traces of twin bands are parallel to {1 1 2} planes.
4. The twins are not planes but consist of many irregular prisms having areas parallel to the ⟨1 1 1⟩ direction; the prismatic faces are not parallel to {1 1 2} planes, but they are often parallel to {1 1 0} planes or to planes of irrational or higher indices.
5. Twinning is accompanied by localized slip in the region of the twin band.

Rhenium. The effects of rhenium additions to molybdenum, tungsten, and chromium, investigated at Battelle,[62] were reported as follows:

—Twinning appears to be associated with rhenium content only and occurs most profusely at the maximum rhenium solubility in molybdenum. No indications of long- or short-range ordering have been found for molybdenum–35 wt.% rhenium. The amount of twinning decreases with increasing temperature for a given composition.

—Twinning effects appear during tensile testing as discontinuities in the stress-strain curves, resulting in serrations in the stress-strain curve similar to the discontinuities caused by interstitial locking. The yield-point behavior in these alloys is attributed to an audible burst of twins as the critical twinning stress is exceeded.

—In tungsten-rhenium alloys the solubility limit for alloys quenched from 1800°C occurs at about 25 wt.% rhenium. Recrystallized tungsten–28 wt.% rhenium (most ductile) has a brittle-to-ductile transition range of 150 to 200°C. Twinning decreases in quantity with increasing temperature and is observed at room temperature in alloys containing 22 to 30 wt.% rhenium. In tungsten–30 wt.% rhenium, twinning during tensile loading was apparent as discontinuities in the stress-strain curve but was not so heavy as in molybdenum–35 wt.% rhenium.

—The solubility of rhenium in chromium lies between 35 and 39 wt.%. Mechanical twinning at room temperature is observed at 35 to 44 wt.% rhenium. Rhenium imparts similar improvements in fabricability and ductility to all three Group VIA metals: chromium, molybdenum, and tungsten.

Additional investigations at Battelle[63] have been concerned with improving the properties of molybdenum, tungsten, and chromium by additions of other metals besides rhenium. Twinning is produced by additions of the platinum-group metals (except palladium). The tendency to twin on deformation increases with increasing alloy content and appears to be at a maximum near the terminal solubility limit. Twinning also is increased by decreasing the deformation temperatures, but homogenizing or annealing the alloys reduces the capacity for twinning. The cast hardness is reduced significantly by additions of Group VIIIA metals at levels of 0.1 to 1 at.%.

Niobium. The niobium-tin phase diagram as reported by Russian investigators[64] contains a compound Nb_3Sn which forms at 2000 ± 25°C. Liquid alloys with 60 wt.% tin and over are laminated. The temperature of monotectic reaction is 730 ± 5°C; a considerable diffusion area was found at the niobium side. The Nb_3Sn (29.87 at.% tin) has a structure with a = ±5.29 A and has a Vickers hardness of 900 kg/mm². Transition of the corresponding state is at 18.05°K. Solid solutions of niobium and tin have better hardness and better oxidation resistance than pure niobium.

A study of the niobium-zinc system was initiated by the Naval Research Laboratory[65] to assist in understanding the high-temperature oxidation resistance of zinc-coated niobium. The existence of three compounds was indicated. On the basis of weight gain, the composition of

the high-zinc compound was estimated to be $NbZn_3$; this was confirmed by a structure determination using the X-ray powder method and by chemical analysis. X-ray examination samples quenched from 475 and 870°C showed no apparent reduction in the intensities of lines with mixed indices. It is concluded that no order-disorder transformation occurs within the temperature range considered, unless the solid-state diffusion rates are sufficiently rapid to allow the transformation to occur during quenching.

Nine binary constitution diagrams and one ternary diagram of some of the refractory metals are presented in a report by Nuclear Metals.[66] The binary diagrams include Hf-Mo, Hf-Re, Hf-W, Nb-Re, Os-Ta, Os-W, Re-Ta, Ru-Ta, Ru-W, and the ternary Re-Ta-W.

(J. A. DeMastry)

Iron- and Nickel-Base Alloys

Graphite coated with Si-SiC was placed in contact with various metals at 1650°F for 1800 hr by investigators at General Atomic.[67] One set of specimens was exposed in ungettered helium, and one set was exposed in helium which had been purified with a zirconium getter. The following conclusions were drawn:

1. Nickel reacted with the Si-SiC layer to a maximum depth of 10 mils.
2. Monel reacted (melted) to a maximum depth of 20 mils.
3. Niobium – 5 wt.% zinc and niobium – 10 wt.% titanium increased considerably in hardness near the edge exposed to Si-SiC. Some specimens showed surface layers that penetrated to a depth of 5 to 10 mils.
4. Inconel reacted with the Si-SiC layer to a depth of 8 to 10 mils and carburized completely; no benefit from zirconium gettering was noted.
5. Types 430 and 430 Ti stainless steel reacted with Si-SiC to a depth of 5 mils and were carburized, no benefit being derived from zirconium gettering.
6. Types 304 and 316 stainless steel reacted to a depth of 2 to 5 mils and were completely carburized, showing no benefit from zirconium gettering.

The age-hardening characteristics of manganese-vanadium-molybdenum austenitic steels were determined by the Naval Research Laboratory[68] as a function of the temperature of the solution treatment. The optimum condition for developing the full age-hardening potential of the alloy is ½ hr at 2100°F, followed by water quenching. Subsequent aging treatments for maximum hardness levels are: 1 hr at 1400°F, 6 hr at 1300°F, or 16 hr at 1200°F. An aging temperature between 1200 and 1300°F is optimum for controlling the balance between yield strength and ductility.

Investigations of the basic slip mechanism of several iron-aluminum alloys for Denver Research[69] indicate crystallographic type slip on the {1 1 0} plane for Thermenol and the binary alloys (Alfenols) containing 10, 13.9, and 16 wt.% aluminum. The mechanism inhibiting banal glide in the binary alloys with increasing aluminum content appears to be in a transitional state at the 8 wt.% level, depending on orientation and the relative complexity of the operating stress systems. The superior ductility of the 8 per cent alloy in comparison with the higher aluminum levels may be accounted for by the fact that fracture occurs by shear rather than cleavage in this composition range. Heat-treatment studies based on resistivity versus temperature curves indicate that room-temperature tensile elongations up to 14 per cent are possible. These latter results were obtained with fully recovered microstructures, indicating that recovered structures may be less notch sensitive than the recrystallized microstructure.

Outside of grain refinement, the beneficial effects of rare-earth scavenging additions on ductility have not been clearly established.

The relative graphitization rates of nickel-copper alloys for graphite cladding were determined by General Atomic.[70] The optimum composition for this application is about 70 wt.% nickel – 30 wt.% copper. The Monel-composition alloys containing less copper graphitize when thermally cycled in contact with graphite, and alloys containing more copper have higher coefficients of expansion and lower melting temperatures. The solution of carbon in Monel does not decrease the strength or ductility at room temperature. Carburized Monel shows elongations greater than 14 per cent in stress rupture in the 1250 to 1650°F range. (J. A. DeMastry)

Ternary Refractory-Metal Alloys

Russian investigators[71] report on the stability of the beta phase in titanium-vanadium-molybdenum alloys as follows: Titanium-molybdenum-vanadium alloys quenched from

900°C, having a metastable beta-phase structure, were heated at 100 to 600°C with a holding time of 15 min to 100 hr. Alloys containing 9.4 to 14.2 wt.% molybdenum and 5.9 to 13.9 wt.% vanadium generally show the same beta-phase stability. The beta phase is preserved for a holding time of 100 hr at 100°C, 25 to 36 hr at 200°C, and 16 to 25 hr at 300°C. The beta-phase then decomposes, forming an omega phase. At 400 to 500°C the omega phase appears in 15 min and is preserved at 400°C for 81 to 100 hr. The omega phase is stable for 4 to 16 hr at 500°C and is then converted to an alpha phase. The hardness increases with the appearance of the omega phase and decreases with the appearance of the alpha phase. Increasing the vanadium content to 20 wt.% produced only a slight improvement in the stability of the beta phase. An alloy with 21.1 wt.% molybdenum and 9.7 wt.% vanadium had the greatest beta-phase stability at 100 to 400°C. The beta-phase stability in titanium-molybdenum-vanadium alloys increases with increasing molybdenum content. Data obtained previously on titanium-molybdenum-manganese alloys show that manganese is more effective than molybdenum in increasing the stability of the beta phase. Thus the titanium alloy with 17.9 wt.% manganese and 4.6 wt.% molybdenum possesses good beta-phase stability on heating at 100 to 600°C, but the titanium alloy with 27.0 wt.% molybdenum and 3.8 wt.% manganese does not. Iron is more effective than manganese or vanadium in stabilizing the beta phase when added in amounts of 5 to 6 wt.% to a titanium-molybdenum alloy.

The stability of the metastable beta phase was investigated in titanium-vanadium alloys by the Russians[72] from −196 to 500°C, with vanadium contents of 3.7, 12.8, 14.2, 15.1, and 19.3 wt.% on a base of titanium made by thermal reduction with magnesium. The results of microstructural and X-ray analyses of alloys quenched in water at 20°C show that the beta phase is fixed in an alloy with 19.3 wt.% vanadium on quenching from 850°C. The alloy with 15.1 wt.% vanadium quenched from 1000°C has a beta-plus-omega phase structure. The 3.7 wt.% vanadium alloy quenched from 900 to 1000°C has the structure of a supersaturated alpha phase (α'). Alloys containing 16, 25, 30, 35, and 40 wt.% vanadium were prepared on a base of titanium made from titanium iodide. The iodide-derived titanium alloy with 15.6 wt.% vanadium had a beta-plus-omega structure on quenching from 900°C, just as was observed for the 15.1 wt.% vanadium alloy with a base of titanium derived by the thermal reduction with magnesium. All the other alloys containing 24.4 wt.% vanadium and higher had a structure of a beta solid solution (the boundary line of the transition from the beta phase to an alpha-plus-beta phase for iodide-derived alloys). The beta solid solution is stable at room temperature and lower, and at 100°C for 81 hr. On heating to 200 to 400°C, the beta solid solution decomposes to an intermediate omega phase which passes over into an alpha phase on increasing the holding time and temperature. The stability of the beta solid solution increases with increasing vanadium content, particularly at 200 to 400°C. Thus the beta-solid-solution alloy with 24.2 wt.% vanadium is stable at a temperature of 200 to 400°C for not more than 4 hr and 15 min, but the beta-solid-solution alloy with 34.3 wt.% vanadium is stable for 100 hr at the same temperature. In the high-vanadium-content (28.8 wt.%) alloys, the beta solid solution decomposes directly to the alpha phase without going through an intermediate omega phase, as the lower vanadium-content (24.4 wt.% and lower) alloy does. The maximum hardness values were found for the beta-plus-omega structure. The hardness of the beta alloys is about the same as that for the alpha-plus-beta alloys.

The electrical resistance and hardness of 32 nickel-chromium-tungsten alloys with a constant tungsten content of 5, 10, 20, and 30 wt.% and with a variable chromium content of 2, 5, 10, 15, 20, 25, 30, and 35 wt.% were investigated[73] after two different heat-treatments. Two sets of samples of each composition were annealed in vacuum at 1200°C for 24 hr and then at 1000°C for 100 hr. Then one set of samples was quenched, and the other set was further annealed at 800°C for an additional 100 hr and cooled in the furnace. It was shown that specific electrical resistance increases with increasing chromium content and attains a maximum in the regions where the ternary solid solution is saturated with respect to chromium and tungsten. Thus the specific electrical resistance of the quenched 5 wt.% tungsten alloy shows a maximum at 35 wt.% chromium, whereas the annealed 5 wt.% tungsten alloy shows a maximum resistivity at 30 wt.% chromium. The electrical resistance of the quenched and annealed samples indicates that the solubilities of

chromium and tungsten in the ternary solid solution of nickel vary with temperature.

Tungsten is more effective than chromium in improving the hardness of the nickel-chromium-tungsten alloy, both at room temperature and at elevated temperatures. An increase in tungsten content of only 7 at.% with a constant chromium content of 9 at.% results in an increase of the hardness of the alloy of 24 per cent at room temperature. At a constant chromium content of 25 wt.%, an increase in tungsten content results in an increase of hardness at moderate temperatures as compared with an alloy with a lower tungsten content. In addition, the decrease in hardness at elevated temperatures is significantly smaller for alloys with a higher tungsten content. Thus the hardness of an alloy with 5 wt.% tungsten and 25 wt.% chromium decreases by 24.7 per cent on increasing the temperature from 100 to 500°C. On increasing the tungsten content to 10 wt.%, the decrease in hardness between 100 and 500°C is 22.9 per cent; at 20 wt.% tungsten the decrease is 17.4 per cent, and at 30 wt.% tungsten the decrease in hardness is only 9 per cent, indicating the important role that tungsten plays in increasing the high-temperature hardness of alloys.

(J. A. DeMastry)

Diffusion Studies

A collection of Russian papers on diffusion of various elements in alloys and in steel and on tracer studies in metallurgy, as well as on various properties of alloys, is available in English.[74] Excerpts of 27 papers presented on these subjects have been translated. Diffusion studies reported in this collection include Co^{60} diffusion in nickel-molybdenum alloys, iron diffusion in iron-chromium alloys, and diffusion of iron and chromium at 900 to 1200°C in alpha Al_2O_3, alpha Cr_2O_3, $NiCr_2O_4$, and $NiAl_2O_4$. A series of investigations of diffusion in zirconium and certain zirconium alloys are also reported. Coefficients were determined for self-diffusion in zirconium at 700 to 1200°C and in niobium-zirconium and tantalum-zirconium at 900 to 1200°C, for tantalum diffusion in zirconium at 700 to 1200°C, and for self-diffusion in zirconium and some of its alloys at 300 to 1200°C. A translation[75] of another Russian article describes a study of the diffusion of zirconium and tin in alpha solid solutions of these metals. The data indicate that alloying alpha zirconium with tin increases the activation energy of zirconium self-diffusion and tin self-diffusion. Also, a compilation of papers is presented in a translation from Russian[76] in which information is given on molybdenum self-diffusion, diffusion of tungsten in molybdenum, and diffusion in high-temperature cobalt-base alloys. In the Russian literature the effect of polymorphic transformation on diffusion of Sn^{113} in titanium has been reported.[77]

The diffusion of hydrogen through zirconium is being studied at Atomics International[78] for a particular application in which liquid sodium is the source of the hydrogen. Concentration-ratio data for various times and temperatures from 250 to 400°C have been obtained. It is pointed out by the author that, if an effective oxide film forms on the zirconium, it would lessen the rate of diffusion as compared to his analysis.

A method to study the diffusion between two metals, one of which is volatile and not very soluble in the other, is described in a French paper.[79] The method was applied to the diffusion of strontium and lanthanum in uranium. Also, the previously reviewed studies by French workers on the effect of external pressure on diffusion in uranium-copper systems have been extended to the uranium-aluminum and uranium-nickel systems.[80] A French paper on uranium-titanium interdiffusion and accompanying Kirkendall effect referenced in the February 1960 issue of *Reactor Core Materials* has been republished in French in *Acta Metallurgica*, with an English abstract.[81]

Preliminary studies were made by Nuclear Metals[5] on the mechanisms and rate constants for liquid-solid interactions between uranium and cladding materials of interest for fast reactors. Although the studies have been discontinued, some data were obtained for the interdiffusion between iron and uranium at temperatures between the threshold for formation of a liquid eutectic (725°C) and the melting point of uranium (1129°C). Limited study of the interaction between liquid uranium and solid zirconium was also made; the rate-determining step for this interaction is the diffusion of zirconium through the molten uranium.

Studies of the diffusion of xenon through aluminum, stainless steel, and the Piqua fuel-element cladding (aluminum plus thin nickel bond) by a radioactive technique are reported by Brookhaven.[82] Xenon was found not to diffuse

through aluminum as thin as 0.010 in. in the temperature range 295 to 473°C. Stainless-steel specimens (0.020 in. thick) showed no evidence of xenon diffusion up to 610°C. Values for the permeability through the Piqua cladding appear anomalous. Also reported in the literature[83] is a study of the diffusion of Xe^{135} in graphite at 400 to 1200°C. Measurements of the mutual diffusion coefficient, D_{12}, of argon and helium in AGOT graphite have been made by Oak Ridge[7] at room temperature, 0°C, and −65°C. All data are reported to fit the equation

$$D_{12} = 4.22 \times 10^{13} D_{12}^{*}$$

where D_{12}^{*} is the classical "free-space" diffusion coefficient of helium and argon in square centimeters per second. It is concluded therefore that the diffusion mechanism is classical and that, if mechanisms such as surface diffusion which might result from an adsorbed (liquid) layer exist, their effects must be less than experimental error (approximately 8 per cent). Also being studied[7] is the diffusion of fission products in porous graphite matrices at reactor operating temperatures. Studies of rates of diffusion of BaO, SrO, Y_2O_3, and ZrO_2 in reactor graphite have shown that the mechanism is a complex, multistep, transfer process. The data presented indicate that, unlike noble-gas transfer (above), surface diffusion and chemical reactions might be significant contributing mechanisms. (D. C. Carmichael)

Selected Mechanical Properties of Cladding and Structural Materials

Zirconium and Zirconium Alloys

The Canadians* have investigated the mechanical properties of two zirconium-base alloys. The room-temperature and 300°C tensile properties of a zirconium−2.5 wt.% niobium alloy are shown in Table IV-5. The inferior strengths of samples 1, 2, and 3 probably resulted from an unintentional slower quench. The impact and creep properties of zirconium−3 wt.% aluminum−0.5 wt.% molybdenum were determined. The total energy absorbed during fracture at room temperature was from 8 to 10 ft-lb. The creep rates after 2000 hr of test at stresses of 40,000 to 50,000 psi at 300°C was 2 to 5×10^{-5} per cent per hour. The properties of a number of zirconium alloys are compared with those of Zircaloy-2 in a review prepared by Thomas.[54] This review also includes properties of several high-strength zirconium alloys.

Hanford workers[2,31,84] have found that the activation energy for creep of 25 and 45 per cent cold-worked Zircaloy-2 in the 330 to 365°C temperature range is between 60,900 and 64,700 cal/g-atom. The lower values are associated with the 25 per cent cold-worked material. Creep tests on PRTR Zircaloy-2 process tubing are being conducted by internal pressurization. Investigations are being made at one test temperature, 345°C, and two stresses, 2250 and 1650 psi. After 100 hr the higher stressed tube had shown almost 13 times the increase in diameter exhibited by the lower stressed tube. Ultimate tensile strengths of extruded Zircaloy-2 tubes as determined by burst tests were consistently higher than those derived from uniaxial tensile tests, as shown in Table IV-6. The differences (9 to 27 per cent) appear to be related to sample history and probably reflect various degrees of preferred orientation.

Workers at Atomics International[85] have investigated contamination of Zircaloy-2 by heating in air at 1000 to 1050°F for 1 hr. No change in mechanical properties related to contamination could be detected. Still another investigation conducted at Bettis[1] has been concerned with changes in mechanical properties as influenced by fabrication practice on Zircaloy-2. The effects of specimen size and geometry and test direction on the tensile properties were studied at room temperature and 600°F. The greatest changes noted were related to direction of test and stages of fabrication. These were evidenced by a difference in 0.2 per cent offset yield strength and elongation. The ultimate tensile strength was relatively insensitive to stages of fabrication or specimen size, at both temperatures studied.

Stress-relaxation studies[2] of Zircaloy-2 at 300°C on annealed 18.5 and 22 per cent cold-worked material have shown that, for stresses between 13,500 and 15,400 psi, the greatest reduction in stress occurs in the first 350 hr. The mechanical properties of Zircaloy-2 sheath have been determined by Du Pont[86] at room temperature. These sheaths had been swaged

*W. R. Thomas, Atomic Energy of Canada, Ltd., 1960. (Unpublished)

Table IV-5 TENSILE PROPERTIES OF ZIRCONIUM–2.5 WT.% NIOBIUM AT ROOM TEMPERATURE AND 300°C*

Specimen	Heat-treatment	Test temp., °C	Yield strength (0.2% offset), 1000 psi	Ultimate tensile strength, 1000 psi	Elongation, %
1	1 hr at 880°C,	RT	90.6	104.9	19.8
4	water quenched + 24 hr	RT	112.4	124.8	11.5
2	at 500°C	300	49.0	60.8	20.5
6		300	80.7	88.6	14.0
3	Water quenched + 6 hr	300	67.2	75.0	13.0
5	at 500°C	300	75.0	83.4	12.0

*W. R. Thomas, Atomic Energy of Canada, Ltd., 1960. (Unpublished)

Table IV-6 MECHANICAL PROPERTIES OF ZIRCALOY-2 TUBES* AT ROOM TEMPERATURE[84]

Condition	Ultimate tensile strength, psi	
	Burst test	Uniaxial tension test
5% cold work	65,400	50,700
11% cold work	65,500	56,000
14.4% cold work	64,900	58,900
17.8% cold work	72,000	63,400
5% cold work and annealed 2 hr at 750°C	41,800	35,400
17.8% cold work and annealed 2 hr at 750°C	52,600	38,600

*Extruded 14:1 at 870 to 900°C.

on fuel tubes of uranium dioxide. The properties of the as-received tubes, as compared with the as-swaged tubes, showed, as would be expected, increased strength resulting from swaging accompanied by a loss of ductility. A summary of creep tests being conducted at Battelle[87] on Zircaloy-2 at elevated temperatures is reported. These tests are expected to continue for as long as 25,000 hr in some instances.

Mechanical Properties of Steels

The creep buckling and collapse of AISI type 304 seamless stainless-steel tubing at 1200°F are being investigated by workers at Oak Ridge.[7] Collapse of 0.75-in.-OD tubes with 0.025-in. wall thickness occurred instantaneously at 800 psi and 1200°F. However, collapse was not evident after 475 hr at 600 psi and after 2225 hr at 400 psi at the same temperature. The effect of heat-treatment on the mechanical properties of AISI type 502 steel, an iron–4.76 wt.% chromium–0.55 wt.% molybdenum–0.53 wt.% manganese having 0.068 wt.% carbon, is also being studied.[7] The tensile, bend, and creep properties were examined at room temperature and 1200°F.

The notch toughness of ASTM A-212B plate is being investigated[7] by testing V-notch Charpy bars where the metal under the notch is made up of equal areas of weld metal and base metal. The heat-affected zone was contained in the base metal. Preheating of base plate to 200°F before welding appeared to lower the transition temperature for double-pass welds but not for the single-pass welds. General Atomic[67] has recently completed a study on the creep-rupture properties of a 1.25 wt.% chromium–0.5 wt.% molybdenum steel and AISI type 316 stainless steel in helium at 1000 and 1300°F. The rupture times up to 1000 hr do not appear to have been affected significantly by the helium atmosphere.

Mechanical Properties of Miscellaneous Alloys

A summary of work done by General Atomic[88] on a study to determine the effect of environment on the creep-rupture properties of Inconel 713C at elevated temperatures is presented. Results show that the rupture life at 1300 and 1500°F and the ductility of this material in helium are similar to the corresponding properties in air at the same temperatures. The fatigue properties of Hastelloy X tubing are being studied at Battelle.[89] An S-N curve will be developed for five temperatures: 1400, 1600, 1735, 1800, and 2000°F.

The creep and tensile properties of niobium–2.37 wt.% chromium, niobium–3.34 wt.% zirconium, niobium–5.2 wt.% vanadium, and niobium–1.56 wt.% zirconium–1.09 wt.% chromium alloys at 650, 800, and 1000°C are being investigated at Battelle.[87] (F. R. Shober)

References

1. Westinghouse Electric Corp., Bettis Atomic Power Laboratory, Bettis Technical Review, Reactor Technology, USAEC Report WAPD-BT-20, September 1960.
2. F. W. Albaugh, Reactor and Fuels Research and Development Operation Monthly Report for October 1960, USAEC Report HW-67254-A, Hanford Atomic Products Operation, Nov. 15, 1960. (Classified)
3. Nuclear Metals, Inc., Fundamental and Applied Research and Development in Metallurgy, Progress Report for September 1960, USAEC Report NMI-2089, Oct. 21, 1960.
4. S. Isserow et al., Monthly Progress Report to E. I. Du Pont de Nemours and Co., USAEC Report NMI-7031, Nuclear Metals, Inc., Sept. 20, 1960. (Classified)
5. Argonne National Laboratory, Reactor Development Program Progress Report, October 1960, USAEC Report ANL-6253, Nov. 15, 1960.
6. Argonne National Laboratory, Reactor Development Program Progress Report, November 1960, USAEC Report ANL-6269, Dec. 15, 1960.
7. Oak Ridge National Laboratory, Gas-Cooled Reactor Project Quarterly Progress Report for Period Ending September 30, 1960, USAEC Report ORNL-3015, Nov. 11, 1960.
8. R. P. Elliott, Columbium-Oxygen System, *Trans. Am. Soc. Metals*, 52: 990–1014 (1960).
9. F. J. Clauss and S. Drake, Study of Halide-Containing Oxide Films on Columbium, in Report LMSD-288140(Vol. II), Paper No. 10, Lockheed Aircraft Corp., January 1960.
10. R. A. Jeffreys and J. D. Gadd, Development and Evaluation of High-Temperature Coatings for Columbium Alloys, Report NP-9416, Thompson Ramo Wooldridge, Inc., July 1960.
11. R. H. Lorenz and A. B. Michael, Oxidation Resistant Silicide Coatings for Columbium and Tantalum Alloys by Vapor-Phase Reaction, Paper Presented at the 118th Meeting of the Electrochemical Society, Houston, Tex., October 1960.
12. J. A. DeMastry and R. F. Dickerson, Niobium—Promising High-Temperature Reactor Core Material, *Nucleonics*, 18(9): 87–90 (September 1960).
13. V. O. Lavrenko, Kinetics and Mechanism of High-Temperature Oxidation of Tantalum in Recrystallized and Cold-Hardened States, Russian Translation NP-tr-491, April 1960.
14. Oak Ridge National Laboratory, Nov. 4, 1960. (Unpublished)
15. E. E. Mathauser et al., Investigation of Problems Associated with the Use of Alloyed Molybdenum Sheet in Structures at Elevated Temperatures, Report NASA-TN-D-447, National Aeronautics and Space Administration, Oct. 25, 1960.
16. Argonne National Laboratory, Reactor Development Program Progress Report, USAEC Report ANL-6234, Oct. 14, 1960.
17. C. T. Fujii and R. A. Meussner, High-Temperature Oxidation of the Mechanism of Iron-Chromium Binary Alloys in Water Vapor, Report NRL-5506, Naval Research Laboratory, Sept. 21, 1960.
18. National Aeronautics and Space Administration, NASA-AEC Liquid Metals Corrosion Meeting, December 7–8, 1960, Washington, D. C., USAEC Report NASA-TN-D-769, February 1961.
19. Brookhaven National Laboratory, Progress Report, Nuclear Engineering Department, September 1–December 31, 1959, USAEC Report BNL-595, July 1960.
20. J. G. Y. Chow and R. A. Meyer, Corrosion of Metals in Fissioning Molten Uranium-Bismuth Solutions, *Trans. Am. Nuclear Soc.*, Session10, Paper 6 (December 1960).
21. J. B. Gibson et al., Dynamics of Radiation Damage, *Phys. Rev.*, 120: 1229 (1960).
22. Oak Ridge National Laboratory, Solid State Division Annual Report for the Period Ending August 31, 1960, USAEC Report ORNL-3017, 1960.
23. A. Grenall, Direct Observation of Fast Neutron Damage in Gold Films, USAEC Report NAA-SR-5062, Atomics International, July 15, 1960.
24. A. N. Goland, Neutron Irradiation of Gray Tin, *J. Phys. and Chem. Solids*, 16: 46 (1960).
25. J. M. Alexander and M. F. Gazdik, Recoil Properties of Fission Products, *Phys. Rev.*, 120: 874 (1960).
26. S. Nenno and J. W. Kauffman, Detection and Determination of Equilibrium Vacancy Concentrations in Aluminum, *J. Phys. Soc. Japan*, 15: 220 (1960).
27. R. O. Simmons and R. W. Balluffi, Measurements of Equilibrium Concentrations in Aluminum, *Phys. Rev.*, 117(1): 51 (1960).
28. R. C. Folweiler and F. R. Brotzen, The Effect of Quenched-In Vacancies on the Elastic Modulus of Aluminum, *Acta Met.*, 7(11): 716 (November 1949).
29. M. J. Makin and F. J. Minter, The Mechanical Properties of Irradiated Niobium, *Acta Met.*, 7(6): 361 (June 1959).
30. G. Biorci et al., Effect of Neutron Bombardment on the Magnetic Properties of Very High Permeability Iron, *J. Appl. Phys.*, 31: 2046 (1960).
31. J. M. Atwood, Unclassified Research and Development Programs Executed for the Division of Reactor Development and the Division of Research (November 1960), USAEC Report HW-67782, Dec. 10, 1960.
32. C. C. Klick, Mechanism for Coloration of Alkali Halides at Low Temperatures, *Phys. Rev.*, 120: 760 (1960).
33. T. S. Noggle and J. O. Stiegler, Electron Microscope Observations of Fission Fragment Tracks

in Thin Films of UO_2, *J. Appl. Phys.*, 31(12): 2199 (1960).

34. T. K. Bierlein and B. Mastel, Damage in UO_2 Films and Particles During Reactor Irradiation, *J. Appl. Phys.*, 31(12): 2314 (1960).
35. T. K. Bierlein and B. Mastel, Fission Fragment Damage in Nonfissionable Thin Films, *J. Appl. Phys.*, 31(12): 2315 (1960).
36. D. A. Young, Surface Heterogeneity in Irradiated Solids, *J. Phys. and Chem. Solids*, 15: 119 (1960).
37. O. Krisement and G. Tromel, Changes of the Properties of SiO_2 Cristobalite by Means of Fast-Neutron Irradiation and the Introduction of Foreign Atoms, *Z. Naturforsch.*, 15a(7): 634 (July 1960).
38. G. Schottky, Theoretical Investigations of Vacancy Complexes in the Noble Metals, *Z. Physik*, 159(5): 584 (1960).
39. V. G. Weizer and L. A. Girifalco, Vacancy-Vacancy Interaction in Copper, *Phys. Rev.*, 120: 837 (1960).
40. K. H. Bennemann and L. Tewordt, Lattice Deformations Around Interstitial Atoms, Vacancies, Interstitial Atom Pairs and Frenkel Pairs in Copper, *Z. Naturforsch.*, 15a(9): 772 (September 1960).
41. A. D. Rossin, Radiation Damage in Steel—Considerations Involving Effect of Neutron Spectra, *Trans. Am. Nuclear Soc.*, 3(2): 538 (December 1960).
42. R. W. Balluffi and R. O. Simmons, Changes in Macroscopic Shape, Lattice Parameter, and Density in Crystals Due to Point Defects, *J. Appl. Phys.*, 31(12): 2284 (1960).
43. J. S. Langer, Theory of Impurity Resistance in Metals, *Phys. Rev.*, 120: 714 (1960).
44. N. H. March and A. M. Murray, Relation Between Dirac and Canonical Density Matrices, with Application to Imperfections in Metals, *Phys. Rev.*, 120: 830 (1960).
45. D. R. Harries, The Effects of Neutron Irradiation on the Properties of Iron and Steel, *J. Iron Steel Inst.*, 194: 289 (1960).
46. S. I. El-Sisi, Effects of Radiation on Structural Materials, *Nuclear Energy*, p. 365 (August 1960).
47. N. L. Parr, Effect of Neutron Irradiation on the Transition Temperature of Structural Steels, *Materials in Design Eng.*, 3(11): 681–683 (1960).
48. Sh. Sh. Ibragimov et al., The Investigation of Properties and Structures of Metals and Certain Steels Irradiated with Fast Neutrons, *At. Energ.*, 8(5): 413–419 (1960).
49. I. M. Voronin et al., Mechanical Properties and Microstructures of Certain Constructional Materials Following Neutron Bombardment, *At. Energ.*, 8(6): 514–518 (1960).
50. A. A. Johnson, The Embrittlement of Molybdenum by Neutron Irradiation, *Phil. Mag.*, 8(5): 413–416 (April 1960).
51. D. Hull and I. L. Mogford, Ductile-Brittle Transition in Steels Irradiated with Neutrons, *Phil. Mag.*, 8(3): 1213–1222 (1958).
52. C. K. Franklin et al., Effects of Irradiation on the Mechanical Properties of Tantalum, USAEC Report BMI-1476, Battelle Memorial Institute, Nov. 18, 1960.
53. J. G. Morgan et al., Irradiation Effects on Boron-Containing Ceramics and Cermets, USAEC Report ORNL-2522, July 1, 1958.
54. W. R. Thomas, Zirconium Alloys for Water-Cooled Power Reactors, IAEA Paper FE-20-1.1, May 13, 1960.
55. R. J. Cometta et al., Transformation Characteristics of Zirconium-Niobium Alloys, USAEC Report TID-6445, Case Institute of Technology, July 31, 1960.
56. R. B. Briggs, Homogeneous Reactor Program Quarterly Progress Report, USAEC Report ORNL-3004, July 31, 1960.
57. F. Bychkov et al., Structural Diagram of Zirconium-Niobium Alloys, *Met. i Metalloved. Chistykh Metal.*, No. 1, 179–191 (1959).
58. D. A. Vaughan et al., Determination of Interstitial Solid-Solubility Limit in Tantalum and Identification of the Precipitate Phase, USAEC Report BMI-1472, Battelle Memorial Institute, Oct. 28, 1960.
59. E. Anderson and W. Hume-Rothery, The Equilibrium Diagram of the System Molybdenum-Rhodium, *J. Less-Common Metals*, 2: 19–28 (February 1960).
60. F. O. Mueller and E. R. Parker, Deformation Twinning and Fracture in Molybdenum, Report NP-9192, University of California, Materials Research Laboratory, June 1960.
61. Reference canceled.
62. W. D. Klopp et al., Further Studies on Rhenium Alloying Effects in Molybdenum, Tungsten, and Chromium, Report NP-9030, Battelle Memorial Institute, July 12, 1960.
63. W. D. Klopp et al., Studies of Molybdenum, Tungsten, and Chromium-Base Alloys with Improved Ductility, Report NP-9178, Battelle Memorial Institute, Aug. 31, 1960.
64. M. I. Agafonova et al., Structure and Properties of Niobium-Tin Alloys, *Izvest. Akad. Nauk S.S.S.R., Otdel. Tekh. Nauk Met. i Toplivo*, No. 5, 138–141 (September–October 1959).
65. C. L. Vold, The Structure of $NbZn_3$, *Acta Cryst.*, 13: 743 (September 1960).
66. A. R. Kaufmann et al., Refractory Metal Constitution Diagrams, Report WADD-TR-60-132 (NMI-9216), Nuclear Metals, Inc., June 1960.
67. General Atomic Div., General Dynamics Corp., Maritime Gas-Cooled Reactor Program, Quarterly Progress Report for the Period Ending December 31, 1959, USAEC Report GA-1195.
68. N. C. Howells and E. A. Lange, Heat Treatment of Mn-V-Mo Age-Hardening Austenitic Steel,

Report NRL-5464, Naval Research Laboratory, May 16, 1960.

69. G. Rauscher et al., Study of Factors Influencing Ductility of Iron-Aluminum Alloys, USAEC Report TID-6694, Denver Research Institute, June 6, 1960.
70. J. C. Bokros, An Evaluation of Nickel-Copper Alloys for Use as Graphite-Cladding Materials at Elevated Temperatures, USAEC Report GA-1281, General Atomic Div., General Dynamics Corp., Apr. 30, 1960.
71. N. V. Ageen and Z. M. Rogachevskoya, Stability of the β-Phase in Titanium-Vanadium-Molybdenum Alloys, *Zhur. Neorg. Khim.*, 5: 619–621 (March 1960).
72. N. V. Ageen and L. A. Petrova, Stability of the β-Phase in Titanium-Vanadium Alloys, *Zhur. Neorg. Khim.*, 5: 615–618 (March 1960).
73. P. B. Budberg and K. I. Shakhova, Properties of Alloys of the Ternary System Nickel-Chromium-Tungsten, *Zhur. Neorg. Khim.*, 5: 415–420 (February 1960).
74. Metallurgy and Metallography: Part I, Russian Translation NP-tr-448 (from *Met. i Metalloved., Acad. Sci.*, USSR, Moscow), 1958.
75. G. B. Fedorov and F. I. Zhomov, The Diffusion of Zr and Sn in Sn Alloys of Alpha Zr, Report JPRS-5167, translated from *Met. i Metalloved. Chistykh Metal.*, No. 1, 162–169 (1959).
76. E. V. Borisov et al., Production and Physical Metallurgy of Pure Metals: Part VIII, Report JPRS-5195, translated from *Met. i Metalloved. Chistykh Metal.*, No. 1, 213–243 (1959).
77. S. Z. Bokshtein et al., Effect of Polymorphic Transformation on the Diffusion in Titanium, *Metalloved. i Termichesk. Obrabotka Metal.*, No. 6, 21–26 (June 1960).
78. K. A. Sense, The Diffusion of Hydrogen Through Zirconium, USAEC Report NAA-SR-Memo-5067, Atomics International, Mar. 10, 1960.
79. Y. Adda et al., A Simple Method To Study the Diffusion Between Two Metals, One of Which Is Volatile and Not Very Soluble in the Other, *Mém. sci. rev. mét.*, 57: 278–284 (April 1960).
80. Y. Adda et al., The Effect of Pressure on Diffusion in U-Al, U-Cu, and U-Ni Systems, *Mém. sci. rev. mét.*, 57: 423–434 (June 1960).
81. Y. Adda and J. Philibert, Study of Uranium-Titanium Diffusion, *Acta Met.*, 8: 700–710 (October 1960).
82. A. W. Castleman et al., Diffusion of Xenon Through Aluminum and Stainless Steel, USAEC Report BNL-624, Brookhaven National Laboratory, July 1960.
83. T. Nakai et al., The Behavior of Fission Products Captured in Graphite by Nuclear Recoil. II. The Diffusion of Xenon-135 in Graphite at a High Temperature, *Bull. Chem. Soc. Japan*, 33: 497–501 (April 1960).
84. J. J. Laidler, Preferred Orientation in Extruded Zircaloy-2 Tubing, USAEC Report HW-64815, Hanford Atomic Products Operation, Apr. 15, 1960.
85. R. K. Wagner, The Effect of Open-Air Heating (1050°F) on the Properties of Zircaloy-2, USAEC Report NAA-SR-Memo-5043, Atomics International, Mar. 1, 1960.
86. R. R. Hood and L. Isakoff, comps., Moderated Power Reactor Progress Report for July 1960, USAEC Report DP-525, E. I. du Pont de Nemours & Co., Inc., October 1960.
87. R. W. Dayton and C. R. Tipton, Jr., Progress Relating to Civilian Applications During September 1960, USAEC Report BMI-1469, Battelle Memorial Institute, Oct. 1, 1960.
88. J. C. Bokros, Effect of Environment on the Creep Rupture Properties of Inconel-713C, USAEC Report GA-1629, General Atomic Div., General Dynamics Corp., Oct. 21, 1960.
89. R. W. Dayton and C. R. Tipton, Jr., Progress Relating to Civilian Applications During November 1960, USAEC Report BMI-1480, Battelle Memorial Institute, Dec. 1, 1960.

Section V

SPECIAL FABRICATION TECHNIQUES

Melting and Casting

The continuing and increasing interest in the preparation of materials by the more sophisticated fusion processes is responsible for a variety of reports covering the broad subjects of vacuum metallurgy and the melting and casting of the refractory and reactive metals.

One particularly informative and comprehensive group of reports (papers presented at the Conference on Vacuum Metallurgy, New York University, June 1–3, 1959) has been edited by Bunshah and published under one cover.[1] Some of the subjects included are vacuum arc melting and casting, vacuum investment casting, vacuum induction melting, vacuum degassing, electron-beam melting, and a bibliography on electron-beam application in metallurgy.

More recently, Noesen[2] has compiled, reported, and commented on his observations on the consumable-electrode melting of reactive metals. With gratifying brevity, he has presented the effect of temperature and pressure on purification during melting and the importance of various factors in controlling electrode melt-off rate.

Johnson,[3] in authoring a Defense Metals Information Center (DMIC) report, summarizes the present status of technology relating to the melting and casting of molybdenum, columbium, tantalum, and tungsten. He concludes that no satisfactory commerical-scale method for producing shape castings of the refractory metals is available, attributing this to the lack of superheat obtainable in present skull type arc-melting practices. He continues by citing the potential of the cold-crucible induction-melting process and recommends its continued development.

With particular reference to the processing of molybdenum-base alloys, both Westinghouse[4] and Santoli[5] have considered the importance of the processing methods. Westinghouse evaluated the molybdenum–0.5 wt.% titanium alloy prepared by arc melting and the molybdenum–0.1 wt.% cobalt alloy prepared by powder-metallurgy techniques. When the alloys were extruded in the temperature range of 2000 to 3000°F at reduction ratios of 2:1 to 5:1 for arc cast, and 2:1 to 3.9:1 for powder product, it was found that:

1. The pressure required to extrude both alloys increased with reduction ratios.
2. Neither product exhibited pronounced changes in microstructure, tensile strength, hardness, or circumferential strength with increasing amounts of work in the temperature range cited.
3. The tensile strength of the molybdenum–0.5 wt.% titanium alloy was higher than that of the molybdenum–0.1 wt.% cobalt alloy at all reduction ratios and extrusion temperatures.
4. The room-temperature tensile strength and hardness of the 0.5 wt.% titanium alloy were not appreciably affected by extrusion temperature.
5. The room-temperature tensile strength and hardness of the 0.1 wt.% cobalt alloy were higher in material extruded at 2300°F than in material extruded at higher temperatures.
6. The pressure required to extrude the arc-cast molybdenum–0.5 wt.% titanium alloy increased with temperature. The opposite effect was observed for the molybdenum–0.1 wt.% cobalt alloy.
7. Load-deformation curves at elevated temperatures (2000 to 2800°F) showed that the compressive yield strengths drop sharply around 2100°F for the molybdenum–0.1 wt.% cobalt alloy and around 2300°F for the molybdenum–0.5 wt.% titanium alloy.

Santoli, in his state-of-the-art study of selected molybdenum alloys, compiled information on consolidation techniques, extrusion technology for their conversion, current industrial capacity for production, and property data. It is considered indicative that the molybdenum alloys with the best high-temperature properties are presently made by arc casting, and only arc-cast alloys and their properties are discussed in detail. Santoli notes further that, in spite of the potential of the powder method in terms of cost, composition control of volatile alloy constituents, control of grain size, and ease of fabrication, these advantages have not been exploited by any significant alloy development.

The successful development, reported by Du Pont, of the fabrication process for high-quality uranium cores for plate type fuel elements was interesting because of the application of steel practices (refined for closer control) to uranium and was gratifying because of the economics in both cost and material yields (70 per cent of forged preformed slabs). Noteworthy in this development was the technical guidance provided by Du Pont and the cooperation and endeavor of the New York and Savannah River AEC offices in locating and selecting the required fabrication (Superior Steel Corporation, Carnegie, Pa.) and heat-treatment facilities (Atlas Steels, Ltd., Willand, Ontario).

Bridgeport Brass reports on a study[6] relating to the fabrication of uranium. The report[6] briefly describes the effect of temperature and grain structure on the formability of uranium. Both fine-grained (as extruded) and coarse-grained (beta or gamma annealed) uranium were impacted with a drop hammer in the alpha- and beta-phase temperature range in an attempt to compare formability between 25 and 750°C. The following conclusions were drawn:

1. The equicohesive temperature (ECT), the temperature where the deformation resistance of fine-grained and coarse-grained uranium is equal, is below the recrystallization temperature.

2. In the hot-work temperature range, above the ECT, the deformation resistance of fine-grained uranium is lower than that of coarse-grained uranium.

3. The formability of uranium in the beta temperature range is equivalent to that of alpha uranium at about 200 to 300°C.

4. Hot-hammer data can be used in estimating the relative extrusion resistance of uranium billets with various grain structures.

5. Surface quality can be improved by employing fine-grained rather than coarse-grained uranium for forming operations.

The forming of 15-in.-diameter hemispheres from Zircaloy-2 sheet was determined to be feasible by Oak Ridge.[7] In operations conducted at Titanium Fabricator (Burbank, Calif.), $\frac{1}{8}$- and $\frac{5}{16}$-in.-thick sheet was formed by power spinning. This was attempted in the interest of reducing the amount of welding necessary to fabricate a core vessel for the Homogeneous Reactor Project. In reducing the quantity of welding, the chances for weld contamination and impairment of corrosion resistance are reduced and economies are effected. Laps and earing difficulties were experienced but were overcome by modification in procedures. Less controllable were thinout and ellipticity, which infers that considerable machining allowances would be required. Even with these difficulties, spinning is considered to be attractive as a primary fabrication operation. (E. L. Foster)

Cladding

Cladding by Rolling and Swaging

Swage cladding of UO_2-fueled, rod type fuel elements is presently receiving major interest. Roll cladding of dispersion fuels is also reported. Prominent among the various laboratories investigating swage cladding and simultaneous densification of UO_2-bearing fuel rods are Chalk River,[8] Savannah River,[9] Babcock & Wilcox,[10] Hanford,[11] Oak Ridge,[12] and Allis Chalmers.[13] The densities achieved by investigations at the different laboratories with various oxide grades and cladding materials are listed in Table V-1.

A theoretical density of 97 per cent has been achieved by swaging fused UO_2 at 800°C in type 304 stainless steel.[8] Sintered oxide yielded 95 per cent under the same conditions. A density of 94 per cent has been achieved[11] with ceramic-grade UO_2 swaged at 800°C. This was an increase from a cold-swaged density of 74 per cent.

Cladding materials also have an effect on the cold-swaged densities obtained. Savannah River[9] reported that much higher densities were ob-

Table V-1 AS-SWAGED DENSITIES OF URANIUM DIOXIDE FUEL ELEMENTS[8–12]

Type of UO_2	Swaging temp., °C	Percentage of theoretical density for UO_2	Sheath material
Fused	RT	94 (ref. 8)	Type 304 S.S.
	RT	93 (ref. 9)	S.S. and Zircaloy-2
	RT	90 (ref. 10)	Zircaloy-4
	RT	91 (ref. 11)	
	RT	83–92 (ref. 13)	S.S.
	800	97 (ref. 8)	Type 304 S.S.
	800	95 (ref. 12)	Type 304 S.S.
Sintered	RT	92 (ref. 8)	Type 304 S.S.
	RT	86 (ref. 11)	
	800	95 (ref. 8)	Type 304 S.S.
	800	82 (ref. 12)	Type 304 S.S.
Ceramic	RT	69 (ref. 8)	Type 304 S.S.
	RT	74 (ref. 11)	
	600	89 (ref. 11)	
	800	86 (ref. 8)	Type 304 S.S.
	800	94 (ref. 11)	
PWR grade	RT	75 (ref. 9)	S.S. and Zircaloy-2
	600	80 (ref. 9)	S.S. and Zircaloy-2
Steam oxidized	RT	80 (ref. 9)	S.S. and Zircaloy-2

tained with stainless steel or Zircaloy-2 as compared with aluminum or mild steel. Investigators at Hanford[11] observed that as-swaged densities below 80 per cent were independent of cladding materials. However, above this density, the low-strength alloys that were yielded under the high swaging pressures produced poor cladding characteristics and no further densification.

A stationary spindle, four-die swage yielded the best combination of cladding characteristics and fuel density, as reported at Hanford.[11] The rolls were skewed to simultaneously feed and rotate the fuel rods.

Rod rolling was studied by Savannah River[9] as a means of producing UO_2 fuel rods. Densities achieved were roughly analogous to swaging, but dimensional control of the as-rolled rods was poor. Attempts were also made to roll a ribbon type fuel element from preswaged rods. Rods containing fused oxide rolled to 80 per cent density, which dropped off with increasing reductions of over 40 per cent.

Production of the Stationary Medium Power Plant No. 1 (SM-1), formerly called the APPR-1, fuel plates was reported by Sylcor.[14] These fuel elements were stainless-steel-clad enriched UO_2 and B_4C dispersed in stainless steel. Production and quality-control techniques are listed.

(E. S. Hodge)

Pressure Bonding

The term pressure bonding, or isostatic bonding, refers to a process that involves the use of gas pressure at an elevated temperature. Materials to be bonded or compacted are sealed in an evacuated container. The sealed assembly is subjected to an external gas pressure at an elevated temperature. The process is essentially an ideal hot-press operation that has been effectively utilized for the bonding and joining of reactor components and for the densification of ceramic, cermet, and dispersion fuels.

Studies conducted at Battelle[15–19] and Sylvania[20,21] indicate that the gas-pressure-bonding process can be effectively utilized for the simultaneous densification and cladding of UO_2. The process involves the densification of cold-compacted UO_2, sealed in a stainless-steel container, at temperatures of 2100 to 2300°F and gas pressures up to 12,000 psi. Sylvania has investigated the use of vibratory, ultrasonic, and sonic techniques for the consolidation of the UO_2 powder prior to gas-pressure compaction. A density of 89 to 90 per cent of theoretical was achieved at 2200°F and 12,000 psi with a fused grade of UO_2 powder. By use of a mixture consisting of 75 per cent coarse fused-grade UO_2 and 25 per cent fine ceramic-grade UO_2, densities of about 96 per cent of theoretical were achieved. This increase in density was attributed to the relatively high oxygen content of the coarse fused UO_2. Studies have also been conducted with niobium and iron-aluminum alloy clad materials. At temperatures of 2700°F, a UO_2 density of 98 per cent was achieved with the niobium cladding. Tests with the iron-aluminum alloys were unsuccessful. The alloys were in cast form, and brittle failures occurred during the gas-pressure treatment.

In the Battelle studies, seven types of commercially available UO_2 powders were investigated. Densities up to 99.5 per cent of theoretical were achieved with a ceramic grade of oxide. The most promising oxide material was a mixture of fused and ceramic grades containing from 30 to 60 per cent ceramic oxide. These mixtures were cold pressed to a sufficient density to prevent distortion of the cladding of tubular and rod type specimens during subse-

quent gas-pressure densification. Permeability measurements of the high-density oxide indicate that the oxide does not possess intercommunicating porosity. The progress of work on this program has been summarized in a topical report.[19]

Bulk UN has been fabricated to a density of 95 per cent of theoretical at 2300°F and 5 tsi and UC to densities up to 99 per cent of theoretical at 2600°F and 5 tsi.[15–18]

Techniques have been developed at Battelle for the fabrication of cermet fuels consisting of 80 vol.% UO_2 and 20 vol.% of the metals chromium, molybdenum, niobium, and stainless steel.[15–18,22] The gas-pressure-bonding technique has been utilized for the simultaneous cladding and densification of these fuel materials. Densities up to 98 per cent of theoretical have been achieved. Specimens of UO_2-chromium, -molybdenum, and -niobium are being fabricated by pressure bonding for irradiation testing.

The technique of gas-pressure bonding has also been extended to the fabrication of other cermet fuels.[15–18] Bonding at 2300°F and 5 tsi gas pressure has produced cermets of 80 vol.% UN possessing the following percentages of theoretical densities: chromium, 90.5; molybdenum, 86.4; niobium, 96.2; and type 347 stainless steel, 91. UO_2 powders coated with Al_2O_3 by a vapor-deposition technique have been densified to 95 per cent of theoretical at 2300°F and 10,000 psi. After bonding, the Al_2O_3 coating was intact on most of the particles. There was evidence of particle fragmentation to fill void space. Future tests are proposed with the selection of a proper particle-size distribution.

At Bettis, techniques are being developed for the production of Zircaloy-clad, compartmented, flat-plate UO_2 fuel plates for the blanket and seed of the PWR.[23–25] The following conditions have been tentatively selected. Zircaloy is abraded to 60 to 120 μin., root mean square, and ultrasonically cleaned prior to assembly. The Zircaloy and UO_2 components are assembled, evacuated, and sealed by electron-beam welding. Bonding is achieved at 1550°F for 4 hr and 10,000 psi gas pressure. Plates 5 by 55 in. are being fabricated by this technique. A facility for the production of the fuel plates is nearing completion. Large pressure vessels have been installed and are currently being instrumented.

An isostatic bonding technique has been developed by Atomics International for the fabrication of fuel elements for the Piqua Organic Moderated Reactor (OMR).[26,27] These fuel plates are tubular in form, consisting of a finned aluminum cladding and uranium–3.5 molybdenum–0.1 wt.% aluminum core. A nickel barrier is used between the core and cladding to minimize diffusion. The elements are bonded at 1000°F and 10,000 psi for 22 min. Fabricated plates have been successfully irradiated in the Organic Moderated Reactor Experiment (OMRE) to a burnup of 2300 Mwd per metric ton of uranium.

Studies concerned with the solid-phase bonding of niobium and molybdenum are summarized in a report by Battelle.[28] Satisfactory bonding was achieved with niobium at temperatures of from 2100 to 2300°F at 10,000 psi for 3 hr. No deleterious effects on the properties of niobium were observed, and the bonds were shown to be as strong as the base metal. Molybdenum was much more difficult to bond. Satisfactory bonds were produced in a temperature range of 2300 to 2600°F; however, after heat-treatment, the molybdenum exhibited the severe directionality common to this material.

Beryllium has also been successfully bonded by this process. Studies at Battelle[15–18] have shown that self-bonding of beryllium can be accomplished at temperatures above 1600°F and gas pressures of 5 tsi. Specimens bonded at 1600°F exhibited some ductility; however, those bonded at 1800°F were extremely brittle. The brittleness of specimens bonded at 1800°F is attributed to grain growth and reaction with the steel container.

A United Kingdom patent[29] has been issued for a fuel-cladding process utilizing the gas-pressure-bonding technique. The cladding is applied by compacting metal powders around the fuel, sealing in a sheath, and subjecting to heat and gas pressure in a furnace. The process is especially recommended for brittle materials such as beryllium.

Battelle is conducting a basic study of the pressure-bonding process to obtain a better understanding of the kinetics and mechanism of the process.[15–18] The effects of pressure, temperature, time, grain size, grain growth, impurities, and surface roughness on the self-bonding of copper have been determined. Microvoids present at the bond interface interfere with the bonding process by preventing the growth of grains across the bond interface. These microvoids are formed through the insufficient flow of metal into voids formed by

asperities or through the condensation of excess vacancies at nuclei such as impurities. During the bonding process, the growth or disappearance of these voids is governed by the availability of vacancy sinks. (S. J. Paprocki)

Diffusion Bonding

A final report has been issued on the eutectic-diffusion-bonding technique developed at Bettis[30] which has been discussed in numerous past reviews. The process was developed for fabricating plate type fuel elements consisting of ceramic (UO_2) fuel wafers contained within a bonded, compartmented Zircaloy-clad structure. The process was originally intended for use in producing PWR core 2 (Shippingport), as discussed in the February 1961 issue of *Reactor Core Materials*. The process involves the formation of a molten layer between the Zircaloy surfaces by means of a eutectic reaction at elevated temperatures between the Zircaloy and a thin eutectic-forming coating, such as copper or iron. This is followed by diffusion of the bonding agent, or eutectic-forming agent, into the adjacent Zircaloy to achieve a continuous Zircaloy-matrix bond. Fuel elements that were eutectic-diffusion-bonded under various conditions were comprehensively tested, and the results are discussed in the report.

A bond-strength test has been developed at Knolls* and has been used to evaluate several types of fuel and poison elements. The punch-and-die test developed provides data on the relative strength of bonds. On the basis of a simplified analysis, it is claimed that the bond strength obtained may be used to determine whether blistering of the element will occur in service, provided that the pressure and unbonded area at the core-to-cladding interface is known. Such predictions have apparently not yet been compared to service behavior, however. (D. C. Carmichael)

Coextrusion

A promising control-rod cruciform containing type 304 stainless steel + ZrO_2 (25 vol.%) clad with type 304 stainless steel has been fabricated at General Dynamics.[31] The coextrusion billet, 5 in. in diameter by 12 in. long, contained the cruciform-shaped dispersion compacted at 35 tsi, type 304 stainless-steel cladding, and mild-steel filler all enveloped in a mild-steel can. The billet was preheated to 1750°F and extruded at a reduction ratio of 22:1 using both Dag 204 and Fiberglas as lubricants. The resulting rod, $1\frac{1}{8}$ in. in diameter by 18 ft 9 in. long, was essentially straight with no obvious surface defects. Examination of the coextruded specimen revealed excellent bonding between the stainless-steel cladding and the matrix and uniform dispersion of the ZrO_2. After the mild-steel can and filler were removed by pickling, further examination of the cruciform revealed that the four blades were not exactly perpendicular, the thickness of the blades was not uniform, and the extrusion was twisted in some localized areas. A fixture that straightened the extrusion at 1400°F was designed and built.

A program was carried out by Nuclear Metals[32] to develop coextruded CP-5 fuel-element tubes. The fuel-element assembly consisted of three nested tubular elements. Pertinent information regarding these elements is given in Table V-2. The objectives of this program were to produce new and realistic fabrication specifications to overcome problems inherent in coextruding this type of tube. The experiments showed that end-seal shift and taper can be held consistently and that an improvement of the shift also brought about improvements in the eccentricity. It was concluded, after fabricating 14 sets of enriched elements, that acceptable tubes can be coextruded if precautions are taken to ensure that perfect alignments are maintained prior to and

Table V-2 CP-5 FUEL-ELEMENT TUBES[32]

Description	Inner tube	Intermediate tube	Outer tube
Inner diameter, in.	2.112	2.516	2.900
Outer diameter, in.	2.234	2.639	3.000
Fuel length, in.	$25\frac{13}{16}$ max.	$25\frac{13}{16}$ max.	$25\frac{13}{16}$ max.
Over-all length, in.	$27\frac{5}{16}$	$27\frac{5}{16}$	$31\frac{5}{32}$
Cladding thickness, in.	0.015	0.015	0.015
End-seal length, in.	$\frac{3}{4}$ min.	$\frac{3}{4}$ min.	$1\frac{1}{2}$ min.
End-seal length, in.	$\frac{3}{4}$ min.	$\frac{3}{4}$ min.	$3\frac{27}{32}$ min.
Core material, %	25 UAl	24 UAl	16.48 UAl
Cladding material	2S Al	2S Al	2S Al
End-seal material, %	$1\frac{1}{4}$ MgAl	$1\frac{1}{4}$ MgAl	0.8 MgAl

*G. J. Sokol et al., Bond Strength Determination in Fuel and Poison Elements, USAEC Report KAPL-M-GJS-3, June 17, 1960. (Classified)

during the extrusion process. The influence of billet temperature, lubrication, liner temperature, temperature uniformity of the billet and liner, extrusion speed, and billet clearance is secondary to the importance of proper alignment for achieving concentric extrusions having uniform dimensions and properties.

Coextruded rods with UO_2 cores and aluminum alloy cladding have been made by the Savannah River Laboratory.[9] The rods extruded at 450°C had an oxide density 75.8 per cent of theoretical; the sieve size of the fused UO_2 used was −16 with an initial density of 52.3 per cent of theoretical. Sheath thickness varied from 0.140 to 0.170 in., and the outside diameters varied from 0.500 to 0.520 in. Types 1100, 5052, and 5154 aluminum alloy were used as cladding. It is anticipated that coextrusion at a higher temperature, 800°C and up, in suitable cladding material will produce extrusions with higher core densities.

An investigation of the use of beryllium as a fuel-element cladding has been conducted by Nuclear Metals.[33] Coextrusion was used as the means of fabrication of three separate core materials. Two major problems encountered in coextruding beryllium involved the differences in the flow characteristics of the individual materials and the inherent brittleness of the beryllium. The coextrusion of beryllium-clad uranium−3.8 per cent silicon, including end sealing, was successful when the extrusion temperature was in the range 1650 to 1750°F. Plots of the relative extrusion constants for epsilon uranium and beryllium were found to intersect at about 1472°F. It was apparent that coextrusion was best accomplished when the core was softer than the cladding; extrusions below 1650°F were not successful. The billets were prepared by packing beryllium powder around the solid-core alloy in a mild-steel container. The billets were evacuated, sealed, heated to the extrusion temperature, and promptly extruded. The mild-steel sheathing was removed by pickling in nitric acid. The extruded rods exhibited good geometric uniformity, cladding integrity, and integral end sealing. Rods of uranium−10 wt.% molybdenum were clad and end sealed, but it was not possible to avoid cracking in the cladding. Experiments using uranium monocarbide as the core material indicated that, when the content was of the order of 58 vol.% or slightly greater, the stiffness of the alloy was of the same order as that of the beryllium at temperatures of 1500 to 1800°F. When solid core material was used, beryllium powder was placed around the core; however, when the core material was in the form of granules, solid beryllium instead of powder was used to contain the core. Experiments indicated such material to be coextrudable with beryllium, including end seals, but this cladding also contained cracks. (C. B. Boyer)

Extrusion Cladding

A rash of low and fluctuating bond strengths in NRU flat-plate production fuel elements was studied at Chalk River.* The trouble was traced to excessively high nitric acid concentration in the pickling tank immediately preceding the nickel-plating bath. Consistently high bond strengths were obtained after the nitric acid concentration was adjusted. In other studies of extrusion-cladding variables, bond strengths of 20,000 to 29,000 psi were obtained by cladding at 1020°F with an aluminum−6 wt.% silicon cladding alloy, provided that sufficient argon was introduced to prevent oxidation of the core. Cladding with type 1S aluminum alloy at 1020°F, with 140 to 400°F core preheating, resulted in 17,000- to 21,000-psi bond strengths. However, some poor bonds were obtained because of oxidation during the preheating operation. Water quenching of the extrusion-clad product as it emerges from the die seems to have raised the bond strengths by 2000 psi. (H. J. Wagner)

Canning

Studies in England[34] have been concerned with a method and apparatus for sealing solid nuclear-fuel bodies, e.g., a uranium rod, in a close-fitting metal sheath with an internal atmosphere such as helium. The apparatus comprises a draw press with a pumping head arranged to be coupled to a sheath during the drawing of the sheath. Before the drawing operation, the aluminum sheath is evacuated by withdrawing air from a cavity at the inner end of the uranium rod via clearance spaces and grooves. Helium is introduced through a needle valve, and then the ram is operated to drive the loaded sheath through the die, trapping the helium gas within the sheath.

*H. Smedley, Atomic Energy of Canada, Ltd., 1960. (Unpublished)

An English patent[35] describes the preparation of steel-plated zirconium cans for fuel elements which are exposed to a surface temperature of more than 300°C. A zirconium tube is coated with steel 30 to 300 μ thick by being forced or shrunk or by welding.

Development of a fuel element consisting of a cluster of stainless-steel-clad, sodium-bonded, uranium–10 wt.% molybdenum fuel rods is described by Atomics International.[36] Such an element has been proposed for the first core loading in the Hallam Nuclear Power Facility (HNPF).

Vacuum casting in graphite molds was proven to be a feasible fabrication method for producing uranium–10 wt.% molybdenum fuel slugs. Extrusion and liquid pouring were both investigated as methods of handling sodium to bond the fuel slugs to the stainless-steel cladding. The extrusion technique was shown to be impractical, because of difficulty in supplying a sufficient volume of sodium to fill the subassembly fuel rods. Satisfactory bonding was obtained by means of the liquid technique. Two full-scale fuel-element mockups were fabricated. Each element contained 19 fuel rods, located by spacers made from spot-welded strips and enclosed in a Zircaloy-2 process tube.

The apparatus is described for the assembly of the fuel-rod components under an inert atmosphere. Also, the equipment is designed to allow for welding the end plugs to the fuel rods after the sodium has been put in. This equipment is so designed as to be completely mechanical once the components have been positioned.

The fuel in the EBR-II power breeder reactor at the National Reactor Testing Station[37] in Idaho is blanketed with depleted unalloyed uranium in type 304 stainless-steel tubes. The loaded tubes, which are called blanket rods, contain sodium metal to facilitate heat transfer across the annulus between the uranium and the tube. The maximum calculated central temperature for blanket slugs adjacent to the fuel is 600°C, and the surface temperature is 520°C. To ensure adequate heat transfer on cooling via the sodium, no voids or unbonded or nonwetted areas greater than $\frac{1}{16}$ in. in any direction can be tolerated. A proper sodium level must also be maintained above the uranium to ensure complete coverage at the top to compensate for fuel-dimension changes resulting from irradiation.

A specially designed inert-atmosphere glovebox facility permits the simultaneous loading of 108 blanket rods. The sodium is loaded into the tubes in a solid form together with the fuel. The tubes are then evacuated, and the sodium is melted by immersion in a portable oil bath of silicone at 200°C.

Assembled blanket fuel rods were subjected to a sodium-bonding treatment to eliminate voids and nonwetted surfaces. The tubes were loaded inside a vertical electric resistance furnace and vibrated at a frequency of 30 cps and an amplitude of $\frac{1}{16}$ in. while being heated simultaneously to 450°C. This bonding treatment required 4 hr, after which the rods were differentially quenched to eliminate shrinkage voids by lowering them vertically into a circulating water bath. This procedure yielded 80 to 90 per cent completely bonded rods.

(E. G. Smith, Jr.)

Nonelectrolytic Chemical-Plating Techniques

The formation of boron coatings on steels[38] by hydrogen reduction of BCl_3 is described. Conditions include a BCl_3-to-H_2 ratio of 0.05, a BCl_3 vaporization temperature of −50°C, and a deposition-temperature range of 750 to 950°C. More diffusion occurred at 950°C. Hardness of the rhombic FeB (eta) phase was measured as 2340 kg/mm^2; the hardness of the Fe_2B (epsilon) phase was measured as 1680–1290 kg/mm^2.

Pyrolytic carbon coatings on graphite render the graphite less permeable.[39] Such coatings are formed from CH_4 at 20 to 80 mm pressure at a coating temperature of 1350 ± 50°C. The impermeability coefficient of a typical layer is 4×10^{-9} cm^2/sec. The presence of silicon in the CH_4 stream may be helpful.

Vapor-phase formation of hafnium and tantalum carbides using methane–metal halide mixtures is outlined by High-Temperature Materials, Inc.[40] The atmosphere injection temperature is 300°C, and the $HfCl_4$-to-CH_4 ratio is 1:1. Hafnium carbide was deposited on tungsten wires at temperatures in the 1700 to 2400°C range. At 1700°C, the coating buildup was 40 mils/hr at a coating efficiency of 10 per cent. At 2100°C, the buildup was 85 mils/hr with increased grain size.

Tantalum carbide coatings are formed in the 1700 to 2300°C temperature range at deposition rates of 36 to 47 mils/hr. Ratios of metal chloride to CH_4 were higher than those for hafnium

carbide deposition. Increased pressure of reactants gave decreased grain size for deposits but also led to decreased deposition rates. Highly oriented, single-phase TaC coatings were formed[41] on 1- by 7-in. extended surfaces at 2000°C at the rate of 20 mils/hr.

A general review covers methods of producing diffusion coatings on nickel alloys, molybdenum, and steels.[42] Chemical vapor-deposition methods are discussed.

In a recent British patent,[43] nickel carbonyl vapor (1 to 3 mm Hg pressure) is caused to impinge on a degassed, heated object in a bell jar initially at a pressure of 10^{-3} mm Hg. A getter body is used to maintain a low partial pressure of oxygen in the coating atmosphere. The coated object is subsequently heated to promote diffusion bonding.

Conversion type coatings can be formed by chemical vapor-phase reaction of substrates with a mixture of commercial $SiCl_4$ and dry (dew point, −40°C) hydrogen.[44] A 2-mil silicide layer was formed on niobium or tantalum alloys in 20 min at 1450°C with 25 to 30 mole % $SiCl_4$ in the coating atmosphere. At lower temperatures and higher $SiCl_4$ contents, silicon was deposited. A zone coating technique, for large objects, is described.

A duplex coating procedure also is described in which molybdenum or a molybdenum compound (e.g., MoO_3) is deposited on the substrate and the resulting molybdenum-rich layer is then converted to $MoSi_2$ by the $SiCl_4$-hydrogen method. For niobium alloys, the best duplex coatings were obtained by immersion of the specimen in liquid MoO_3 at 800°C, hydrogen reduction of the MoO_3 to molybdenum at 800°C, and, finally, conversion of the molybdenum-rich surface to $MoSi_2$ by reaction with $SiCl_4$ plus hydrogen for 20 min. The duplex coating, thus formed, consisted of a 2- to 3-mil outer layer of $MoSi_2$ and a 2-mil layer of substrate silicides.

The best test life obtained for conversion silicide coatings was 40 hr at 1260°C in air for niobium-tantalum-tungsten-zirconium and niobium-tantalum-zirconium alloys. The duplex silicide coating method yielded 70-hr lives in air at 1260°C for the above two alloys. Use of appropriate elements as diffusion barriers should reduce the rate of oxidation of silicide coatings.

"Pure" TiC can be deposited on steel by the reaction of gaseous $TiCl_4$ with volatile hydrocarbons.[45]

A general review of the characteristics of vapor-deposited tungsten coatings on graphite, copper, iron, molybdenum, and nickel has been published.[46] Hydrogen reduction of WF_6 at substrates heated to about 1200°C was used as the vapor-phase reaction. (E. M. Sherwood)

Coated Particles

A method is described[47] for coating aerosolized refractory particles with nickel by vapor-phase decomposition of $Ni(CO)_4$ near 150°C and with tantalum by hydrogen reduction of $TaCl_5$ at 1000°C. Special Al_2O_3 particles were fed at 1 g/min with $Ni(CO)_4$ at 33 g/min (25 cm^3/min) through a nozzle and into a reaction chamber with nitrogen as the fluidizing carrier gas. Coated particles were collected in a bag filter. Chemical analysis[48] showed 12 wt.% nickel present in a batch of particles magnetically separated from the collected material.

The coating of UO_2 spheres with niobium−5 wt.% vanadium alloy, chromium, and molybdenum is being continued by Nuclear Materials and Equipment.* A coating buildup rate of 2 μ/hr for the niobium−5 vol.% vanadium alloy was obtained under the following conditions:

Parameter	Value
VCl_4 vaporizer temp., °C	45−50
$NbCl_5$ vaporizer temp., °C	150−160
Mass ratio, $NbCl_5/VCl_4$	4:1
Hydrogen gas flow, liters/min	4.0
Argon gas flow, liters/min	0.5
Reactor temp., °C	1020

Chromium was deposited on niobium-coated (thickness, 2 μ), 100-mesh UO_2 by hydrogen reduction of $CrCl_2$. Coating conditions were:

Parameter	Value
$CrCl_2$ vaporization rate, g/hr	10
Hydrogen flow rate, liters/min	2
Reactor temp., °C	770
Plating rate, μ/hr	1

"Chewing" of the niobium coating to 0.5 μ was noted. Chromium coatings, obtained by pyrolysis of chromium dicumene in a bomb technique, contained carbon.

*Nuclear Materials and Equipment Corporation, 1960. (Unpublished)

Molybdenum coatings were obtained on 100-mesh UO_2 spheres in a 180°-rotated, horizontal, stainless-steel reactor by hydrogen reduction of $MoCl_5$, under the following conditions:

Parameter	Value
$MoCl_5$ vaporization temp., °C	165
Hydrogen flow rate, liters/min:	
Through vaporizer	1.6
Through reactor	2.4
Plating rate, μ/hr	1.6

Control of the reactor inlet temperature was critical to prevent premature decomposition of $MoCl_5$.

Coatings of chromium and Al_2O_3 were deposited on 0.075-in. cylindrical UO_2 particles as a possible means of improving the abrasion resistance of these particles.[16] A chromium coating 16 to 17 μ thick was applied by thermal decomposition of chromium dicumene at 325°C in a rotating basket reactor. The Al_2O_3 coating, 137 to 206 μ thick, was applied at 950°C by hydrolysis of $AlCl_3$ in a fluidized bed of the UO_2 particles. In a 5-hr abrasion test, chromium reduced the weight loss by a factor of 20, relative to uncoated particles. The Al_2O_3 coating did not improve abrasion resistance.

Work was continued on pyrolytic carbon coatings to render solid-solution, thorium-uranium dicarbide particles moisture resistant during fuel-element fabrication. Carbon, deposited by pyrolysis of acetylene in a fluid bed of the carbide particles, may also help retain fission products during reactor operation. The coating thickness on nine lots of mixed carbide which were coated at temperatures between 1650 and 2750°F ranged from 2 to 55 μ. Coating density appeared to vary with the partial pressure of acetylene in the coating atmosphere.

In previous work on the fluidized-bed coating of UO_2 powders with Al_2O_3, trouble has been caused by the undesirable settling of by-product Al_2O_3 dust. Improvements in reactor design and adjustment of operating conditions minimized this difficulty.[17]

In the coating of UO_2 with Al_2O_3 by hydrolysis of Al_2Cl_6 vapor in a fluidized bed, it was found that the Al_2O_3, formed at or below 500°C, was porous and amorphous.[18] Alpha Al_2O_3 was formed at 1000°C. The Knoop hardness number of the 1000°C coating was 2000; that of the material formed at the lower temperature was 600.

In the high-temperature coating of fuel particles with pyrolytic carbon, care must be taken to prevent premature decomposition of the hydrocarbon used. This requires use of a cooled-vapor injector, maintained at a temperature below 1200°C. In coating at temperatures above 1500°C, a technique resembling barrel plating was used. The reactor was an induction-heated rotating graphite tube containing a charge of 16-mesh graphite particles and 120-mesh UC_2 particles, previously coated with pyrolytic carbon at 1200°C in a fluidized bed. A 20- to 30-μ-thick coating of pyrolytic carbon was laid down at 2000°C and a 10-μ-thick coating at 1800°C. Both coatings were free of voids. However, uncoated particles were found in the material processed at 1800°C. (E. M. Sherwood)

Electroplating

Nickel plating is considered[27] to be one of the most important steps in the procedure for cladding uranium alloy fuels for the Piqua reactor. Extruded, finned aluminum tubing was isostatically bonded to the cast-uranium cylinders after a 0.001-in.-thick nickel plate was adherently deposited on the castings to serve as a diffusion barrier. Surface pores in the casting, which were described as being 0.010 in. in diameter, were bridged by the nickel, but blistering occurred at these sites during the subsequent bonding operation. Electrolyte entrapped in the pores produced high-pressure gases when it corroded the substrate and was vaporized. This result duplicates previous experience with nickel plating of uranium and other active metals and emphasizes the importance of providing dense surface layers on castings that require coatings for either protective or cladding purposes.

The nickel-plating development at Piqua takes advantage of auxiliary anodes to improve the thickness uniformity and of changing contacts without interrupting the current to ensure pore-free deposits. These are examples of procedures adopted to ensure high-quality coatings. At an early stage in the development,[26] the grit-blasted fuel elements were etched first anodically in an alkaline solution and then in nitric acid solution. Later, both etching treatments were omitted when evaluation of bond quality in both out-of-pile and in-pile tests showed no failure of the aluminum-clad elements attributable to a plating deficiency. Prior to these tests, bond quality was evaluated by several proce-

dures, including, in addition to mechanical tests such as the peel test, newer tests employing sonic, ultrasonic, eddy-current, transient-heating, and infrared scanning devices. Infrared scanning was judged as the "most promising," but no details were described.

A recent patent[49] dealing with aluminum plating of barrier-coated uranium disclosed a procedure for improving the adherence of the electroplated aluminum to the barrier surface. Immersion in a fatty acid prior to plating in an aluminum chloride–lithium hydride plating solution was suggested. The aluminum-plating procedure was more completely described previously.[50] Nickel proved to be a better diffusion barrier than iron when aluminum-plated uranium was heated. The best method for activating the nickel surface, prior to aluminum plating, included successive immersions in alcohol and in oleic acid. The aluminum deposited in the aluminum chloride–lithium hydride bath was more resistant to corrosion during immersion in distilled water than that deposited in an ethyl pyridinium bromide–aluminum chloride–toluene solution. The weight gain for the aluminum plated in the latter solution was attributed to the hydration of occluded organic matter.

Chromium was deposited on Zircaloy with no measurable pickup of hydrogen by a vapor-deposition process employing dicumene obtained from Union Carbide.[51,52] Although the coatings were nonuniform in thickness and ranged from 0.6 to 2 μ, they served as a barrier to hydrogen absorption by Zircaloy-2 during exposure to a hydrogen-containing atmosphere at 400°C. Zircaloy was adherently electroplated with copper in an alkaline solution, but plating conditions were exacting.[52]

Hydrogen pickup by thorium during preplating activation treatments was related to blistering of nickel- and chromium-plated thorium, observed after many hours of exposure to water-saturated air[18] at 200°F. Specimens activated anodically in hydrochloric acid solution contained 18 or 22 ppm hydrogen; electropolished and chemically pickled specimens contained <2 and 8 ppm, respectively. A 25-ppm hydrogen content of an activated and nickel-plated specimen was reduced to 7 ppm by outgassing at 500°F in vacuum. Rapid heating to 500°F usually caused blisters in the coating.

(W. H. Safranek)

Ceramic Coatings

Sanderson and Porter[53] reports that subsurface coatings can be developed in graphite spheres. Both nickel and glass were found to penetrate or fill the pores of a graphite shell when heated uniformly in an out-of-pile furnace.

A coating for the protection of tungsten in air at 3000°F or higher for up to 10 hr was reported by the University of Illinois.[54] The coating, which consisted of a mixture of 35 per cent glass and 65 per cent zircon, was initially heated in vacuum at temperatures up to 2600°F and then fired in argon at 2850°F. (B. W. King)

Welding and Brazing

Joining studies at Hanford (references 51, 52, 55, and 56) related to fuel-element closures involve a variety of joining processes. Weld fabrication of Zircaloy components for the Plutonium Recycle Test Reactor (PRTR) is described.[55] This work involved various welding techniques for closures and spacer attachments and subassembly fabrication. Techniques for tungsten-arc inert-gas, magnetic-force butt, tungsten-arc spot, projection, high-frequency resistance, and conventional resistance-seam welding are described.

Additional studies of magnetic-force butt welding for beryllium and stainless steel are in progress. Beryllium joints between ½-in.-diameter by 0.040-in. wall tubing and ½-in.-diameter end plugs produced by this method were satisfactory. Similar joints in stainless steel were satisfactory when the tubing wall thickness was 0.015 in. but were not satisfactory for thinner wall material.

An article similar to reference 55 describes English experience with welding problems encountered in fuel-element fabrication.[57]

A recent DMIC memorandum presents a compilation and discussion of unclassified information on the welding of niobium and niobium alloys.[58]

Oak Ridge studies[12] of beryllium welding are continuing. Cracking at the root of seal welds made on tubing end plugs can be limited by press fitting the plug into the tube. A study of the joint efficiency of welds in various types of tubing and configurations also seems to indicate a correlation between joint fit-up and properties. The data obtained in this study are summarized in the tabulation below:

Tubing material	Joint efficiency
Hot-press rod	56.4
	85.2
Warm-extruded rod	100
	75.2
English hot-extruded	100
	100
	100
French hot-extruded	78.5

(R. E. Monroe)

Nondestructive Testing

Ultrasonic Techniques

The various agencies doing research in atomic energy have contributed much toward advancing the use of ultrasonic energy for nondestructive testing. Since 1952, Hanford[59] has been using ultrasonic energy to measure grain size. A transformation test (Sonotest) has developed from this work as a semiautomatic go, no-go test for untransformed, small-grain material. Rejects range from 0 per cent on large-grained lots to 15 per cent on some small-grained lots, the average reject rate being 2 per cent. Over 15 tons of bare uranium cores have been tested at the rate of 5 sec per 8-in. core. By means of digital techniques, the Sonotest provides a readout of "finest," "average," and "variation" in grain size.

The attenuation of a pulse of ultrasonic energy due to scattering at grain boundaries depends on the relation between the wavelength and the dimensions of the grain. The Sonotest transmits a 5-Mc pulse through a specimen. The amplitudes of the received pulses vary inversely with grain size.

Perhaps one of the most difficult problems facing the ultrasonics engineer has been that of inspecting adhesive bonds for bond strength.[60,61] Four instruments evaluated at Martin are capable of distinguishing bond defects, such as voids and porosity, from control bonds, as well as variations in glue-line thickness. However, none of the instruments used could separate low-strength bonds due to poor surface preparation or undercured adhesive from the control bond. Although there is a difference in the physical properties between a weak bond and a good bond which should cause a variation in acoustic impedance between the two, the total variation is extremely small compared with the differences in acoustic impedance between the base metal and either type of bond. The difference between the acoustic impedances of a void and a bonded area is more pronounced and thus easily detected.

The use of Lamb waves for detecting unbonded areas has been investigated.[62,63] While carrying out this work, Argonne discovered that Lamb-wave propagation is not limited to thin plates but can be generated very weakly in plates as thick as 4 in. Theory indicates that the frequency-thickness curves extend to infinity, but from a practical standpoint Lamb waves have been considered to be limited to thin plates. The resolution to be expected using Lamb waves in detecting nonbound areas in 4-in.-thick plates has not been established.

Another interesting development at Argonne[62] has been the discovery of a couplant which has been used to measure elastic constants of a small single crystal of alpha zirconium with shear waves at temperatures ranging from 25 to 780°C. The couplant is a mixture of sodium silicate and calcium carbonate in solution, which forms (after drying) a solid transmission layer between the buffer and the specimen, and which efficiently transmits both the shear and the longitudinal modes of ultrasonic energy into the specimen.

While studying methods of inspecting thin-wall tubing, Hanford[64] has discovered wave motion in the tubing similar in many respects to Lamb waves. These waves have been studied from a fundamental approach, and, as a result, work has been started on the development and design of an advanced ultrasonic testing system for thin-wall fuel sheath tubing. Plans call for four transducers for flaw inspection (two for radial flaws and two for transverse flaws) and two more for thickness measurements.

Partial evaluation[64] of PZT and lead metaniobate transducers for Lamb-wave testing shows that these materials appear superior to barium titanate, although PZT exhibits peculiar "ringing" characteristics which are now being investigated.

Work is in progress on an ultrasonic resonant method of measuring plate thickness without the use of grease or liquid couplant between the transducer and the metal surface.[64] The ultrasonic waves are induced by eddy currents. The vibrations are detected by means of a capacitive

type pickup. Although the idea seems sound, not enough information is available for evaluation; for instance, the reports do not disclose to which resonance modes the thickness is to be related.

Regarding the sensitivity of a Curtiss-Wright Immerscope, model 424A, Hendricks at Savannah River[65] reports that a 1-Mc lithium sulfate plane-wave transducer detected V notches 1 mil deep, 15 mils wide, and 62 mils long. Better resolution and stronger signals were received from ID flaws with a focused barium titanate transducer with less effort expended to position the transducer. (D. Ensminger)

Nondestructive Testing by Eddy-Current and Cyclographic Methods

The application of the eddy-current technique to the measurement of fuel-element plate, coolant-channel width has not met with success at Oak Ridge. The sensor is made with a small flat coil backed up by a flexible ferromagnetic leaf spring. The change in flexing of the spring with channel spacing is detected in the coil as a change in inductive coupling. The range of the first model is 30 to 70 mils with a sensitivity of ±1 mil. An improved model has been devised with a sensitivity of ±0.5 mil.

Atomics International has used cyclographic examination of SRE fuel elements for the detection of NaK bonding.[36] Voids as small as $\frac{1}{16}$ in. in diameter have been successfully detected; however, an experienced observer is required to interpret the cyclograph charts because of sensitivity to specimen changes other than the presence of voids. (D. R. Grieser)

References

1. R. F. Bunshah, ed., *Transactions of the Vacuum Metallurgy Conference, June 1–3, 1959*, New York University Press, 1960.
2. S. J. Noesen, Consumable Electrode Melting of Reactive Metals, *J. Metals*, 12(11): 842–849 (November 1960).
3. W. H. Johnson, Melting and Casting of the Refractory Metals Molybdenum, Columbium, Tantalum, and Tungsten, Report DMIC-139, Battelle Memorial Institute, Defense Metals Information Center, Nov. 18, 1960.
4. Westinghouse Electric Corp., Lamp Div., Research and Development Work on the Extrudability and Extruded Properties of Sintered and Arc-Cast Molybdenum Alloys, Final Report, Report NP-9108, Mar. 31, 1960.
5. P. A. Santoli, Molybdenum Alloy Extrusion Development Program, First Interim Technical Progress Report for June 15, 1960, to September 15, 1960, Report ASC-TR-7-785, Allegheny Ludlum Steel Corp. Research Center, October 1960.
6. Q. C. Carloni and L. Robins, Effect of Temperature and Grain Structure on the Formability of Uranium, USAEC Report BRB-56, Bridgeport Brass Co., Oct. 28, 1960.
7. F. W. Cooke, A Study of the Forming of Zircaloy-2 Hemispheres by Power Spinning, USAEC Report CF-60-4-121, Oak Ridge National Laboratory, Apr. 8, 1960.
8. W. M. Campbell, Atomic Energy of Canada, Ltd., 1960. (Unpublished)
9. G. R. Cole et al., Fabrication of Uranium Oxide Fuel Elements, USAEC Report DP-430, E. I. du Pont de Nemours & Co., Inc., Nov. 23, 1960.
10. R. R. Hood and L. Isakoff, Heavy Water Moderated Power Reactor Progress Report for July 1960, USAEC Report DP-525, E. I. du Pont de Nemours & Co., Inc., October 1960.
11. Hanford Atomic Products Operation, Novel Ceramic Fuel Fabrication Processes, USAEC Report HW-64629, Apr. 15, 1960.
12. Oak Ridge National Laboratory, Gas-Cooled Reactor Project Quarterly Progress Report for Period Ending September 30, 1960, USAEC Report ORNL-3015, Nov. 11, 1960.
13. Allis-Chalmers Mfg. Co., Pathfinder Atomic Power Plant Technical Progress Report for April–June 1960, USAEC Report ACNP-6007, Oct. 15, 1960.
14. Production of Fuel Elements for Nuclear Reactors, *Machinery*, 97(2491): 313–320 (Aug. 10, 1960).
15. R. W. Dayton and C. R. Tipton, Jr., Progress Relating to Civilian Applications During September 1960, USAEC Report BMI-1469, Battelle Memorial Institute, Oct. 1, 1960.
16. R. W. Dayton and C. R. Tipton, Jr., Progress Relating to Civilian Applications During October 1960, USAEC Report BMI-1473, Battelle Memorial Institute, Nov. 1, 1960.
17. R. W. Dayton and C. R. Tipton, Jr., Progress Relating to Civilian Applications During November 1960, USAEC Report BMI-1480, Battelle Memorial Institute, Dec. 1, 1960.
18. R. W. Dayton and C. R. Tipton, Jr., Progress Relating to Civilian Applications During December 1960, USAEC Report BMI-1489, Battelle Memorial Institute, Jan. 1, 1961.
19. S. J. Paprocki, ed., Progress on the Use of Gas-Pressure Bonding for Fabricating Low-Cost Ceramic, Cermet, and Dispersion Fuels, USAEC Report BMI-1475, Battelle Memorial Institute, Nov. 7, 1960.
20. I. Sheinhartz and J. Fugardi, Ceramic Fuel Ele-

ments Made by Hot Isostatic Pressing, USAEC Report SCNC-311, Sylvania-Corning Nuclear Corp., September 1960.
21. I. Sheinhartz and J. Fugardi, Isostatic Pressing of UO_2 in High-Temperature Metals, USAEC Report SCNC-312, Sylvania-Corning Nuclear Corp., September 1960.
22. S. J. Paprocki et al., Preparation and Properties of UO_2 Cermet Fuels, USAEC Report BMI-1487, Battelle Memorial Institute, Dec. 19, 1960.
23. Westinghouse Electric Corp., Bettis Atomic Power Laboratory, Technical Progress Report, Pressurized Water Reactor (PWR) Project for the Period April 24, 1960, to June 23, 1960, USAEC Report WAPD-MRP-86.
24. Westinghouse Electric Corp., Bettis Atomic Power Laboratory, Technical Progress Report, Pressurized Water Reactor (PWR) Project for the Period June 24, 1960, to August 23, 1960, USAEC Report WAPD-MRP-87.
25. Westinghouse Electric Corp., Bettis Atomic Power Laboratory, Technical Progress Report, Pressurized Water Reactor (PWR) Project for the Period August 24, 1960, to October 23, 1960, USAEC Report WAPD-MRP-88.
26. M. H. Binstock, Fuel Element Development for Piqua OMR, USAEC Report NAA-SR-5119, Atomics International, June 30, 1960.
27. E. E. Garrett et al., Hot Pressure Bonding of OMR Tubular Fuel Elements, USAEC Report NAA-SR-5120, Atomics International, July 30, 1960.
28. S. J. Paprocki et al., The Bonding of Molybdenum and Niobium-Clad Fuel Elements, USAEC Report BMI-1451, Battelle Memorial Institute, July 12, 1960.
29. Leslie Mark Wyatt, Improvement in or Relating to Metal Coatings, British Patent 832,807 (to UKAEA), Apr. 13, 1960.
30. R. A. Wolfe et al., Eutectic-Diffusion-Bonding of Plate Type Fuel Elements Containing Ceramic Fuel, USAEC Report WAPD-211, Westinghouse Electric Corp., Bettis Atomic Power Laboratory, October 1960.
31. General Atomic Div., General Dynamics Corp., Maritime Gas-Cooled Reactor Program, Quarterly Progress Report for the Period Ending December 31, 1959, USAEC Report GA-1195.
32. J. Wong, Development Work on the Fabrication of CP-5 Fuel Element Tubes, Final Report to Argonne National Laboratory, USAEC Report NMI-4852, Nuclear Metals, Inc., May 13, 1960.
33. J. Greenspan, Fabrication Development of Beryllium-Clad Uranium–3.8 Wt.% Silicon, Uranium–10 Wt.% Molybdenum, and Uranium–Uranium Monocarbide Cermets, USAEC Report NMI-1236, Nuclear Metals, Inc., Aug. 30, 1960.
34. G. W. Ford et al., Improvements in or Relating to Sheathed Elements, British Patent 845,181, Aug. 17, 1960.
35. Plated Cans for Fuel Elements, British Patent 840,609, July 6, 1960.
36. S. M. Cobb, Uranium Alloy Fuel Element Fabrication Development for HNPF Core I, USAEC Report NAA-SR-5291, Atomics International, Nov. 1, 1960.
37. R. L. Salley and C. H. Bean, Assembly, Sodium Bonding, and Inspection of EBR-II Blanket Rods, *Trans. Am. Nuclear Soc.*, 3(2): 448–449 (December 1960).
38. M. A. Pchelkina and Yu. M. Lakhtin, Boron Coating from the Vapor Phase in Boron Trichloride Medium, *Metalloved. i Termichesk, Obrabotka Metal.*, No. 7, 40–42 (July 1960).
39. General Atomic Div., General Dynamics Corp., 40-Mw(e) Prototype High-Temperature Gas-Cooled Reactor Research and Development Program, USAEC Report GA-1235, September 1960.
40. High-Temperature Materials, Inc., Pyrolytic Carbide Development Program for U. S. Navy, Bureau of Weapons, Monthly Progress Report No. 7, Oct. 31, 1960.
41. High-Temperature Materials, Inc., Pyrolytic Carbide Development Program for U. S. Navy, Bureau of Weapons, Monthly Progress Report No. 8, Nov. 30, 1960.
42. Diffusion Coatings, *Mech. World Eng. Record*, 140: 392–393 (September 1960).
43. L. W. Owen, Improvements in or Relating to the Deposition of Nickel Coatings, British Patent 843,531, Aug. 4, 1960.
44. R. H. Lorenz and A. B. Michael, Oxidation-Resistant Silicide Coating for Cb and Ta Alloys by Vapor Phase Reaction, Paper Presented at the 118th Meeting, Electrochemical Society, Houston, Tex., Oct. 9–13, 1960.
45. W. Ruppert, The Deposition of Titanium Carbide on Steel Surfaces, *Metalloberfläche*, 14: 193–198 (July 1960).
46. W. Beller, Tungsten Nozzles by Vapor Deposit, *Missiles and Rockets*, 7: 23–24 (Sept. 12, 1960).
47. Aeroprojects, Inc., Aerosol Preparation of Composite Metal Powders for Dispersion Strengthening, Bimonthly Progress Report No. PR-N-311-7, July 16–September 15, 1960, Report NP-9703.
48. Aeroprojects, Inc., Aerosol Preparation of Composite Metal Powders for Dispersion Strengthening, Bimonthly Progress Report No. PR-N-311-8, September 16–November 15, 1960.
49. W. C. Schickner, Process of Electroplating Metals with Aluminum, U. S. Patent 2,934,478 (to AEC), Apr. 26, 1960.
50. J. G. Beach and C. L. Faust, Electroclad Aluminum on Uranium, *J. Electrochem. Soc.*, 106: 654 (1959).
51. F. W. Albaugh, Reactor and Fuels Research and Development Operation Monthly Report for September 1960, USAEC Report HW-66960-A, Hanford Atomic Products Operation, Oct. 15, 1960. (Classified)

52. Hanford Atomic Products Operation, Reactor and Fuels Research and Development Monthly Report for November 1960, USAEC Report HW-67532-A, Hanford Atomic Products Operation, Dec. 15, 1960. (Classified)
53. Sanderson and Porter, Fuel-Element Development Program for the Pebble Bed Reactor, A Topical Report on Subsurface Coatings for Fueled Graphite Spheres, USAEC Report NYO-9060, June 30, 1960.
54. C. G. Bergeron et al., Protective Coatings for Refractory Metals, Report WADC-TR-59-526 (Pt. 2), University of Illinois, Dept. of Ceramic Engineering, August 1960.
55. L. E. Mills, Zircaloy Welding, *Welding J.*, 40(2): 141–151 (1961).
56. F. W. Albaugh, Reactor and Fuels Research and Development Operation Monthly Report for October 1960, USAEC Report HW-67254-A, Hanford Atomic Products Operation, Nov. 15, 1960. (Classified)
57. A. F. Taylor, Welding Problems Associated with Nuclear Fuel Elements, *Brit. Welding J.*, 7(10): 594–622 (October 1960).
58. W. J. Lepkowski and R. E. Monroe, Welding of Columbium and Columbium Alloys, Report DMIC-Memo-69, Battelle Memorial Institute, Defense Metals Information Center, Oct. 24, 1960.
59. C. L. Frederick, Ultrasonic Grain Size Testing of Hanford Fuel Elements, USAEC Report HW-64971, Hanford Atomic Products Operation, May 11, 1960.
60. J. P. Reese et al., Evaluation of Ultrasonic Test Devices for Inspection of Adhesive Bonds, Quarterly Progress Report No. 2 for October 1959 Through December 31, 1959, Report ER-10911-2, Martin Co., January 1960.
61. Martin Co., Evaluation of Ultrasonic Test Devices for Inspection of Adhesive Bonds, Quarterly Progress Report No. 3 for January 1, 1960, Through March 31, 1960, Report ER-10911-3, April 1960.
62. W. J. McGonnagle et al., Argonne National Laboratory, November 1960. (Unpublished)
63. Argonne National Laboratory, Reactor Development Program Progress Report, USAEC Report ANL-6269, November 1960.
64. Hanford Atomic Products Operation, Jan. 17, 1961. (Unpublished)
65. H. D. Hendricks et al., Savannah River Laboratory, Nov. 21, 1960. (Unpublished)

LEGAL NOTICE

This document was prepared under the sponsorship of the U. S. Atomic Energy Commission. Neither the United States, nor the Commission, nor any person acting on behalf of the Commission:

A. Makes any warranty or representation, expressed or implied, with respect to the accuracy, completeness, or usefulness of the information contained in this report, or that the use of any information, apparatus, method, or process disclosed in this report may not infringe privately owned rights; or

B. Assumes any liabilities with respect to the use of, or for damages resulting from the use of any information, apparatus, method, or process disclosed in this report.

As used in the above, "person acting on behalf of the Commission" includes any employee or contractor of the Commission, or employee of such contractor, to the extent that such employee or contractor of the Commission, or employee of such contractor prepares, disseminates, or provides access to, any information pursuant to his employment or contract with the Commission, or his employment with such contractor.